LINE PROFILES IN NUCLEAR MAGNETIC RESONANCE ABSORPTION.

Thesis by

John Stewart Waugh

In Partial Fulfillment of the Requirements

for the Degree of

Doctor of Philosophy

California Institute of Technology

Pasadena, California

1953

ACKNOWLEDGEMENTS

It is a privilege to acknowledge the great benefit which I have derived from my happy association with Professor Don M. Yost. His unique and illuminating approach to science and to life mark him, in the words of the prophet, as a "...tahta gemi ve çelik insan güulerinin şanlik hatirasi."

I would also like to thank Professor Robert F. Christy for his willing and helpful clarification of some aspects of the theory, and Mr. William J. Karzas for several discussions of quantum mechanical problems. Thanks are due Mr. Bart Locanthi for his advice on matters of electronics.

I am grateful to the United States Rubber Company for a predoctoral fellowship awarded to me during the academic year 1951 - 1952, and to the E. I. DuPont de Nemours Company for a research grant in the summer of 1952. The construction of most of the apparatus was supported by a generous grant - in - aid to Professor Yost by the Research Corporation.

ABSTRACT

The general theory of line shapes in nuclear magnetic resonance experiments is first outlined in some detail, and results important to the ensuing discussion are derived.

A radiofrequency spectrometer has been assembled, and its design, construction, and operation are described.

The fine structure problem for collinear systems of three interacting spins is solved by application of perturbation theory. Application is then made to the special case represented by the bifluoride ion. Experimental determinations of the line shapes and mean square line widths are made for the proton and fluorine resonances in potassium bifluoride, and interpreted in terms of the configuration of the ion. The equilibrium position for the proton is found to be within $\pm$ 0.05 A.U. of the center of the ion axis. Similar experiments performed on sodium bifluoride are less conclusive, but limits are set on the possible configurations of the HF_2^- ion in this salt.

Line width studies have been made on a number of crystalline coordination complexes. It is found that the cobalt (III) hexammine ion possesses freedom of reorientation in the lattice, but that no such freedom exists in other related compounds which were studied.

Finally, an attempt to determine the third proton configuration in phosphorous acid is briefly described.

TABLE OF CONTENTS

I. GENERAL THEORY OF LINE SHAPES IN NUCLEAR MAGNETISM.

To explain the existence of hyperfine structure in atomic spectra, Pauli in 1924 postulated that atomic nuclei in general possess intrinsic angular momenta and associated magnetic moments.[1] Since that time, the experimental ramifications of the nuclear spin in both physics and chemistry have grown steadily in number and importance, to the extent that an acceptance of Pauli's postulate and its consequences is an established part of the modern scientific weltanschauung. It is the purpose of this section to describe a particular method for obtaining information concerning the structures of certain crystalline solids, from the observation of interactions among the nuclear moments which they contain.

1. Spin and Magnetic Moment Properties of Nuclei:

The spin $\vec{I}$ of a free nucleus, like any other angular momentum, may be defined by the commutation rules for its components:

$$\begin{aligned} [I_x, I_y] &= i\hbar I_z \\ [I_y, I_z] &= i\hbar I_x \\ [I_z, I_x] &= i\hbar I_y \end{aligned} \qquad (1.1)$$

where

$$\vec{I} \cdot \vec{I} = I_x^2 + I_y^2 + I_z^2 ; \qquad \hbar = h/2\pi .$$

Since $\vec{I} \cdot \vec{I}$ commutes with I_x, I_y and I_z, we may obtain simultaneous eigenvalues for $\vec{I} \cdot \vec{I}$ and one of the components, which we shall take to be I_z. By manipulation of the above rules[2] we find the allowed values to be

$$\vec{I} \cdot \vec{I} = I(I+1)\hbar^2 \quad (I = 0, \tfrac{1}{2}, 1, \tfrac{3}{2}, \ldots)$$
$$I_z = m\hbar \qquad (m = I, I-1, \ldots, -I). \tag{1.2}$$

Here I is a quantum number, not to be confused with the magnitude of the angular momentum vector. It is the maximum possible value of I_z in units of $\hbar$, and is the quantity customarily referred to as "the spin." For the purposes of the experiments to be described, in which we shall consider processes accompanied by energy exchanges on the order of 10^{-13} electron volt, the spin I is a permanent, unalterable property of the nucleus. We shall therefore explicitly label the states of interest only by the degree of freedom corresponding to the $(2I + 1)$ possible values of the magnetic quantum number m.

As in the case of electron spin, there is associated with the spin of a nucleus a magnetic dipole moment $\vec{\mu}$, collinear with the angular momentum, and defined by

$$\vec{\mu} = g \frac{e}{2M_p c} \vec{I} \tag{1.3}$$

where e is the electronic charge, M_p is the proton mass, and c

is the velocity of light in a vacuum. g is a splitting factor, analogous to the Landé g, and can be determined at the present time only by experiment.

The quantity usually called the magnetic moment, μ , is defined as the maximum possible time average of an observable component of $\vec{\mu}$, i.e., :

$$\mu = \langle \mu_z \rangle_{max.} = g \frac{e\hbar}{2M_p c} I = g\beta I \qquad (1.4)$$

where β is the nuclear magneton, 5.049×10^{-24} erg gauss^{-1}.

For a nucleus of spin $I \geq 1$, there exist in general higher electric and magnetic multipole moments which may interact with fields present at the nucleus. Only electric 2^{21}-pole and magnetic 2^{21+1}-pole moments are possible;[3] and of these only the electric quadrupole moment has been of any experimental interest. None of these, however, will directly concern us here.

2. Magnetic Resonance of Isolated Spins:

The interaction of a nuclear magnetic moment with an external magnetic field $\vec{H}_0$ is given by

$$W_0 = - \vec{\mu} \cdot \vec{H}_0 \qquad (2.1)$$

whence the possible energy levels for a nucleus in such a field are

$$W_0 = - mg\beta H_0 \qquad (2.2)$$

adjacent levels being separated in energy by $\Delta W_0 = g\beta H_0$. Here H_0 is the magnitude of the field, which is taken to lie in the z direction. In classical terms, the field exerts a torque on the moment, equal to

$$\vec{\mu} \times \vec{H}_0 = \vec{L} = \frac{\vec{dI}}{dt} \tag{2.3}$$

by Newton's second law.[4] From (1.3) we then have

$$\frac{\vec{dI}}{dt} = - g \frac{e}{2M_p c} \vec{H}_0 \times \vec{I}. \tag{2.4}$$

That is, the vector $\vec{I}$ precesses about $\vec{H}_0$ with angular frequency

$$\vec{\omega}_L = - g \frac{e}{2M_p c} \vec{H}_0 \tag{2.5}$$

in which ω_L is called the Larmor frequency.[5] In connection with the physical reality of this frequency, it may be noted that by the Bohr frequency condition, $\Delta W = \hbar \omega$, a transition between adjacent levels is accompanied by the emission or absorption of a quantum of radiation at the Larmor frequency:

$$\omega = \frac{\Delta W}{\hbar} = \frac{-1}{\hbar} g \frac{e\hbar}{2M_p c} H_0 = \omega_L. \tag{2.6}$$

For protons ($I = \frac{1}{2}$, $g = 5.586$) in a field of 5000 gauss*, this frequency, in units of cycles per second, is 21.4×10^6 sec^{-1}, which is in the range of radiofrequencies. For all other nuclei except that of H^3 the magnetic moment is smaller than this, so that the Larmor precession is slower for the same field strength, or requires a larger field for the same precessional frequency.**

Transitions between Zeeman levels may be produced by interaction of the rotating component of magnetic moment with a rotating magnetic field. Majorana(6) and Rabi(7) have solved the problem exactly for an isolated spin. However the results are given with sufficient accuracy and considerably greater simplicity by the usual perturbation theory formula for magnetic dipole transition probabilities:

$$\frac{d}{dt} P_{m \to m'} = \frac{2\pi}{3\hbar^2} \left| \langle m' | \underline{M} | m \rangle \right|^2 \rho(\omega_L) \qquad (2.7)$$

where $\underline{M}$ is the magnetic moment operator. Because I_z is fixed by the quantization, the effective parts of $\underline{M}$ are the rotating components in the xy plane,

---

* Strictly speaking, field intensity should be measured in oersteds. However, since we shall be dealing only with substances of nearly unit permeability, the induction and field strength are numerically the same. We therefore perpetuate the inaccuracy to conform with the existing literature.

** It is clear that we can regard either the frequency or the field as the independent variable, with the same results. Owing to the nature of the experimental arrangement to be described, the latter convention is ordinarily the more convenient, and we shall usually regard H_0 as the explicit variable, with a Larmor value H_0^*.

$$\underline{M}_{eff} = \frac{\mu}{2} \left(\underline{I}_x \pm \underline{I}_y \right). \tag{2.8}$$

$\rho(\omega)$ is the energy density per unit frequency range in the weak, isotropic, unpolarized field. We shall wish to deal instead with a small oscillating field polarized in the x direction, $H_1 \cos \omega t$. For this case the transition probability per unit time becomes

$$\frac{d}{dt} P_{m \to m'} = \frac{H_1^2}{2\hbar^2} \left| \langle m' \left| \underline{I}_x \right| m \rangle \right|^2 \delta (H_0, H^*) \tag{2.9}$$

where H_0 is now regarded as the independent variable and $\delta (H_0, H^*)$ is a Dirac delta function. The behavior indicated here is the nuclear magnetic resonance effect. It may be noted at this point that, if this sharp resonance can be detected, we have a method for determining either the g factor of the nucleus or the magnetic field strength by means of a simple frequency measurement. Much experimental activity has recently centered in these areas[9,10] owing partly to the convenience and high accuracy of the measurements.

Expression (2.9) is symmetrical in the states $|m\rangle$ and $|m'\rangle$, so that the probability per nucleus per unit time is the same for induced emission as for absorption. In order for continuous absorption to occur in an ensemble of nuclei, there must at all times be a greater population in the lower (absorbing) state

than in the upper (emitting) one. We must then inquire concerning the relative populations of states of different m in the steady state.

3. The Establishment of Thermal Equilibrium:

At equilibrium, in the absence of any radiation field but with a constant magnetic field, H_0, the population of state $|\, m \,\rangle$ is described by a Boltzmann distribution:

$$N_m = \frac{N_0}{Z}\, e^{\frac{-gm\beta H_0}{kT}} \quad ; \quad T >> \frac{gm\beta H_0}{k} \quad . \tag{3.1}$$

Here N_0 is the total number of spins under consideration and Z is the partition function, which for this case is very nearly $2I + 1$. For protons ($I = \frac{1}{2}$, $g = 5.586$) at room temperature in a field of 5000 gauss we find the ratio of the populations of the two levels to be

$$\frac{N_{\frac{1}{2}}}{N_{-\frac{1}{2}}} \simeq 1 + 3.5 \times 10^{-6} \quad . \tag{3.2}$$

Clearly, it is the very small excess number in the state of lower energy which must be responsible for any net absorption of energy by the ensemble.

In the absence of any effects other than those so far considered, the application of a radiation field at the Larmor frequency will

result in an exponential approach of this population ratio to unity. For the ensemble of protons we are free to define a "spin temperature", T_s, such that (3.1) always holds. The absorption of radiation then results in an unbounded linear increase of T_s, which is concerned only with the spin variables of the thermodynamic system, and the disappearance of any net absorption. In order to preserve an excess in the lower state, there must be a mechanism other than induced emission for lowering the spin temperature by loss of energy by the spin system to the other degrees of freedom of the system.* There are two possibilities involved:

A. The excited spins may decay by spontaneous magnetic dipole emission. The average life with respect to such decay, however, is found to be on the order of 10^{22} seconds[12], and the process may therefore be neglected.

B. Energy may be given up to the lattice motion of the surroundings. (Here the term "lattice" is loosely used to include all of the surroundings, whether in a solid, liquid, or gas, which embody the translational, rotational and vibrational degrees of freedom of the medium.) It will be shown in a later section that such motions are effective in bringing about equilibration of the entire thermodynamic system only when the changing magnetic fields at the excited nuclei have Fourier components in the vicinity of ω_L or $2\omega_L$. As a measure of the effectiveness of these

---

* If this were not so, it would be possible to prepare a spin system with a real negative spin temperature.[11]

processes, we may define for any material a "spin - lattice relaxation time", T_1 by

$$N_m - N_{m'} \sim e^{-t/T_1}.$$

Note that competition between the resonant absorption and the thermal relaxation affords a possible method of measurement of T_1.

In single crystals where the only motions are high frequency lattice vibrations, T_1 is characteristically of order 10^4 seconds. Very small and unpredictable amounts of paramagnetic impurities may reduce these times enormously, and so no significant relationship can be deduced between the empirically determined relaxation time and the dynamical properties of the crystal. In gases and liquids, where the Fourier spectrum of perturbing dipole fields is a random one, T_1 is typically on the order of 1 second.

It will be seen that the slowness of the relaxation process imposes a limitation on the attainable rate of absorption, there being an optimum size of H_1 for the greatest possible steady state value of $N_m - N_{m+1}$. While this limitation is often severe, it is still possible to obtain measurable absorptions in most cases.

It is well to remark parenthetically that the measurement of spin - lattice relaxation times as a function of temperature provides an important method for studying changes in the constitution and internal motion in solids occurring at second order phase transitions.[13]

A third type of interaction is that between nuclear dipoles, in which a quantum is emitted by one and absorbed by the other. This spin - exchange coupling cannot produce thermal relaxation of the spin system since the total energy is conserved. But it, together with the static dipole fields in the sample, is responsible for the effect of principal interest in the investigations described in this thesis.

4. The Local Field:

Up to this point we have considered the nuclear magnetic resonance effect for nuclei which are regarded as not mutually interacting. In any real material the moments do of course influence one another, and it is of interest to examine the nature and size of the observable effects produced.

To take a naive but heuristic view, we may think of the mutual interaction in classical terms, as follows: for a given exciting frequency, the resonant value of the magnetic field is in general not simply the applied field $\vec{H}_0$. Instead it is the vector sum of $\vec{H}_0$ and whatever local perturbing fields may be present at the resonant nucleus, due to the nature of the sample itself. In materials which are electronically diamagnetic the only important disturbances of this sort are the dipole fields of the nuclei themselves. (So long as we restrict ourselves to nuclei of spin $\frac{1}{2}$, we encounter no trouble due to coupling of nuclear quadrupole moments to the gradient of the electric

field of the lattice.) If we assume that only the static z components of these fields are of importance, we may write the field at nucleus i due to the others as

$$H_{loc.} = \sum_j \mu_{zj} r_{ij}^{-3} (1 - 3 \cos^2 \theta_{ij}) \qquad (4.1)$$

where θ_{ij} is the angle between $\vec{H}_0$ and the radius vector $\vec{r}_{ij}$ connecting i and j. For protons separated by 1 A. U., μ/r^3 has the value 14.1 gauss, so it is evident that $H_{loc.}$ is a small but appreciable perturbation on the 10^3 gauss fields ordinarily used to remove the space degeneracy.

If (4.1) is averaged over a sphere, as would be the proper procedure for a sample in which the internuclear vectors are rapidly and randomly changing in direction, the local field is seen to vanish. In gases and liquids, where such averaging occurs due to the thermal motion and is essentially complete within one Larmor precession period, this result is observed: the magnetic resonance occurs very sharply at H^*. (A natural line width of ca. 10^{-5} gauss remains, owing to the finite lifetimes of the excited states.) In "rigid" crystalline solids, however, where the nuclei are bound closely to fixed equilibrium positions, quite a different situation prevails.

Suppose, for instance, that a sample consists entirely of a set of nuclear pairs in each of which nucleus 1 has a different

magnetic moment than nucleus 2. If $\vec{r}_{12}$ is the same for all these pairs, the local field at nuclei of type 1 is always

$$\left[H_{loc.} \right]_1 = \pm \frac{\mu_2}{r_{12}^3} (1 - 3 \cos^2 \theta_{12}) \qquad (4.2)$$

with the sign determined by which of the two allowed states the second spin occupies. If all dipole - dipole interactions other than those within the individual pairs are neglected, there will then be two distinct values of the external field for which resonance of 1 occurs at a given excitation frequency:

$$H_0 = H^* \pm \frac{\mu_2}{r_{12}^3} (1 - 3 \cos^2 \theta_{12}) . \qquad (4.3)$$

If more distant neighbors are considered, it is clear qualitatively that each of the two absorption lines will be split into many more components, the amounts of the splittings being proportional to $\mu_j r_{1j}^{-3}$. For a very large number of such components, the end effect is a broadening of the entire absorption line, in which the fine structure due to the 1 - 2 interactions may still be discernible if these are sufficiently dominant.

It should be remarked here that the above treatment actually gives the correct result for the case that the interactions are all between unlike spins. This will be made clear in the more complete treatment to follow, as will the fact that a correction is necessary when interactions between identical spins are of importance.

5. The Effect of Motion on the Line Width:

As we have seen, rapid random reorientation of the internuclear vectors causes averaging of the local field to zero, producing an extremely narrow absorption line. However, motion which is not of a spherically symmetric type may produce incomplete averaging and a line of intermediate width.* For a nuclear pair of the type discussed above, rotating about an axis normal to the internuclear vector, the line is one half as broad as if no motion occurred, although the structure of the line remains the same. This sort of behavior is useful in studying the internal motions of crystalline solids, as will be pointed out in more detail in a later section.

Even if the orientation of a group remains fixed, any large internal vibrations have an effect on the line shape. For the nuclear pair, the local field of interest involves an average of r_{12}^{-3} over the state of motion. For harmonic stretching vibrations, to take an example, this average is certainly not the same as the inverse cube of the equilibrium separation; and this fact must, in principle, be taken into account. Fortunately for the simplicity of the calculations, most vibrations in solids are not of a large enough amplitude to introduce errors if they are neglected.

6. Quantum Mechanical Description of the Dipole - Dipole Coupling:

While the classical local field viewpoint often leads to correct results, there are many cases where corrections are needed. For this

---

* A more rigorous discussion of the types of averaging necessary, and the conditions under which they are valid, will be given in Section IV.

reason, and in order to place the entire treatment on a more rigorous basis, it is desirable to consider the quantum mechanical situation in some detail.

The energy of an assembly of classical magnetic dipoles in a magnetic field $\vec{H}_0$, assuming its internal configuration to be rigid, is given by

$$W = \sum_i \mu_i \cdot \vec{H}_0 + \sum_i \sum_{j>i} \left[\frac{\vec{\mu}_i \cdot \vec{\mu}_j}{r_{ij}^3} - 3 \frac{(\vec{\mu}_i \cdot \vec{r}_{ij})(\vec{\mu}_j \cdot \vec{r}_{ij})}{r_{ij}^5} \right] \tag{6.1}$$

where the first term is the "Zeeman" energy of interaction with the external field, and the second represents the "dipolar" energy, or coupling of the moments with one another. $\vec{r}_{ij}$ is the radius vector joining nuclei i and j. For a system of nuclei of spin $\frac{1}{2}$ we may write the corresponding Hamiltonian operator as follows:

$$\mathcal{H} = \sum_i \sum_{j\ i} \mathcal{H}_{ij}$$

$$\mathcal{H}_{ij} = g_i g_j \beta^2 \left[\frac{\vec{\sigma}_i \cdot \vec{\sigma}_j}{r_{ij}^3} - 3 \frac{(\vec{\sigma}_i \cdot \vec{r}_{ij})(\vec{\sigma}_j \cdot \vec{r}_{ij})}{r_{ij}^5} \right]. \tag{6.2}$$

Here the σ's are Pauli spin operators, whose components are given by

$$\sigma_x = \begin{pmatrix} 0 & 1 \\ 1 & 0 \end{pmatrix} ; \quad \sigma_y = \begin{pmatrix} 0 & -i \\ i & 0 \end{pmatrix} ; \quad \sigma_z = \begin{pmatrix} 1 & 0 \\ 0 & -1 \end{pmatrix} . \qquad (6.3)$$

The same Hamiltonian is valid for any other spin if we replace these operators by the corresponding $(2I + 1)$ by $(2I + 1)$ angular momentum matrices[14] so long as we consider only magnetic interactions.

For a spin system of any complexity, it is apparent that the above Hamiltonian is an exceedingly complicated one. In principle one should take into account the effects of all the 10^{20} or so spins in the macroscopic sample. Such a system has an enormous number of states, all highly degenerate in the absence of any coupling. The introduction of the perturbation partly removes the degeneracy, and establishes a set of fine structure components for the absorption. These will nearly all be in the immediate vicinity of the unperturbed line at H^*, since the great majority of the characteristic values of $\mathcal{H}$ are small in comparison with the Zeeman energies of the states. The very high density of fine structure components in this small range permits the problem to be treated by continous methods, the totality of the fine structure being described by a continuous line shape function, $f(H_0)$.

Adopting this point of view, Waller[15] Broer[16] and Van Vleck[17] have devised a rigorous, if not completely practical, method for calculating $f(H_0)$ from the molecular data. The line shape is described in terms of its moments about the center, which are defined by

$$\overline{(H_0 - H^*)^n} = \int_0^\infty (H_0 - H^*)^n f(H_0 - H^*)\, dH_0; \tag{6.4}$$

$$\int_0^\infty f(H_0 - H^*)\, dH_0 = 1 .$$

A knowledge of all the moments is equivalent to a knowledge of the function itself.[18] The theory expresses the moments in terms of the traces of the magnetic moment matrix and its commutator with the Hamiltonian, the traces being evaluated in a representation in which the nuclei are independent. Because of the invariance of the trace to transformation from one representation to another, the results are valid for the coupled system.

Unfortunately, the calculation of the higher moments is extremely tedious, and the solution has been carried out only through $\overline{(H_0 - H^*)^4}$. Furthermore, the higher moments are very sensitive to small changes in the wings of the line, and these are the regions in which experimental measurements are the least accurate. The second moment, however, retains considerable utility in the matching of experimental data to theoretical models. It is found to have the form

$$\overline{(H_0 - H^*)^2} = \overline{\Delta H^2} = \frac{3}{4N_s} I(I+1)\, g^2 \beta^2 \sum_k r_{jk}^{-6} P_2(\cos \theta_{jk}) + \frac{1}{3N_s} I'(I'+1)\, g'^2 \beta^2 \sum_{k'} r_{jk'}^{-6} P_2(\cos \theta_{jk'}). \tag{6.5}$$

Here the unprimed letters apply to the nuclei at resonance, and the primes denote whatever other perturbing nuclei are involved. N_s is the number of nuclei at resonance in the group for which the second moment is calculated. In practical cases, $\overline{\Delta H^2}$ converges rapidly as N_s is increased.

The second moment alone gives very little information regarding the shape of the absorption. However in many cases it is possible to use this quantity in conjunction with the results of another treatment to obtain detailed line profiles in excellent agreement with experiment. The sample is imagined to be divided into small, magnetically identical "elementary interaction cells", each containing only a few nuclei. The internal interaction energy of each of these cells is to be large in comparison with its coupling to the surroundings. By a method to be described in the next section, the line profile for such a cell is calculated assuming it to be completely isolated. The second moment contributed by the surroundings alone is then computed, and a bell - shaped curve of appropriate half width is substituted for each (discrete) component of the elementary cell fine structure. The validity of this procedure rests on the assumptions that the surroundings are approximately isotropic in their magnetic effects, and that the external broadening is produced by many more nuclei than occupy the elementary interaction cell. In many real crystals this assumption turns out to be justified. Furthermore, if the external

broadening is very small in comparison with the total width of the absorption, the line calculated by this procedure is quite insensitive to the exact shape of the broadening function used. Indeed, in some of the calculations a rectangular component line gives substantially the same results as a Gaussian.

We shall now discuss the method to be employed in calculating the fine structure to be expected from the highly anisotropic elementary interaction cell alone.

7. The Energy Levels of the Elementary Interaction Cell:

We now restrict the discussion to a small group of two or three nuclei, so that the Hamiltonian (6.2) becomes tractable. Since the matrix elements $\mathcal{H}_{ij}$ are small relative to the splitting of the Zeeman levels, we may expect to obtain valid results by considering the former as small perturbations on the latter. We label the states of the system by the magnetic quantum numbers m_i of the individual spins, and assume that this characterization is still valid after the introduction of the perturbation. It is convenient to sort out the effects of various parts of the Hamiltonian[19] by expanding it as follows:

$$\mathcal{H}_{ij} = \frac{g_i g_j \beta^2}{r_{ij}^3}\Big[\sigma_{x_i}\sigma_{x_j}(1-3\alpha_{ij}^2) + \sigma_{y_i}\sigma_{y_j}(1-3\beta_{ij}^2) + \sigma_{z_i}\sigma_{z_j}(1-3\gamma_{ij}^2) - 3(\sigma_{x_i}\sigma_{y_j}+\sigma_{y_i}\sigma_{x_j})\alpha_{ij}\beta_{ij} - 3(\sigma_{x_i}\sigma_{z_j}+\sigma_{z_i}\sigma_{x_j})\alpha_{ij}\gamma_{ij} - 3(\sigma_{y_i}\sigma_{z_i}+\sigma_{z_i}\sigma_{y_i})\beta_{ij}\gamma_{ij}\Big] \tag{7.1}$$

in which α_{ij}, β_{ij}, and γ_{ij} are the direction cosines of $\vec{r}_{ij}$ relative to a set of Cartesian axes whose z axis is along $\vec{H}_0$.

We now introduce the operators[20]

$$\sigma_{+_i} = \sigma_{x_i} + i\,\sigma_{y_i}$$

$$\sigma_{-_i} = \sigma_{x_i} - i\,\sigma_{y_i} \tag{7.2}$$

for which the selection rules are

$$\sigma_{+_i} : \quad m_i = +1$$

$$\sigma_{-_i} : \quad m_i = -1 \ . \tag{7.3}$$

These have the advantage that they are more strict than the restriction $\Delta m_i = \pm 1$ on σ_x alone. Re-expressing the results in spherical polar coordinates (r, θ, ϕ) and adding the appropriate Heisenberg time factors exp $(-iEt/h)$ for the various states the Hamiltonian matrix becomes

$$\mathcal{H}_{ij} = \frac{g_i g_j \beta^2}{r_{ij}^3} \ (A + B + C + D + E + F) \tag{7.4}$$

where

$$A = \sigma_{z_i} \sigma_{z_j} (1 - 3 \cos^2 \theta_{ij})$$

$$B = -\frac{1}{4}(1 - 3\cos^2\theta_{ij})\left[\sigma_{-_i}\sigma_{+_j} e^{\frac{i\beta H_0 t}{\hbar}(g_j - g_j)} + \sigma_{+_i}\sigma_{-_j} e^{\frac{i\beta H_0 t}{\hbar}(g_i - g_j)}\right]$$

$$C = -\frac{3}{2}\sin\theta_{ij}\cos\theta_{ij} e^{-i\phi_{ij}}\left[\sigma_{+_i}\sigma_{z_j} e^{\frac{i\beta H_0 t}{\hbar} g_i} + \sigma_{+_j}\sigma_{z_i} e^{\frac{i\beta H_0 t}{\hbar} g_j}\right]$$

$$D = -\frac{3}{2}\sin\theta_{ij}\cos\theta_{ij} e^{i\phi_{ij}}\left[\sigma_{-_i}\sigma_{z_j} e^{\frac{-i\beta H_0 t}{\hbar} g_i} + \sigma_{-_j}\sigma_{z_i} e^{\frac{-i\beta H_0 t}{\hbar} g_j}\right]$$

$$E = \frac{3}{4}\sin^2\theta_{ij} e^{2i\phi_{ij}}\sigma_{+_i}\sigma_{+_j} e^{\frac{i\beta H_0 t}{\hbar}(g_1 + g_2)}$$

$$F = \frac{3}{4}\sin^2\theta_{ij} e^{-2i\phi_{ij}}\sigma_{-_i}\sigma_{+_j} e^{\frac{-i\beta H_0 t}{\hbar}(g_1 + g_2)}. \qquad (7.5)$$

The changes in $m = \sum m_i$ which may be induced by this perturbation are, for each term

A : $\Delta m = 0$	D : $\Delta m = -1$
B : $\Delta m = 0$	E : $\Delta m = +2$
C : $\Delta m = +1$	F : $\Delta m = -2$

Term A represents the static dipole - dipole interaction between the z components of magnetic moment, and as such is identical with the "local field" perturbation described in § 4. If all interacting pairs (i, j) have sufficiently different g factors, all of the other terms vanish in time average, and the classical calculation is correct and complete. For pairs of identical nuclei, only terms C - F vanish, and the secular part includes both A and B. The latter may be thought of as corresponding to the simultaneous reversal of two antiparallel spins, brought about by the precessing component of dipole field produced by each at the other. For a simple pair or an equilateral triangle of identical spins, the contribution of B is one half that from A, so the splittings obtained are 3/2 the classical values. This factor does not hold for all systems, however, the reason being connected with the fact that $\mathcal{H}_{ij}$ and $\mathcal{H}_{ik}$ do not in general commute.

For a spatially rigid elementary interaction cell, terms C, D, E, and F always vanish, owing to their rapid periodicity. However, if the lattice undergoes motions producing fluctuating magnetic fields which have a Fourier component at $g\beta H_0/\hbar$ or $2g\beta H_0/\hbar$, this part of the Hamiltonian allows exchange of energy between the spins and the lattice degrees of freedom. This

phenomenon is of interest in the theory of the spin - lattice relaxation process,[12] but will not occupy our attention further here. We shall be interested, indeed, only in crystals in which all the motions are of a far higher frequency when ω_L.

The problem remaining is to calculate the matrix elements of A and B between all pairs of states of the spin system under consideration. The matrix is then diagonalized by solving a secular equation. The eigenvalues of the energy are added as corrections to the energies of the appropriate unperturbed Zeeman states to obtain the complete energy level scheme for the system.

In order to relate the various energy differences which obtain to the expected fine structure, we must first calculate corresponding magnetic dipole transition probabilities. In simple cases of high symmetry, these often can be obtained on inspection by a consideration of the symmetry properties of the wave functions and of the magnetic dipole operator. In somewhat more complicated cases it will be necessary actually to insert the operator and calculate its matrix elements. In order to do this, we must first determine the correct zero'th order wave functions for the system by finding the unitary matrix which diagonalizes the Hamiltonian. These linear combinations of the most elementary states are then used to calculate the relative transition probabilities, and the magnetic resonance spectrum is thus obtained.

8. Line Shapes in Single Crystals and Powders:

The structure of the absorption still depends on all the r_{ij} and θ_{ij}. If a model is now assumed for the elementary interaction cell, this dependence reduces to a single one on the orientation of the cell in the Zeeman field. If the macroscopic sample is a single crystal, in which all the cells are identical in structure and orientation, the observed absorption should clearly agree with the results of the above calculation. In any real material, however, the cells do of course interact, though the strength of this coupling is assumed small compared with the internal interactions. As mentioned in the previous section, we take this into account by substituting for each fine structure component a Gaussian:

$$S(H) = \frac{1}{\xi\sqrt{2\pi}}\, e^{\frac{-(H - H_0)^2}{2\xi^2}} \qquad (8.1)$$

where the half width ξ includes the "extramolecular" broadening as well as any contributions due to crystal imperfections and magnetic field inhomogeneity.* If the assumed model is correct, and if the proper broadening has been introduced, the result should be in good agreement with experiment. This has indeed been the case in the few experiments which have been performed with compounds of known structure. So long as the overlap of the Gaussian com-

---

* to be discussed in a later section.

ponents is slight, the observed peaks fall on the positions predicted by the first order perturbation theory, and thus a simple and direct determination of the interatomic distances is possible.

In only a few cases is it feasible, or even possible, to obtain single crystals of a sufficient size and perfection to carry out the experiment required by the above analysis. It is therefore important to inquire what the shape of the absorption line will be in the case that the sample is a grossly isotropic powder of microcrystals. To do this we regard the resultant line as the superposition of a continuum of components, in which the strength of the component at H_0 is taken as being proportional to the probability that its center lies between H_0 and $H_0 + dH_0$. Each of the components is to be a Gaussian whose half width is given by the characteristic supplementary broadening ξ, and the probability required is related to the field strength through the dependence on orientation of the elementary interaction cell.

From the Hamiltonian (7.5) it is evident that the only angular dependence for a nuclear pair (i, j) resides in the factor $(1 - 3 \cos^2 \theta_{ij})$. For a set of such pairs with different θ_{ij}, the line shape becomes a rather complicated function of cell orientation, and the introduction of all the necessary constraints on these angles may become tedious. For the special case of linear elementary interaction cells, however, the angular dependence may be treated as a scale factor for the total splitting,

and its averaging carried out independently of the exact geometry of the interacting group.

If all orientations over a sphere are equally likely, we may take the probability as a function of θ to be

$$\frac{d\rho}{d\theta} = \frac{1}{2} \sin \theta \tag{8.2}$$

where θ is the angle between any axis fixed in the interaction cell and the external field, and $p(\theta)$ is normalized to unit probability for finding θ somewhere in the range $(0,\pi)$. We can write the unbroadened fine structure analytically as

$$\phi(H_0 - H^*) = K \sum_{\alpha} d_\alpha \delta (H_0 - H^*, \pm \alpha)(1 - 3 \cos^2 \theta) \tag{8.3}$$

where there is one (symmetrical) pair of components for each value of α, and d_α is the degeneracy of the transitions corresponding to splitting α. Using this expression to obtain $\sin \theta$ in terms of H_0, we have for one of the allowed values

$$\frac{dp}{dH_0} = \frac{1}{4\alpha\sqrt{3}} \left(1 \mp \frac{H_0 - H^*}{\alpha} \right)^{-1/2} . \tag{8.4}$$

Here the upper sign holds in the range $-2\alpha \leq H_0 - H^* \leq \alpha$ and the lower one for $-\alpha \leq H_0 - H^* \leq 2\alpha$. In the overlapping region, dp/dH_0 is given by the sum of these.

The line shape for the pair of components at $\pm\alpha$ is obtained by folding the Gaussian component line into the probability distribution function (8.4), that is:

$$f(H) = \int_{-\infty}^{\infty} \frac{dp}{dH_0} e^{\frac{-(H - H_0)^2}{2\xi^2}} dH_0. \qquad (8.5)$$

Owing to the linearity of this Gauss transform[21] we can carry out the integration for just one sign in (8.4) and add to the result its reflection in $(H_0 - H^*) = 0$. It is helpful at this point to simplify the notation by introducing more convenient dimensionless variables. We write

$$\frac{H_0 - H^*}{\alpha} = x \qquad \frac{H - H^*}{\alpha} = y$$

$$\frac{\xi}{\alpha} = \beta \qquad (8.6)$$

Choosing the upper sign in (8.4) the transform is

$$G(\alpha y + H^*) = \int_{-2}^{1} \frac{\alpha}{\sqrt{1 - x}} e^{-\frac{1}{2\beta^2}(y - x)^2} dx. \qquad (8.7)$$

This integral has not been evaluated in closed form and so it is necessary to carry it out numerically. The difficulty with the branch point at $x = 1$ is removed by an integration by parts:

$$G(\alpha y + H^*) = -2\alpha\sqrt{1-x}\; e^{-\frac{1}{2\beta^2}(y-x)^2}\Big|_{-2}^{1}$$

$$+\frac{2\alpha}{\beta^2}\int_{-2}^{1}\sqrt{1-x}\,(y-x)\,e^{\frac{1}{2\beta^2}(y-x)^2}\,dx.$$

Introducing the commonly tabulated error function

$$\Phi(z) = \frac{1}{\sqrt{2\pi}}\, e^{\frac{-z^2}{2}} \qquad (8.8)$$

and discarding some multiplicative constants, we have

$$g(y) = \sqrt{3}\beta^2\,\Phi\left(\frac{y+2}{\beta}\right) + \int_{-2}^{1}\sqrt{1-x}\,(y-x)\,\Phi\,\frac{y-x}{\beta}\,dx \qquad (8.9)$$

This function has been evaluated by multiple application of Simpson's rule and the results are recorded in Table 1. Where necessary, more accurate analogues of Simpson's rule for more finely divided intervals have been employed. The figures given are presumed reliable within ± 1 in the last figure.

As noted above, the line shape is proportional to $g(y) + g(-y)$. This function appears in Table 2. In both tables all transforms are normalized to unit total area.

9. Use of g(y) in Prediction of Real Line Shapes:

The application of the above analysis is reasonably straightforward. A model is assumed for the elementary interaction cell, the basic fine structure is calculated by perturbation theory and a value of ξ is then estimated. For each component α_j the transform for the appropriate value of $\beta_j = \xi/\alpha_j$ is obtained by interpolation in Table 2 (or more simply by choosing the nearest tabulated transform). The arguments are then multiplied by α_j and the entries by α_j^{-1} to preserve the normalization. The results for all components are plotted and added graphically to obtain the theoretically predicted total absorption.

If the assumed model for the spin system is qualitatively correct, some agreement will be found with the experimental data. The parameters α_j and β_j are now adjusted to give the best possible correspondence, and the internuclear distances calculated from the values of α_j are obtained. These are always of the form $\alpha_j = K \mu r^{-3}$. In favorable cases, little or no adjustment of β_j is necessary, for this quantity is frequently predictable with reasonable accuracy from previously known features of the crystal structure. If the basic structure of the lattice is unknown, however, some adjustment will be necessary, and the value obtained may give some small amount of information concerning the type of packing in the crystal. The procedure yields the most clear - cut results when β_j is considerably less than 1. Otherwise so

much of the elementary interaction cell detail may be obscured as to lead to considerable ambiguity on the interpretation of data. It is an unfortunate fact that even in the most favorable cases, the smearing of the fine structure by the extramolecular interactions hides many of the more closely spaced fine structure components.

TABLE 1

Gauss transform of the Fine Structure for a Spherically Symmetric Distribution.

y	$\beta = 0.10$	$\beta = 0.15$	$\beta = 0.20$	$\beta = 0.25$	$\beta = 0.30$	$\beta = 0.35$
-2.70	.000	.000	.000	.000	.000	.001
-2.60	.000	.000	.000	.000	.000	.006
-2.50	.000	.000	.000	.000	.005	.014
-2.40	.000	.000	.000	.004	.011	.022
-2.30	.000	.005	.010	.016	.021	.033
-2.20	.005	.017	.037	.040	.039	.051
-2.10	.030	.046	.079	.076	.069	.072
-2.00	.081	.084	.112	.104	.099	.092
-1.90	.145	.139	.134	.124	.120	.115
-1.80	.171	.160	.150	.141	.137	.133
-1.70	.177	.165	.160	.155	.153	.150
-1.60	.180	.169	.167	.166	.165	.165
-1.50	.182	.174	.173	.173	.173	.172
-1.40	.186	.181	.181	.181	.181	.180
-1.30	.190	.189	.189	.189	.189	.187
-1.20	.195	.195	.196	.196	.194	.192
-1.10	.200	.200	.201	.202	.200	.198
-1.00	.204	.204	.205	.207	.206	.205
-0.90	.209	.209	.210	.212	.212	.212
-0.80	.215	.215	.216	.217	.218	.219
-0.70	.221	.221	.222	.223	.225	.225
-0.60	.228	.228	.229	.231	.233	.232
-0.50	.236	.236	.237	2.39	.241	.240
-0.40	.245	.245	.246	.248	.250	.250
-0.30	.254	.254	.255	.257	.259	.261
-0.20	.264	.264	.266	.268	.272	.278
-0.10	.275	.276	.279	.282	.287	.297
0.00	.288	.290	.294	.298	.304	.319
0.10	.304	.306	.312	.318	.325	.341
0.20	.324	.326	.335	.344	.353	.364
0.30	.348	.351	.367	.375	.384	.391
0.40	.376	.387	.410	.417	.424	.421
0.50	.415	.433	.457	.462	.467	.455
0.60	.468	.494	.519	.521	.515	.489
0.70	.571	.599	.602	.578	.546	.503
0.80	.742	.724	.671	.605	.550	.498
0.90	.952	.772	.664	.581	.518	.468

TABLE 1 continued

y	β = 0.10	β = 0.15	β = 0.20	β = 0.25	β = 0.30	β = 0.35
1.00	.780	.640	.461	.469	.452	.417
1.10	.295	.380	.312	.352	.367	.350
1.20	.044	.154	.207	.250	.270	.276
1.30	.002	.077	.129	.158	.171	.203
1.40	.000	.029	.061	.079	.099	.137
1.50	.000	.002	.010	.032	.056	.087
1.60	.000	.000	.000	.006	.025	.050
1.70	.000	.000	.000	.000	.010	.029
1.80	.000	.000	.000	.000	.002	.014
1.90	.000	.000	.000	.000	.000	.004

TABLE 2

Normalized Line Shape Functions.

y	β = .10	β = .15	β = .20	β = .25	β = .30	β = .35
0.00	.288	.290	.294	.298	.304	.319
0.10	.290	.291	.295	.300	.306	.320
0.20	.294	.295	.300	.306	.312	.321
0.30	.301	.302	.310	.316	.322	.326
0.40	.310	.316	.327	.332	.337	.336
0.50	.325	.334	3.46	.350	.354	.348
0.60	.348	.361	.373	.376	.374	.360
0.70	.396	.410	.412	.400	.386	.364
0.80	.478	.470	.443	.411	.384	.359
0.90	.580	.490	.438	.396	.365	.340
1.00	.492	.422	.332	.338	.328	.311
1.10	.298	.290	.256	.272	.283	.274
1.20	.120	.175	.202	.223	.232	.234
1.30	.096	.133	.160	.174	.180	.195
1.40	.093	.105	.121	.130	.140	.159
1.50	.091	.088	.092	.102	.115	.130
1.60	.090	.085	.084	.086	.095	.107
1.70	.088	.082	.080	.077	.081	.090
1.80	.085	.080	.075	.070	.070	.083
1.90	.072	.070	.076	.062	.060	.060
2.00	.040	.042	.056	.052	.050	.046
2.10	.015	.023	.040	.038	.035	.036
2.20	.003	.009	.019	.020	.020	.025
2.30	.000	.003	.005	.008	.010	.016
2.40	.000	.000	.000	.002	.005	.011
2.50	.000	.000	.000	.000	.002	.007
2.60	.000	.000	.000	.000	.000	.003
2.70	.000	.000	.000	.000	.000	.001

II. DESIGN, CONSTRUCTION, AND OPERATION OF THE APPARATUS.

The first experimental detection of resonant transitions between nuclear Zeeman levels was made by the molecular beam magnetic resonance method of Rabi[22] et. al. This technique is still in widespread use. However by its basic nature it excludes from study any materials in the solid or liquid state. Partly in order to overcome this shortcoming, several variations of the nuclear magnetic resonance have been developed in the postwar period. The two approaches are in no sense competitive, but rather are complementary in that each is suitable for attacking problems inaccessible to the other.

In the nuclear induction apparatus of Bloch and his collaborators[23], the sample is contained in an excitation coil whose axis is at right angles to the external field $\vec{H}_0$. At resonance, a voltage is induced in a second coil with its axis in the third perpendicular direction, and the resulting signal is amplified and detected to obtain the final resonance signal.

The nuclear magnetic resonance absorption technique, simultaneously developed at Harvard by Purcell and co - workers;[24] omits the third coil. Instead it measures the energy losses from the excitation coil at resonance by means of the unbalancing of a radiofrequency bridge.

Investigations have also been made in which the signal of interest is a change in the level of oscillation of a regenerative or superregenerative detector[25]. The inductance in its tank circuit is again a coil whose axis is at right angles to $\vec{H}_0$, and contains the sample of interest. This approach has been found useful chiefly in the construction of fluxmeters. By this means, magnetic field measurements accurate to one part in 10^5 or better are conveniently possible.

A more radical departure is taken by Hahn[26] and his colleagues. Here the sample is excited by two or more short pulses of high level radiofrequency energy. One or more delayed pulses are then observed at a later time by detection of the voltage in the same coil which is used for the excitation. This technique is not applicable to the study of line profiles.

The apparatus to be described is a nuclear magnetic resonance absorption spectrometer. A general view of the equipment in substantially complete form appears in Figure 1, page 35, and a block diagram in Figure 2, page 36. The main features of its design and construction will now be described.

1. Magnet and Power Source:

The Zeeman splitting field is produced by a large electromagnet,[27] which is stored by the Office of Naval Research in the Gates Laboratory. The original pole pieces, designed with an eye to cosmic ray momentum measurements, have been replaced by more

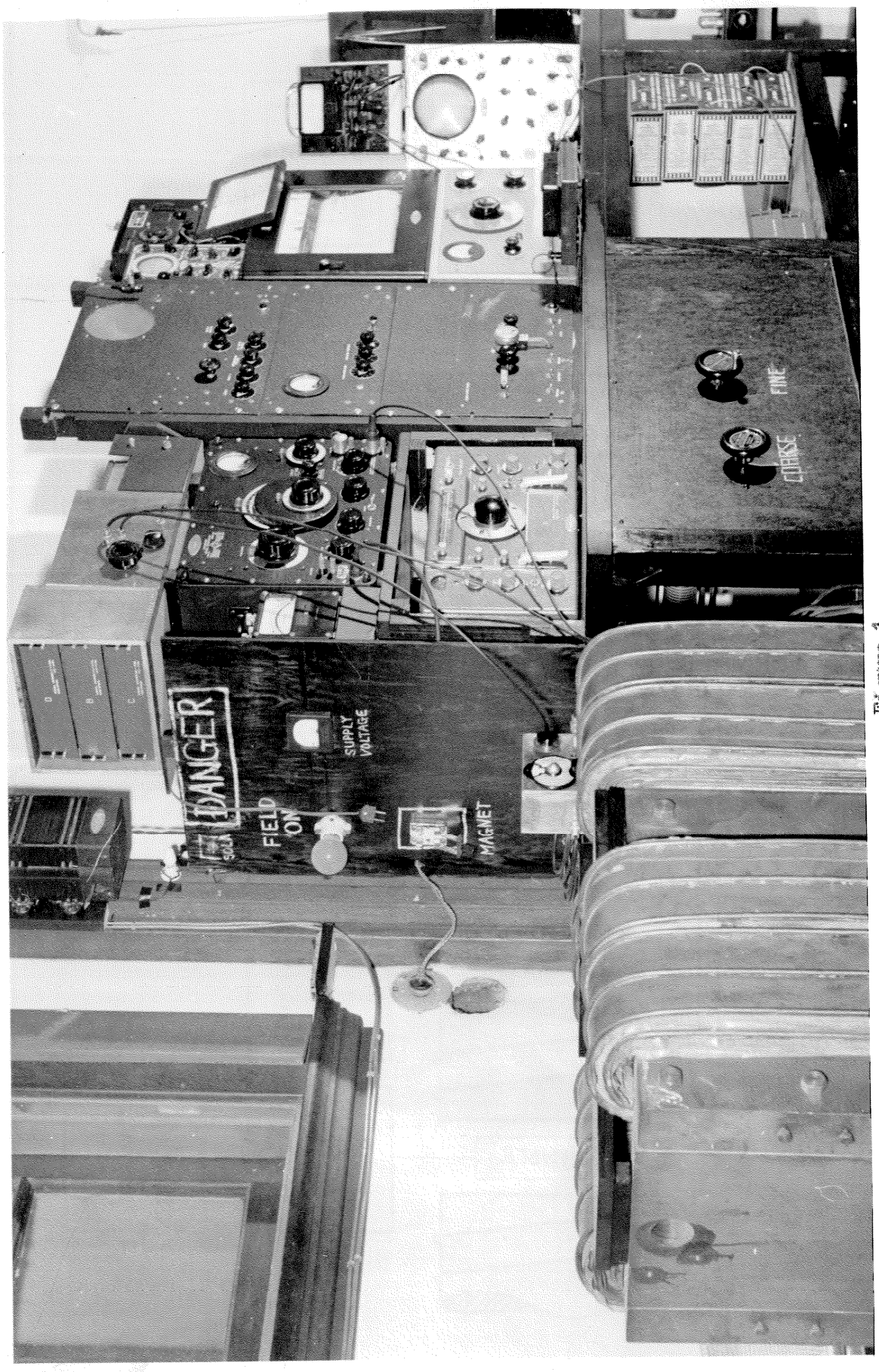

Figure 1

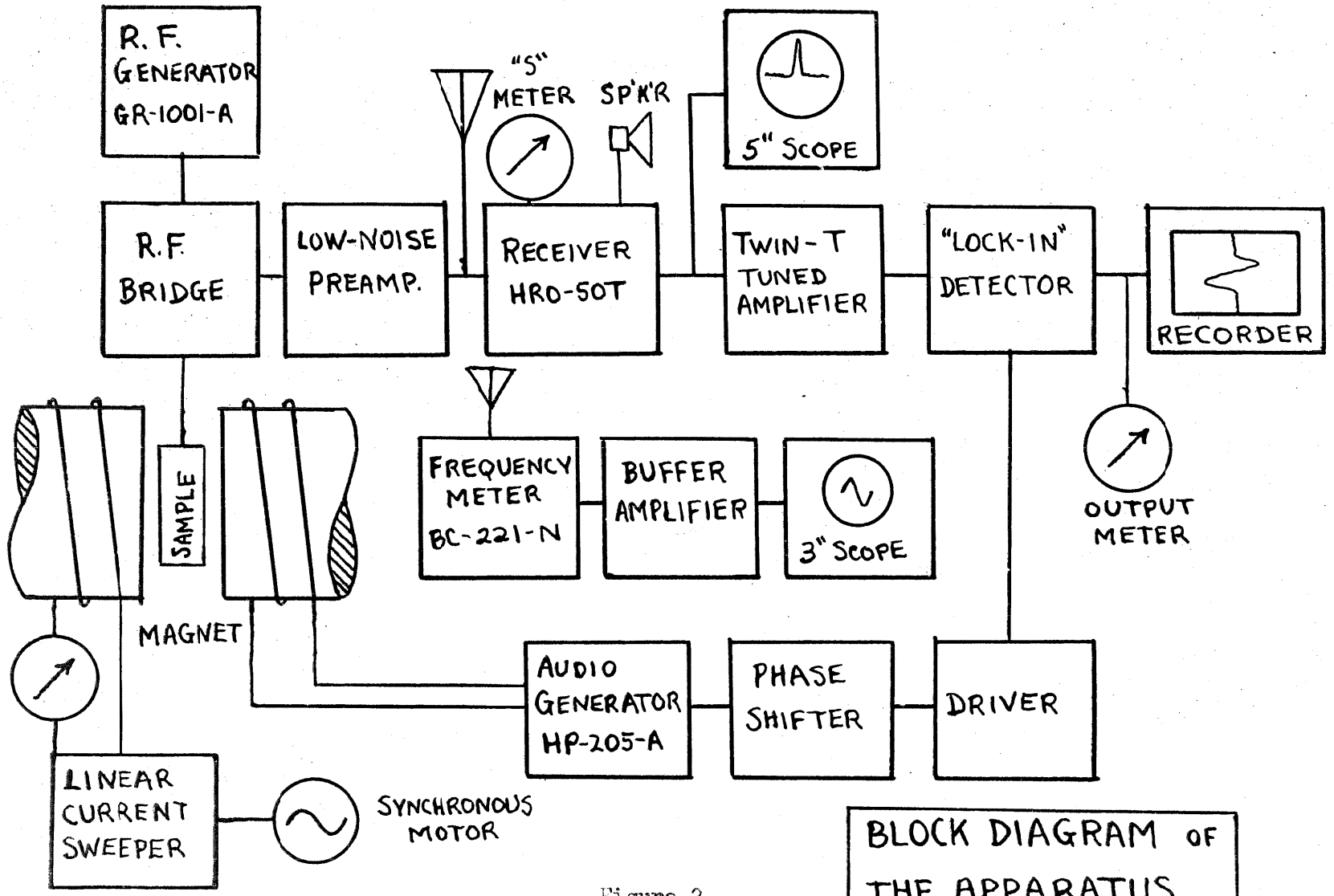

Figure 2

BLOCK DIAGRAM OF THE APPARATUS

suitable ones of Armco magnet iron, which has desirable homogeneity and saturation properties. The pole faces are six by fourteen inches in size, and are separated by a gap of 1.455 ± .001 inch. The yoke is of a rectangular shape, with its two longer sides joined centrally by the pole area, and is built of cold rolled steel. With all of the eight independent windings connected in series to give a resistance of 6.7 ohms, the field in the region of interest amounts to 460 gauss ampere^{-1}, and the magnetization curve is linear. A calibration of field versus current appears in Figure 3 page 38. At 5000 gauss, the mean inhomogeneity over areas of order 1 cm^2 is roughly ± 0.2 gauss.

Power is supplied by a bank of sixty large lead storage cells, which are normally charged continuously during use by a direct current generator, and controlled by a system of rheostats (figure 9). The power drain is ordinarily about 0.8 KW, although the magnet is designed to operate safely at a dissipation of 10 KW. The windings are interleaved and covered with copper sheets to which are soldered copper tubes carrying water for cooling purposes. In the experiments to be described, a flow of about 1 liter per minute was maintained, and no perceptible heating of water occurred.

2. Fine Adjustment and Sweeping of the Magnetic Field:

For purposes of fine control, the magnet is supplied with an auxiliary winding of 2200 turns of 28 ga. enameled copper wire,

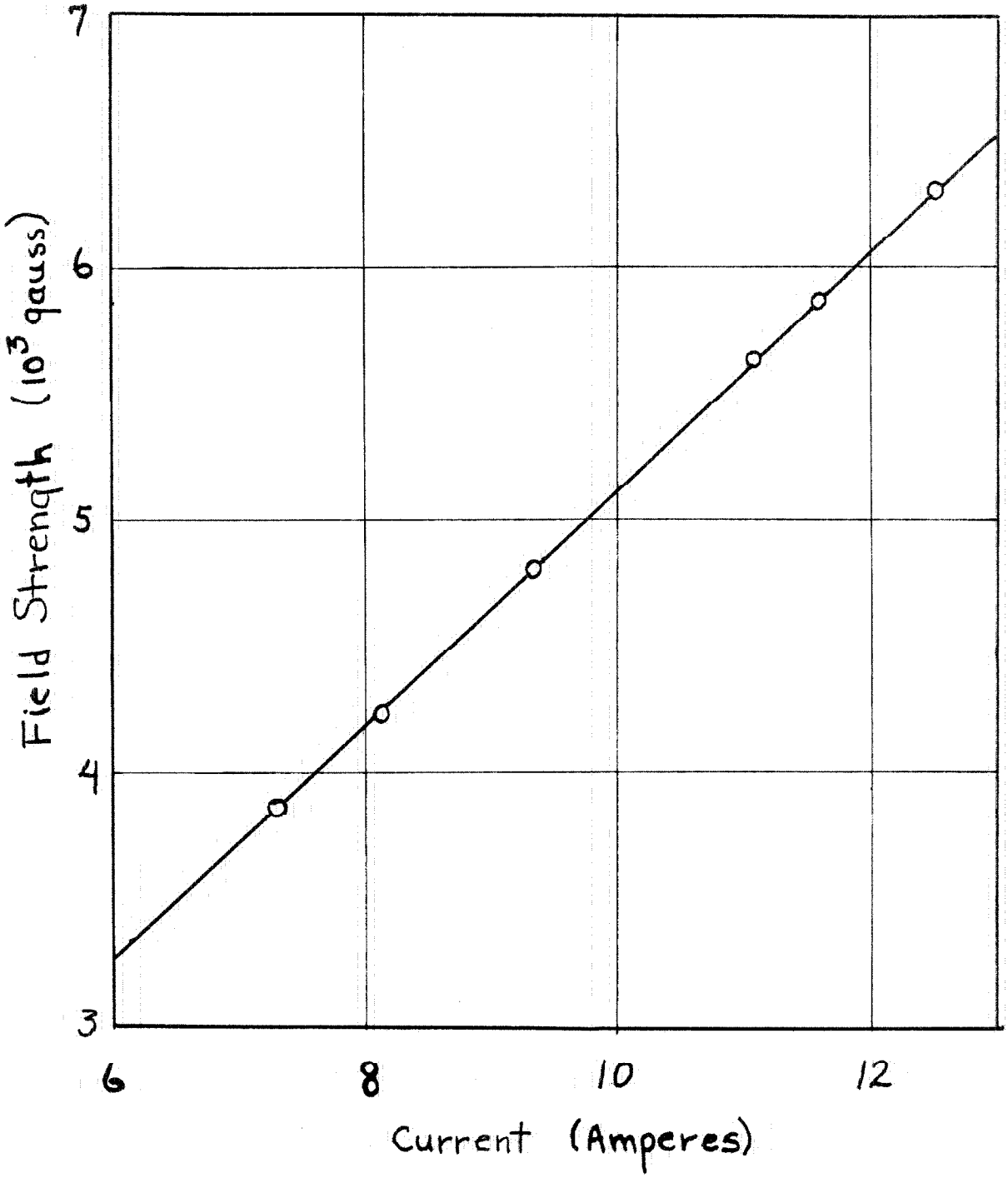

Figure 3

whose resistance is 540 ohms. It is desirable to be able to change the value of the field slowly and linearly in time, as a resonance peak is traversed. Since the magnetization curve is linear in the region of normal operation, a linear change of the current in the auxiliary winding accomplishes this end, and is obtained as follows:

The output of a specially designed current regulator[28] shown in Figure 4, page 40 is connected to the auxiliary magnet winding. In the absence of any pulses from its thyratron, the bias on the 6L6's decays through the low pass grid circuit, allowing the magnet current to increase. The bias on the thyratron simultaneously becomes less negative, until the point is reached at which this tube fires on each peak of its alternating plate voltage. The train of negative pulses which thus appears on the 6H6 cathode rebiases the 6L6 grids until the thyratron is again cut off and the same process begins again. The hunting characteristics are principally controlled by the constants of of the integrating network. The helical potentiometer is driven by a slowly geared synchronous motor, so that the controlled current changes in a linear fashion.

The sweeping system has been calibrated at total fields of zero and 5000 gauss by means of a ballistic galvanometer calibrated against both a standard permanent magnet and an effectively infinite solenoid of calculable characteristics. A calibration was also

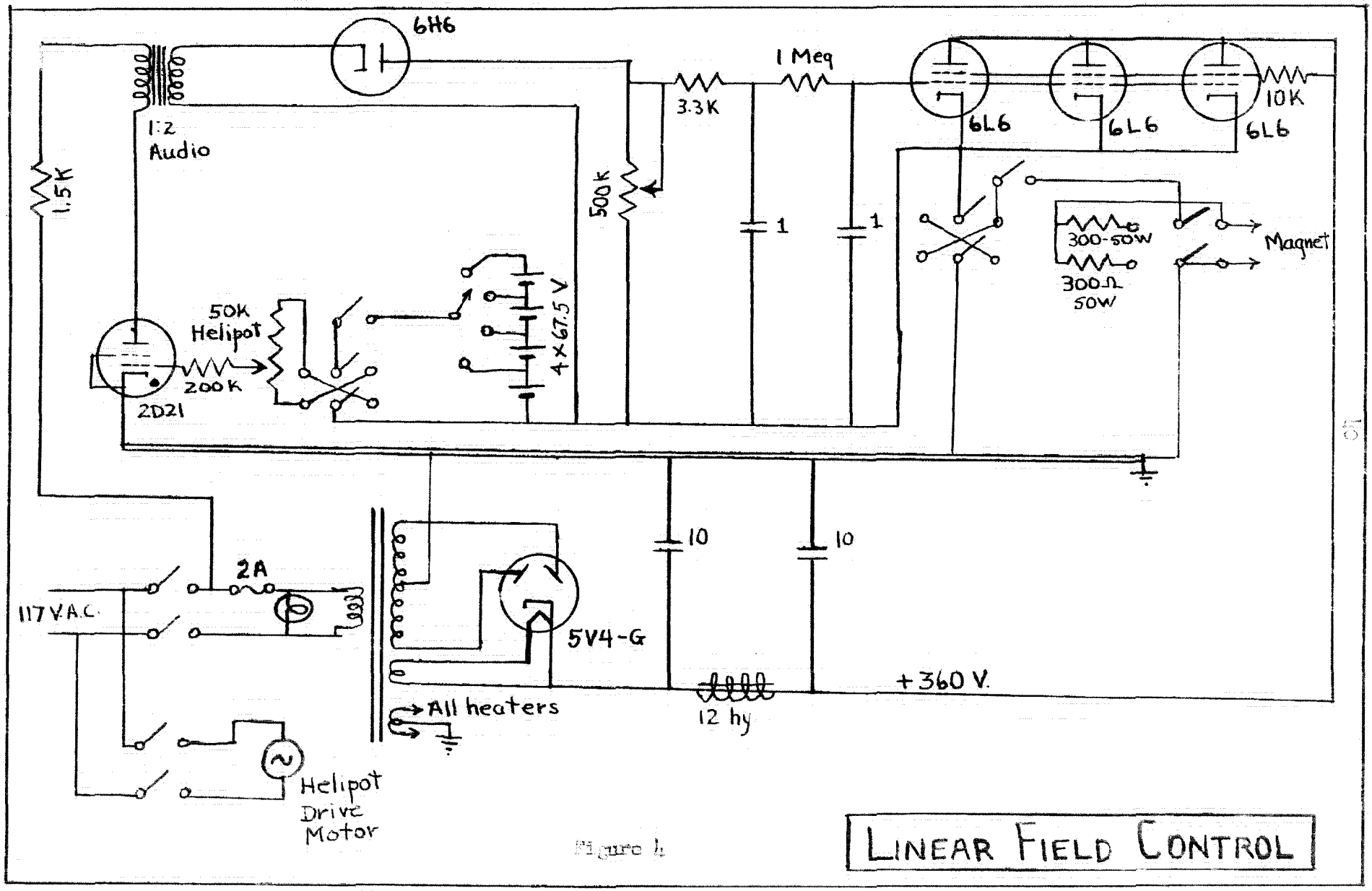

Figure 4

LINEAR FIELD CONTROL

performed with a nuclear magnetic resonance fluxmeter, constructed by Mr. F. B. Humphrey. All calibrations agreed with ± 3%, and the proton resonance data were taken as final. Provision was made for continuous monitoring of the voltage across the helical potentiometer, since aging of the batteries has a strong effect on the field calibration.

Inasmuch as line widths and fine structure splittings depend inversely on the cubes of the internuclear distances, determinations of the latter are subject only to one third as large a relative error as are the line width data themselves. The error in relative field measurements in these experiments is conservatively taken to be ± 2%.

3. Radiofrequency Power Source:

The high frequency voltage necessary to excite the sample at the Larmor frequency is obtained from an R. F. signal generator, General Radio Model 1001 - A. This unit employs a Wien bridge oscillator to provide a continuously variable output of 0 - 200 millivolts and two volts over the range 5 Kc. to 50 Mc. Most of the experiments to be described were carried out at a frequency of 18.61 Mc. from a source impedance of 50 ohms.

The frequency drift after a ten minute warm-up period is slight. Performance is rendered more stable with respect to rapid fluctuations in amplitude by the interpolation of a Sola constant voltage transformer between the signal generator and its power source.

4. Radiofrequency Bridge Detection of the Nuclear Resonance:

The output of the signal generator is loosely coupled through terminated 50 ohm coaxial lines (RG-58/U) of equal length to the inputs of two arms of a radiofrequency bridge. One arm includes a tuned parallel resonant LC circuit, whose inductance contains the sample. The coil is placed in a coaxial brass probe of low shunt capacitance, and has its axis aligned perpendicular to the external field $\vec{H}_0$. When a nuclear resonance occurs, the energy loss to the sample produces a reduction in the Q of this resonant circuit, and the bridge is consequently thrown out of balance. The Anderson bridge[29] (Figure 5, page 43) whose dummy arm contains a nonresonant T section, is easy to construct and is convenient to balance at any frequency. However it has been found to be somewhat less stable and definitely less sensitive than the Bloembergen bridge[12] (Figure 5), although with ideal components the two are electrically equivalent.[30] The Bloembergen bridge employs two arms which are electrically identical, so that the output signals are alike in amplitude and phase. They are connected to an output junction by two coaxial lines, one of which is one half wave length longer than the other at the frequency of operation. The 180° phase shift thus introduced brings about cancellation of the two signals when the bridge is completely balanced.

It is well at this point to investigate the character of the resonance signal appearing at the bridge output, and verify the

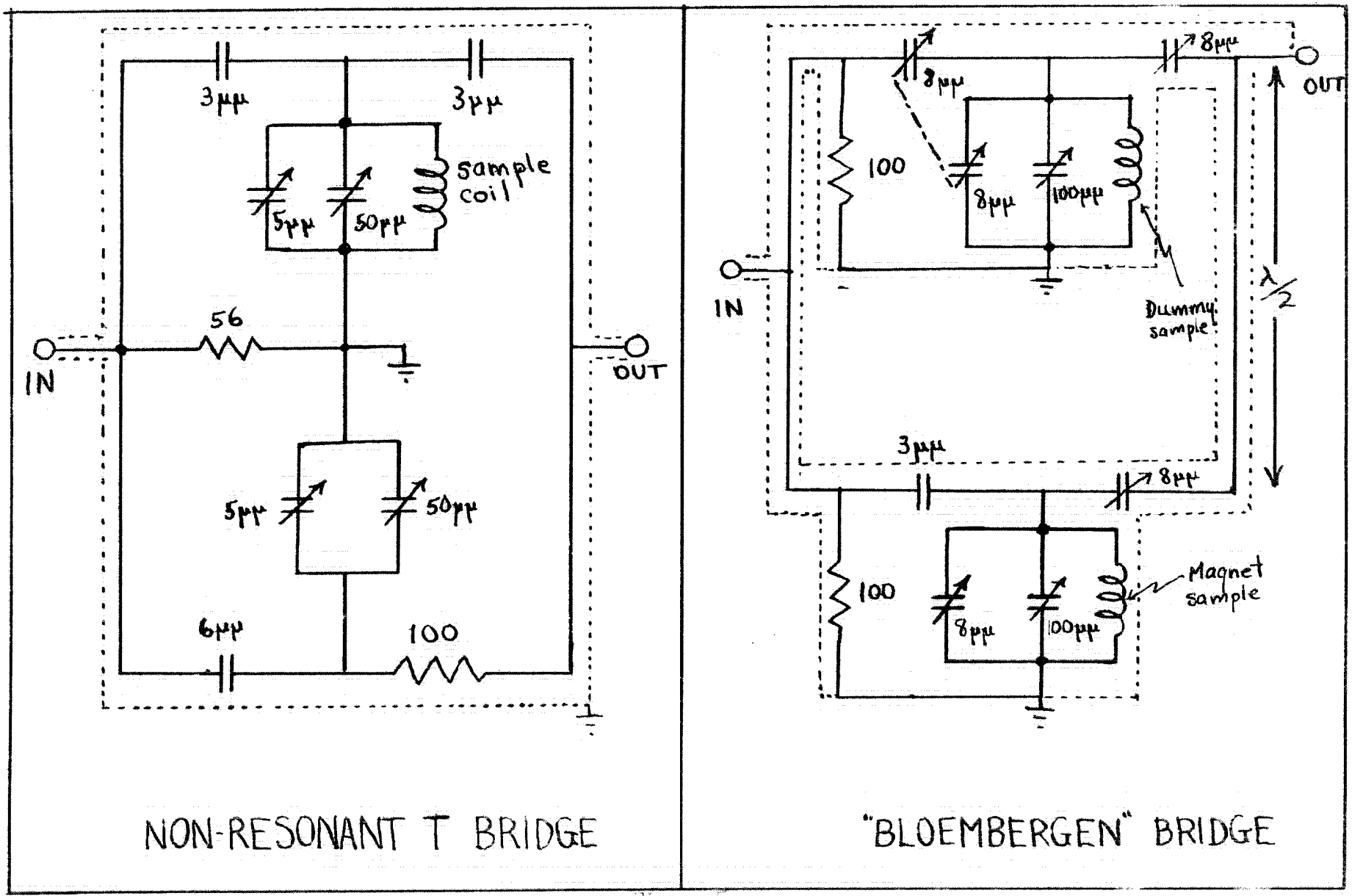
3μμ
3μμ
sample coil
5μμ
50μμ
56
IN
OUT
5μμ
50μμ
6μμ
100
NON-RESONANT T BRIDGE
8μμ
8μμ
OUT
100
8μμ
100μμ
IN
Dummy sample
λ/2
3μμ
8μμ
100
8μμ
100μμ
Magnet sample
"BLOEMBERGEN" BRIDGE

Figure 5

expectation that it should be large enough to measure experimentally. By an analysis of the tuned circuits of the Bloembergen bridge under the assumption that the generator signal is derived from a constant current source, Pake[31] finds the unbalance signal originating from the nuclear resonance to be

$$4\pi QV_0(X' \sin\theta - X'' \cos\theta).$$

Here Q is the "figure of merit" for the tuned circuit, V_0 is the amplitude of the imput voltage, and $X = X' - iX''$ is the complex nuclear magnetic susceptibility. θ is a phase parameter, adjustable by means of the trimmer condensers of figure 4b. When $\theta = 0$ or π, the bridge is unbalanced off resonance in amplitude but balanced in phase, and the output signal is proportional to the absorption.* $\theta = \pi/2$ or $3\pi/2$ is the condition for pure phase unbalance and the observation of resonant dispersion. Intermediate values of θ lead to the undesirable mixtures of absorption and dispersion, from which it is difficult to abstract any useful information. The intelligence we desire is carried by the absorption signal, which is observed directly although it could be calculated by means of the Kramers - Kronig relations[32] between the dispersion and the absorption. In order to observe the pure absorption signal, the bridge is deliberately unbalanced in amplitude, so that the resonant variations observed are to

---

* This is readily shown by calculating $\mathrm{Rl} \int \vec{M} \cdot d\vec{H}$ around a hysteresis loop.

first order those for $\theta = 0$ or π.

If the absorption is described phenomenologically in terms of its shape $f(H_0)$, taking $\int_0^\infty f(H_0)\, dH_0 = 1$, it is possible to write[12]

$$X''(H_0) = \frac{\pi H_0 X_0}{2} f(H_0) \qquad (4.1)$$

where X_0 is the static Curie susceptibility. Taking the typical numerical values

$$f(H_0)_{max} \approx \overline{\Delta H^2}^{-2}, \quad \frac{\overline{\Delta H^2}^{-2}}{H_0} \approx 10^{-2} - 10^{-5},$$

$$X_0 = 10^{-10} \text{ cgs.}$$

we have $X''_{max} = 10^{-8}$ to 10^{-5} cgs. Hence from (4.1), if $Q = 100$, $V_0 = 10^{-2}$ volt., the output signal is seen to have an amplitude of roughly 10^{-7} to 10^{-4} volt. Amplification can serve to make such a signal detectable only if it is at least of the same order of magnitude as the noise voltage contributed by the amplifiers. To a good approximation, the noise figure of the entire spectrometer is produced in the first stage of amplification, which in the present apparatus has a noise figure of about 4 db. The noise voltage at the preamplifier input is given by

$$N = \sqrt{kTBFR} \qquad (4.2)$$

where B is the bandwidth of the system in sec^{-1}, F is the noise figure, and R is the equivalent source resistance. In the spectrometer here described, the bandwidth is ordinarily taken to be about 5 c.p.s., and R is roughly 100 ohms. At room temperature, then, the noise voltage at the bridge output junction is on the order of 10^{-8} volt. Thus the theoretical peak signal to noise ratio is expected to be in the range 10 to 10^4. These orders of magnitude are corroborated experimentally.

It is worth noting that the signal to noise ratio may be improved by cooling the bridge or by narrowing the bandwidth. The former is found ordinarily to introduce greater difficulties than it cures, owing to the establishment of fluctuating temperature gradients and concomitant balance instability. Any decrease in the bandwidth increases the time required to make a measurement. In summary, it then appears that noise is often a difficult, but usually not an insuperable, problem.

5. Audiofrequency Field Modulation:

In principle, one could trace out the shape of an absorption line simply by measuring the amplitude of the amplified bridge output at a number of values of H_0 for a given excitation frequency. However, the small size of the resonant variation compared with the total unbalance signal and the slow drifts inherent in the apparatus make this an impractical procedure.

Furthermore, it is desirable to detect the envelope of the radio-frequency carrier at as early a stage as possible, and it would be difficult to avoid instability in the DC amplification which would then become necessary.

A satisfactory solution of these difficulties is found in a technique analogous to the use of a beam chopper in optical spectroscopy, or Stark modulation in microwave spectroscopy. The magnetic field H_0 is modulated sinusoidally at a low frequency ω_m over a small region about a point at which we desire to know the absorption. If this point lies somewhere on an absorption line, the absorption becomes periodic with repetition rate $\omega_m/2\pi$ sec^{-1}. Thus we may regard the shape function $f(H_0)$ as a modulation on the sinusoid at ω_m which in turn modulates the radiofrequency carrier. Upon demodulation of the latter, there results an alternating signal of period $2\pi / \omega_m$ which may then be amplified by ordinary, stable, resistance coupled amplifiers. The amplitude of this signal depends upon the absorption.

An advantage of this procedure will be evident in the fact that, since the field modulation presumably does nothing except to introduce a periodic perturbation on the nuclear Zeeman levels, any signal observed at the proper repetition rate must have its origin in the nuclear absorption and not in noise sources in the remainder of the apparatus. (This is true so long

as there is no pickup of the modulation voltage in the equipment.)

The maximum potentialities of the modulation method can be realized only if means are available for rejection of all signals except those produced by the modulation. A later section describes a satisfactory way to approximate this behavior.

In the present apparatus, the modulation is produced by an auxiliary magnet winding of 600 turns, excited by an audio-frequency signal generator, (Hewlett Packard 205A). The more easily available 60 cycle modulation which could be obtained directly from the power lines is avoided to obviate difficulty with the pickup of that frequency which is certain to be present in many parts of the apparatus.

The amplitude of the modulation has been determined by measuring the alternating voltage induced in an air core solenoid placed in the magnet gap. The solenoid was calibrated similarly in a larger solenoid of effectively infinite length and presumably calculable characteristics. The maximum amplitude available at a total field of 5000 gauss is about 3 gauss, which is more than sufficient for the experiments to be described.

6. Low Noise Preamplifier:

The bridge output is matched through a 50 ohm coaxial line into a specially designed cascode wide - band amplifier, (figure 6)

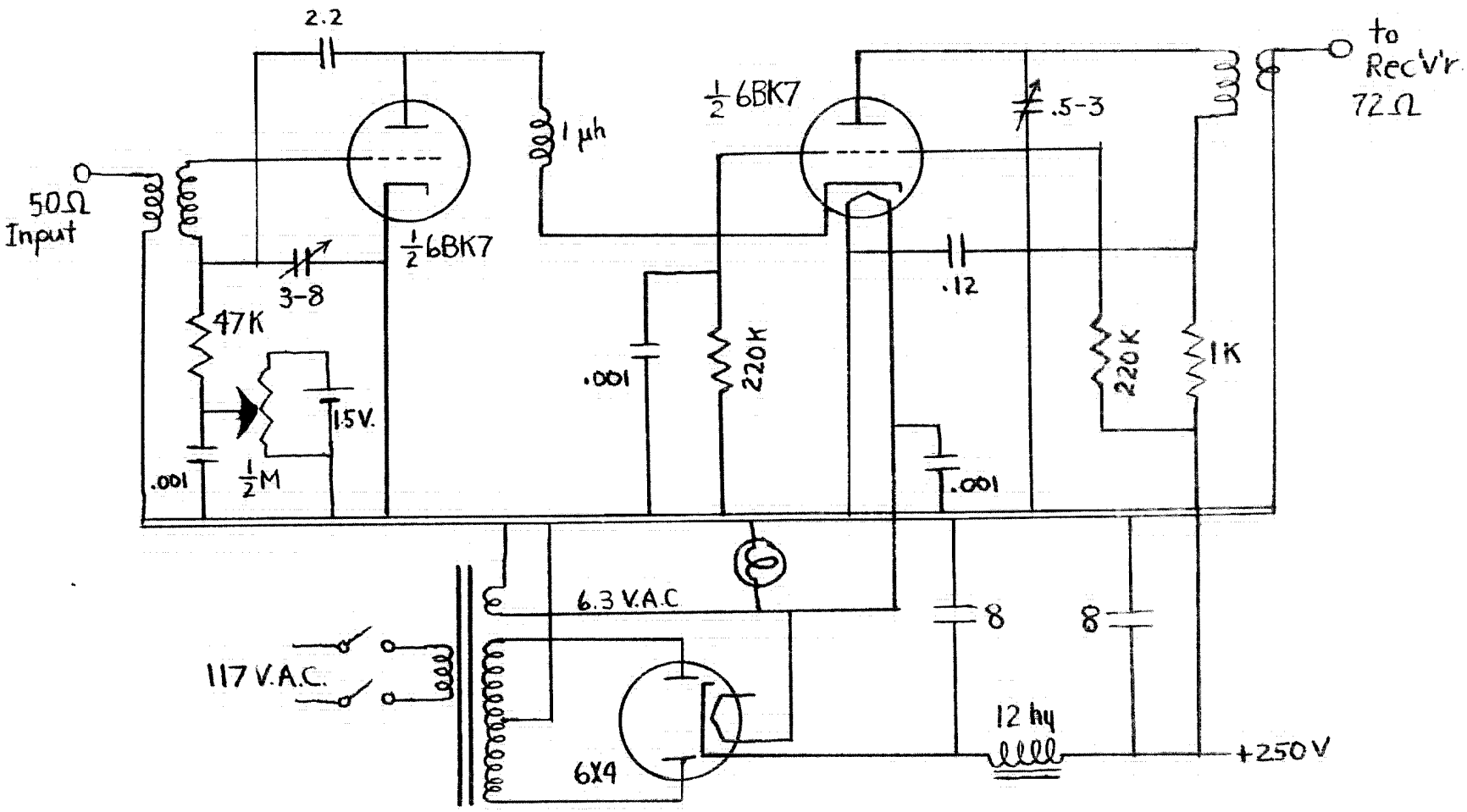

Low-Noise R.F. Preamplifier

Figure 6

This circuit is a modification of a television tuner manufactured by the Standard Coil Products Co., Inc. Its R.F. transformers are mounted in a rotatable turret, permitting convenient switching from one 4 Mc. - wideband to another. The preamplifier has a noise figure of ca. 4 db., or about 10 db. less than does the subsequent part of the apparatus. This circumstance makes possible the observation of signals roughly three times weaker than could be detected without it.

7. The Receiver:

The output of the preamplifier is introduced through an unbalanced 72 ohm coaxial line to a communications receiver, National Co. Model HRO 50 - T. Here it is amplified and detected, and its audiofrequency envelope appears at the speaker terminals. Interchangeable coil sets are used to obtain a tuning range of 450 Kc. to 30 Mc. While the local oscillator is already both voltage - regulated and temperature compensated, more stable and quieter operation is obtained by using as a power source the same Sola transformer that supplies the signal generator. Maximum stability is obtained using the automatic volume control and a total signal level sufficient to drive the intermediate frequency stages to the edge of the remote cutoff region. An automatic noise limiter is available, but its use brings about no improvement.

By this time it is obvious that it is far more convenient to traverse an absorption by varying the external field at fixed frequency, than to use the opposite alternative. Any change in frequency involves retuning both the signal generator and the receiver, and requires rebalancing the bridge. In addition, any large changes in frequency require the replacement of the bridge's half wave line. The circuitry is found, on the other hand, to be remarkably insensitive to even large changes in the magnetic field.

8. Oscilloscope Presentation:

The output of the receiver may be connected to the vertical deflection plates of 5" oscilloscope (Dumont # 281). If a sample of the modulating voltage is than put on the horizontal plates, the result is a linear plot of absorption versus field strength, over the range covered by the modulation. This method of observation is particularly suited to the strong, sharp resonances characteristic of liquids and gases. In such cases the modulation is ordinarily taken to be a few times the line width, and a direct comparison between the two is possible. Under conditions such that the line width is determined solely by the field inhomogeneity, it is therefore possible to obtain an accurate estimate of the latter (see § 1).

9. Selective Audiofrequency Amplification of the Resonance Signal:

As mentioned in § 5, it is desirable to detect only the part of the total available signal which has its origin in the Zeeman modulation of the spin energy levels. It is possible to show, by means of a Taylor expansion, that if the amplitude of the modulation signal is much less than the characteristic width of the absorption peak, the Fourier component at ω_m has an amplitude proportional to $d/dH_0 \left[f(H_0) \right]$. Even when the modulation amplitude is of the same order of magnitude as the line width, a surprisingly faithful reproduction of the first derivative is obtained. Thus, if the audio system is given a very narrow bandpass, the derivative signal will be obtained, and yet all of the random noise will be eliminated except for the small amount residing in the passband.

In the present spectrometer an extremely narrow bandwidth is obtainable by use of a "lock - in" detector, shown in figure 7, page 53. In this device the input signal is put onto the control grid of a mixer tube, whose suppressor grid is driven by a sinusoidal reference signal.

Let us designate the frequency of a Fourier component of the input signal by ω_s. When this signal is mixed with a sinusoidal signal of angular frequency ω_m, the plate voltage of the mixer stage contains components at ω_s, ω_m and $\omega_s \pm \omega_m$. If, now, the plate circuit is provided with a low pass filter network,

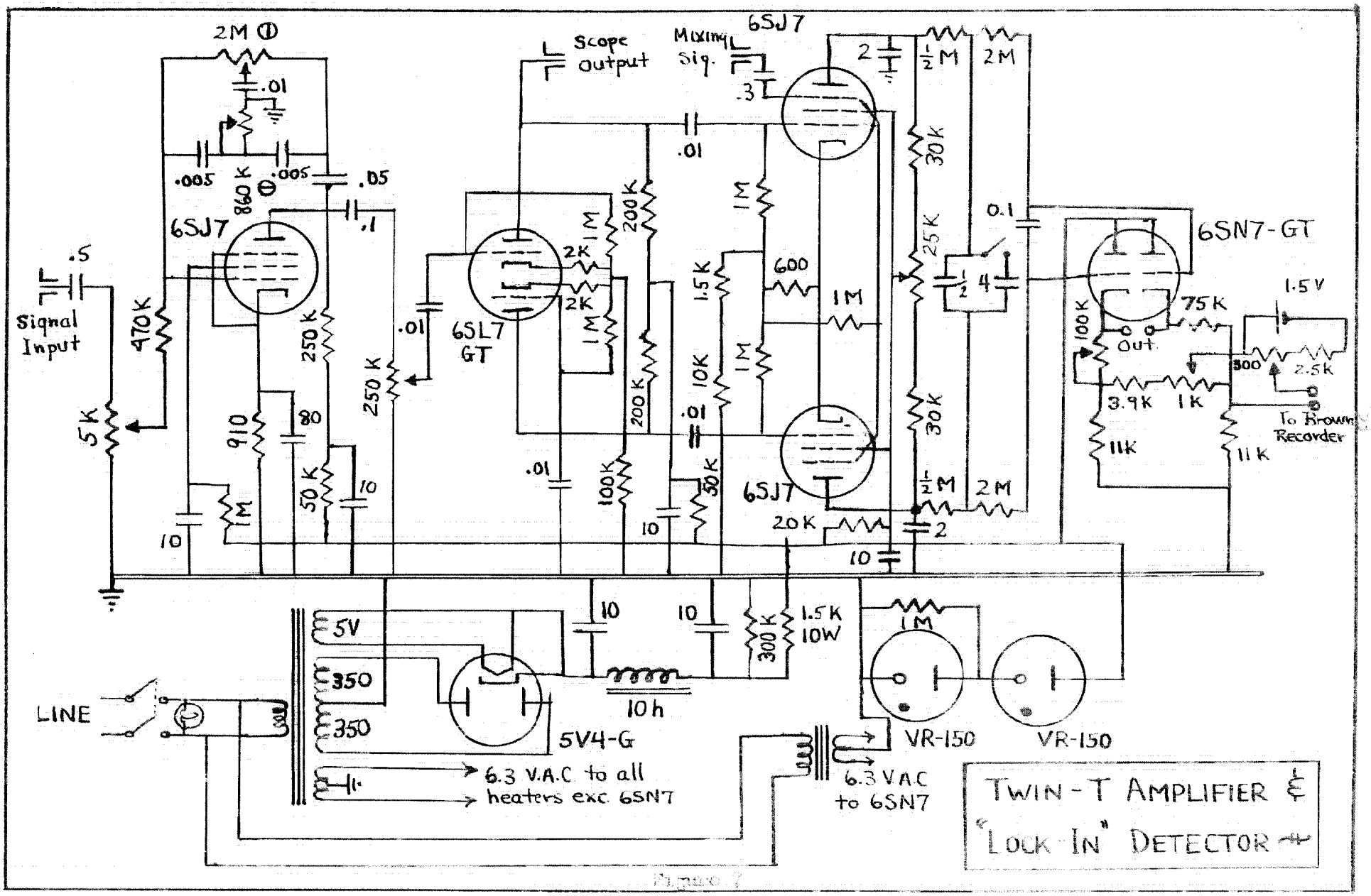
2M
.01
.005
860 K
.005
.05
.1
6SJ7
.5
Signal Input
470K
5K
250 K
910
80
50 K
10
1M
10
250 K
.01
6SL7 GT
Scope output
Mixing Sig.
6SJ7
.3
.01
2K
2K
1M
200K
1M
200 K
.01
100K
10
1.5K
10K
1M
1M
600
1M
.01
30K
10
2
1/2 M
2M
30K
25K
1/2 M
2M
20K
2
10
0.1
1/2 4
6SN7-GT
1.5 V
75K
100 K
Out
300
2.5K
3.9K
1K
11K
11K
To Brown Recorder
5V
350
350
5V4-G
10
10
10 h
300K
1.5K 10W
1M
VR-150
VR-150
LINE
6.3 V.A.C to all heaters exc. 6SN7
6.3 VAC to 6SN7
TWIN-T AMPLIFIER & "LOCK-IN" DETECTOR

all components will be rejected except $\omega_s - \omega_m$ when $\omega_s \approx \omega_m$. If $\omega_s = \omega_m$, a D.C. output is obtained whose amplitude depends on the phase between ω_s and ω_m. (For this reason the device is often called a phase sensitive detector.) By using a filter with a sufficiently long time constant, the bandwidth of the amplifier may thus be reduced to as small a range as desired about a center at ω_m. In the present unit, by use of a triple pi - section RC network, the 10 db. bandwidth may be reduced to a measured value of about $\pm$ 0.1 sec^{-1}. Care must be taken that the bandwidth is kept wide enough to avoid distortion of the resonance signal as the field is slowly swept through an absorption line. Also with a narrow bandpass, the magnet modulation and the lock - in mixing signal must be maintained carefully at the same frequency, and in the same phase relationship. The most convenient method of accomplishing this is to derive both signals from the same signal generator.

The lock - in signal is amplified by the driver shown in figure 8, page 55. Since maximum D.C. output of the detector occurs when the grid and suppressor signals are in phase, a 180° constant amplitude phase shifter is incorporated. Thus a compensation is possible for the various phase shifts occurring throughout the chain of apparatus between the signal generator and the control grid of the phase sensitive detector.

In the present equipment, the detector is preceded by a

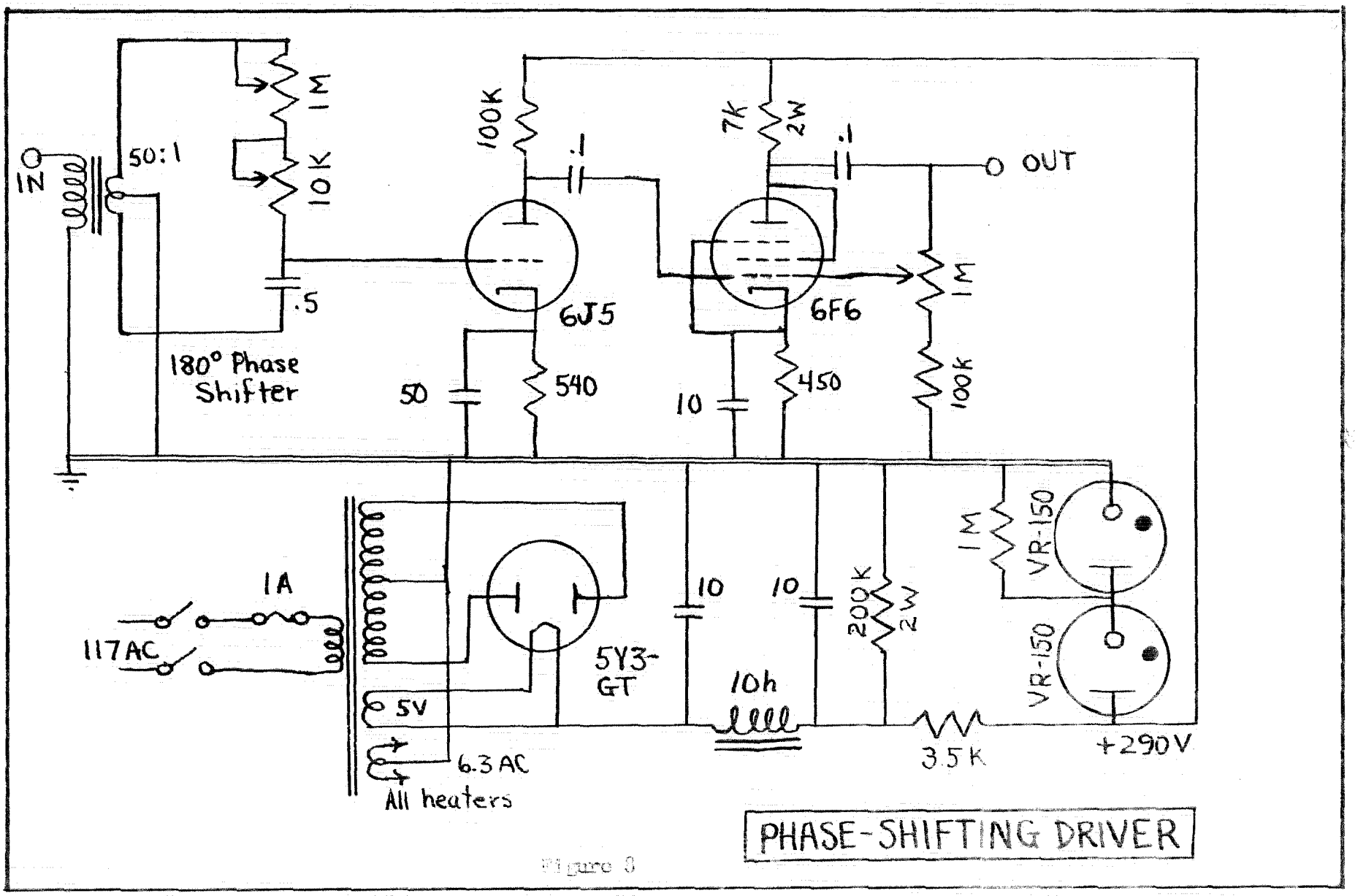
IN
50:1
1M
10K
.5
180° Phase
Shifter
100K
.1
6J5
50
540
7K
2W
.1
OUT
6F6
1M
100K
10
450
1A
117AC
5V
6.3 AC
All heaters
5Y3-
GT
10
10
10h
200K
2W
1M
VR-150
VR-150
3.5K
+290V
PHASE-SHIFTING DRIVER

Figure 3

stage of amplification which incorporates inverse feedback through a twin - T rejection network tuned at the modulation frequency.[34] This stage has a 10 db. bandwidth of approximately 10 sec^{-1} centered at ω_m. Its function is to prevent overloading of the lock - in stage by 60 c.p.s. hum pickup and high frequency random noise fluctuations.

10. Recording Meter Presentation:

The D.C. output of the lock-in detector is directly coupled into a differential cathode follower, thus providing an output of low impedance. A voltage divider is employed to divert a part of this signal into a Brown recording potentiometer with full scale sensitivity of 0.01 volt. As the modulated field is slowly swept through a resonance, the derivative of the absorption peak is thusplotted on the chart. Experiments have been made to insure that the signal thus obtained is directly proportional to the bridge signal over the entire scale. The running axis of the chart is linear in the field strength, by virtue of the use of the linear current regulator described in § 2.

11. Frequency Measurement:

For the accurate determination of the positions of resonance lines and the measurement of magnetic fields, it is necessary to have a means for precise measurement of frequency. While this

necessity does not exist in the case of line shape determinations, it was nevertheless felt desirable to increase the versatility of the spectrometer by installing provisions for such measurements. A surplus Signal Corps frequency meter, BC 221 - N has been modified by Mr. F. B. Humphrey by insertion of a buffer amplifier input to prevent loading of the oscillator. Its output is connected to the vertical amplifier of a three inch cathode ray oscilloscope, (Triumph Model 830). The frequency meter dial is set to zero beat with the input signal, and the frequency read directly from the dial to five significant figures. By allowing the frequency meter to radiate into a receiver tuned to National Bureau of Standards Station WWV, the meter calibration may be checked whenever desired at frequencies of 2.5, 5, 10, 15, 20 and 25 Mc./sec.

12. Operation of the Spectrometer:

The signal generator is first connected as shown in figure 9A, page 58. Using the 2 volt output, it is tuned until a minimum galvanometer deflection is obtained, indicating the frequency for which the line L is one half wave length long. The signal generator is now turned down to an output level of 10 to 100 millivolts and connected through one bridge arm at a time to the receiver. The main bridge tuning condensers are tuned to give a maximum reading of the "S" meter, indicating resonance of the tuned circuits.

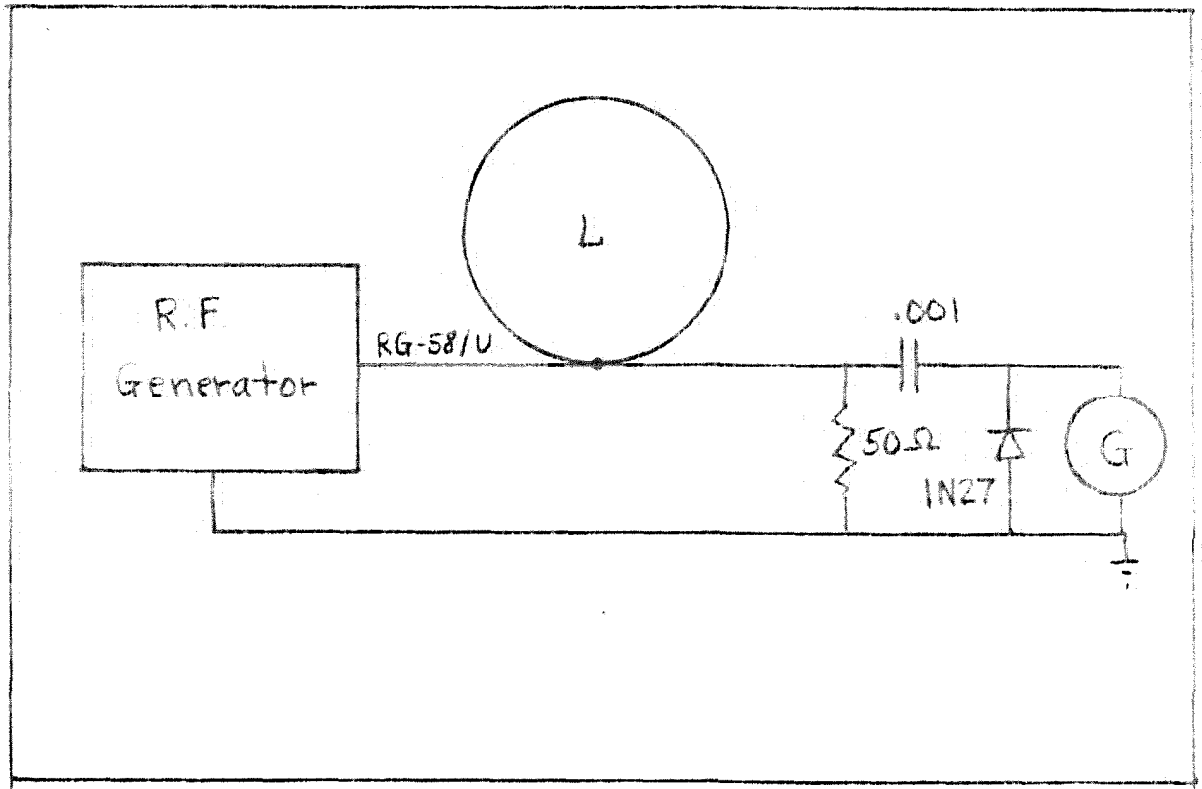

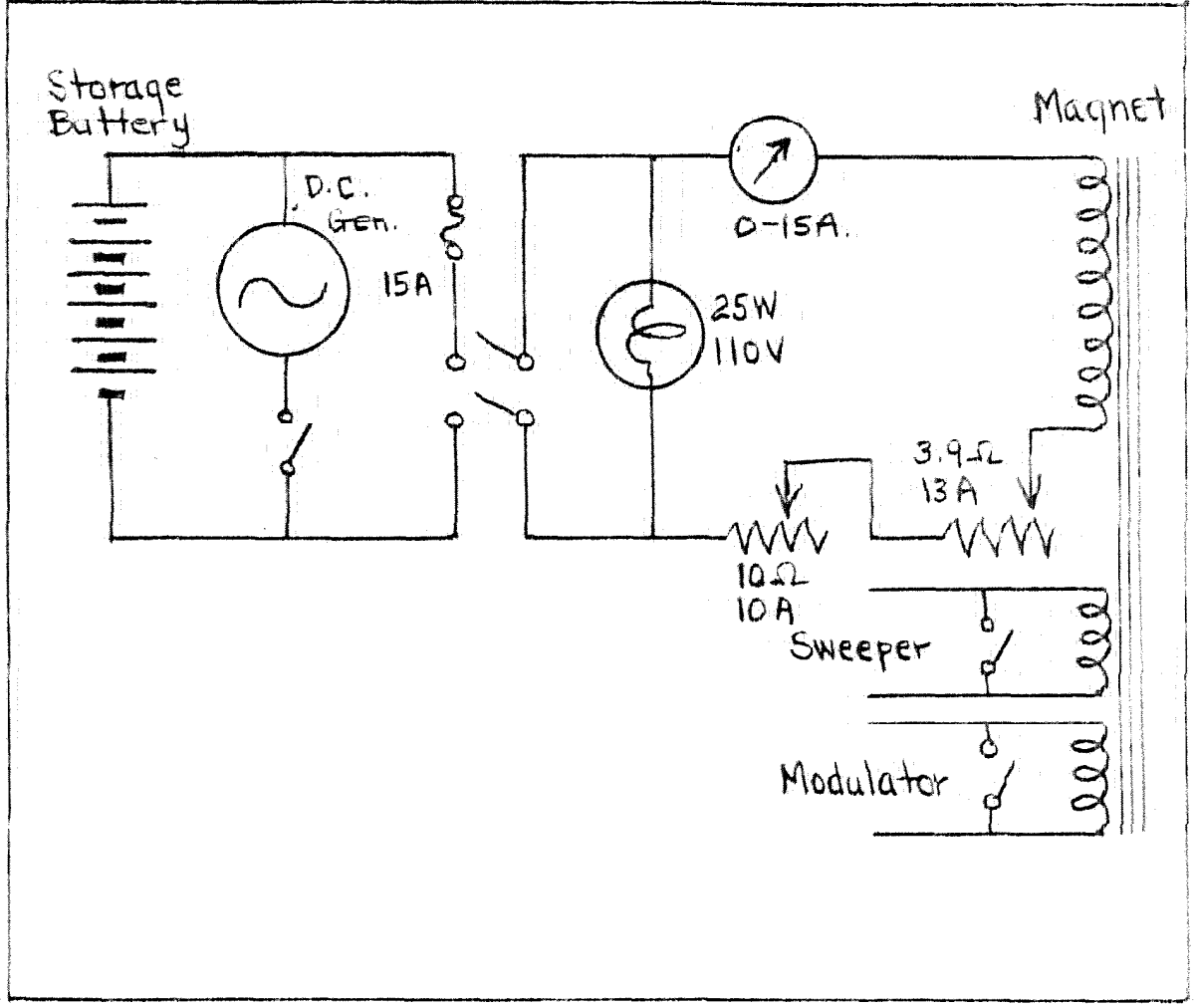

Figures 9A and 9B

The entire bridge is now put into the circuit, and the fine tuning controls adjusted alternately until a minimum reading of the "S" meter is obtained. Then the fine control on the dummy arm of the bridge is deliberately detuned to obtain a considerable amplitude unbalance. (The two fine controls give substantially independent control over amplitude and phase.) The "S" meter should now indicate stable balance roughly 30 to 50 db. below the signal generator output.

With the R.F. gain control set for a reading of about S9, the audio system gain is increased to the point where random noise becomes evident above the hum pickup on the oscilloscope. The magnetic field is slowly varied by means of the main rheostat system (figure 9B) until a sudden deflection is noted on the Brown recorder. With the field set at a value slightly above or below this point, the linear current regulator is now started and allowed to sweep the field through the region of interest. If an absorption is actually present, it will be mapped out on the Brown recorder. The system gain is then adjusted to give a convenient deflection, and the line is traversed slowly and repeatedly in both directions until sufficient data have been obtained.

Throughout this process the receiver tuning changes slowly, and the bridge gradually drifts out of balance. Continual adjustment of the controls thus becomes necessary if an optimum

signal is to be obtained. The appearance of asymmetry in the recorded line shape derivative is a symptom of large phase unbalance, and requires complete rebalancing of the bridge.

A provision is made for connection of the vertical amplifier of the five inch oscilloscope to one of the plates of the phase inverter which follows the twin - T tuned amplifier. If the oscilloscope is synchronized with a signal taken from the field modulation supply, passage through a strong resonance produces a characteristic sine wave pattern, which reverses sharply in phase as the peak of the resonance is passed. Even in cases where the signal is too weak to make this detection possible, the arrangement is a convenient one for continuous monitoring of the system gain by observation of the noise level.

To avoid distortion of the line shapes it is advantageous to use the smallest field modulation consistent with adequate signal strength. Furthermore, some adjustment of the R.F. level at the signal generator is necessary to obtain a large signal without saturation and consequent broadening of the absorption.

In the case of strong resonances it is sometimes found that the necessary data can be gathered more rapidly if the output of the lock - in detector is read on a vacuum - tube voltmeter rather than on the Brown recorder. Under these circumstances the field is changed in discontinuous steps, and the average

reading of the output meter determined at each point. Care must be taken in either case that no drifting of the main field occurs during the time taken to trace out an absorption line. Since the only drift of the field is downward, this may safely be assumed to be the case if lines taken by traversing the absorption in both directions have the same width.

In turning the main field on and off, the two auxiliary windings should be short circuited to avoid breakdown of the insulation by the high surge voltages produced as the field collapses. The main magnet windings are protected somewhat in this way by a 25 watt, 100 volt light bulb which is connected across the power line.

III. FINE STRUCTURE FOR ABSORPTION BY A THREE - SPIN SYSTEM.

The bifluoride ion, which will be discussed in detail in next section, is an example of a collinear three - spin system of the type B - A - B. It is expected, for reasons to be mentioned later, that the resonance absorption of this ion corresponds to the special case in which the two A - B separations are the same. However it is of some interest to develop the more general case of a collinear system of either of the types B - A - B or B - B - A, in which the separations are all independent and may take on any values whatever.* Limiting cases of the results will be found to give the absorption for two simpler systems which have been studied by other investigators.

1. The Energy Levels:

It is convenient to write the secular part of the Hamiltonian (7.5) of Part I in the form

$$\mathcal{H} = \sum_{i<j}\sum \frac{g_i g_j \beta^2}{8 r_{ij}^3} \left(\vec{\sigma}_i \cdot \vec{\sigma}_j - 3\sigma_{iz}\sigma_{jz} \right)\left(3\cos^2\theta_{ij} - 1\right) \tag{1.1}$$

Taking into account the collinearity of the spin system of

---

* The somewhat fatuous restriction must be made that the internuclear distances must be much smaller than the wave length of the absorbed radiation. The latter is ordinarily on the order of 10 meters.

interest, and the fact that the A - B interactions involve only σ_z terms, this becomes:

$$\mathcal{H} = a\sigma_{1z}\sigma_{2z} + c\sigma_{1z}\sigma_{3z} + b(\sigma_{2x}\sigma_{3x} + \sigma_{2y}\sigma_{3y} - 2\sigma_{2z}\sigma_{3z}) \tag{1.2}$$

where

$$a = \frac{-g_A g_B \beta^2}{4r_{AB}^{(1)\,3}} P_2(\cos\theta) \qquad c = \frac{-g_A g_B \beta^2}{4r_{AB}^{(2)\,3}} P_2(\cos\theta)$$

$$b = \frac{g_B^2 \beta^2}{8r_{BB}^{2}} P_2(\cos\theta). \tag{1.3}$$

θ is the angle between the system axis and the external field, and the operators are labelled in such a way that 1 refers to nucleus A and 2 and 3 refer to nuclei of type B. It is assumed that none of the nuclei possess higher multipole moments, and that the substance in which they reside is electronically diamagnetic.

It is convenient in calculating the energy levels to use as unperturbed stationary states the simple product wave functions

$$\begin{aligned} |1\rangle &= (+++) & |5\rangle &= (+--) \\ |2\rangle &= (++-) & |6\rangle &= (-+-) \\ |3\rangle &= (+-+) & |7\rangle &= (--+) \\ |4\rangle &= (-++) & |8\rangle &= (---). \end{aligned} \tag{1.4}$$

in which

$$(+) = \begin{pmatrix} 1 \\ 0 \end{pmatrix} \qquad (-) = \begin{pmatrix} 0 \\ 1 \end{pmatrix}.$$

The first symbol in each function corresponds to nucleus A, and the others to B_1 and B_2, the two other nuclei in the system. This representation is not diagonal under the perturbation (1.2), and the Hamiltonian matrix is:

$$\mathcal{H} = \begin{pmatrix} a+c-2b & & & & & & & \\ & a-c+2b & 2b & & & & 0 & \\ & 2b & -a+c+2b & & & & & \\ & & & -a-c-2b & & & & \\ & & & & -a-c-2b & & & \\ & & & & & -a+c+2b & 2b & \\ & 0 & & & & 2b & a-c+2b & \\ & & & & & & & a+c-2b \end{pmatrix} \tag{1.5}$$

The roots of the secular equation are

$$\begin{aligned} E_{11} &= a + c - 2b & E_{55} &= -a - c - 2b \\ E_{22} &= 2b + \sqrt{4b^2 + (a-c)^2} & E_{66} &= 2b + \sqrt{4b^2 + (a-c)^2} \\ E_{33} &= 2b - \sqrt{4b^2 + (a-c)^2} & E_{77} &= 2b - \sqrt{4b^2 + (a-c)^2} \\ E_{44} &= -a - c - 2b & E_{88} &= a + c - 2b \end{aligned} \tag{1.6}$$

The chosen system of quantization is diagonal with respect to the Zeeman energies of the uncoupled spins, which are found to be

$$W_1 = A + 2B \qquad W_5 = A - 2B$$
$$W_2 = A \qquad W_6 = -A$$
$$W_3 = A \qquad W_7 = -A$$
$$W_4 = -A + 2B \qquad W_8 = -A - 2B \qquad (1.7)$$

where

$$A = \frac{1}{2} g_A \beta H_0 ; \qquad B = \frac{1}{2} g_B \beta H_0 . \qquad (1.8)$$

Combining the Zeeman and dipolar energies, the perturbed energy levels are those shown in Figure 10, page 66.

2. Selection Rules and Intensities:

The intensities for magnetic dipole absorption are proportional to the squares of the matrix elements of the properly rotating components of magnetic moment between the states of interest. To calculate these, it is convenient to use a representation in which the dipolar perturbation is diagonal. By calculating the unitary transformation which diagonalizes (1.2), we find that the states in which the spins of type B are antiparallel are mixed to give

$$|2\rangle' = (R^2 + 1)^{-1/2} \left[(++-) + R(+-+) \right]$$
$$|3\rangle' = (R^2 + 1)^{-1/2} \left[R(++-) - (+-+) \right]$$
$$|6\rangle' = (R^2 + 1)^{-1/2} \left[R(-+-) + (--+) \right]$$
$$|7\rangle' = (R^2 + 1)^{-1/2} \left[(-+-) - R(--+) \right] . \qquad (2.1)$$

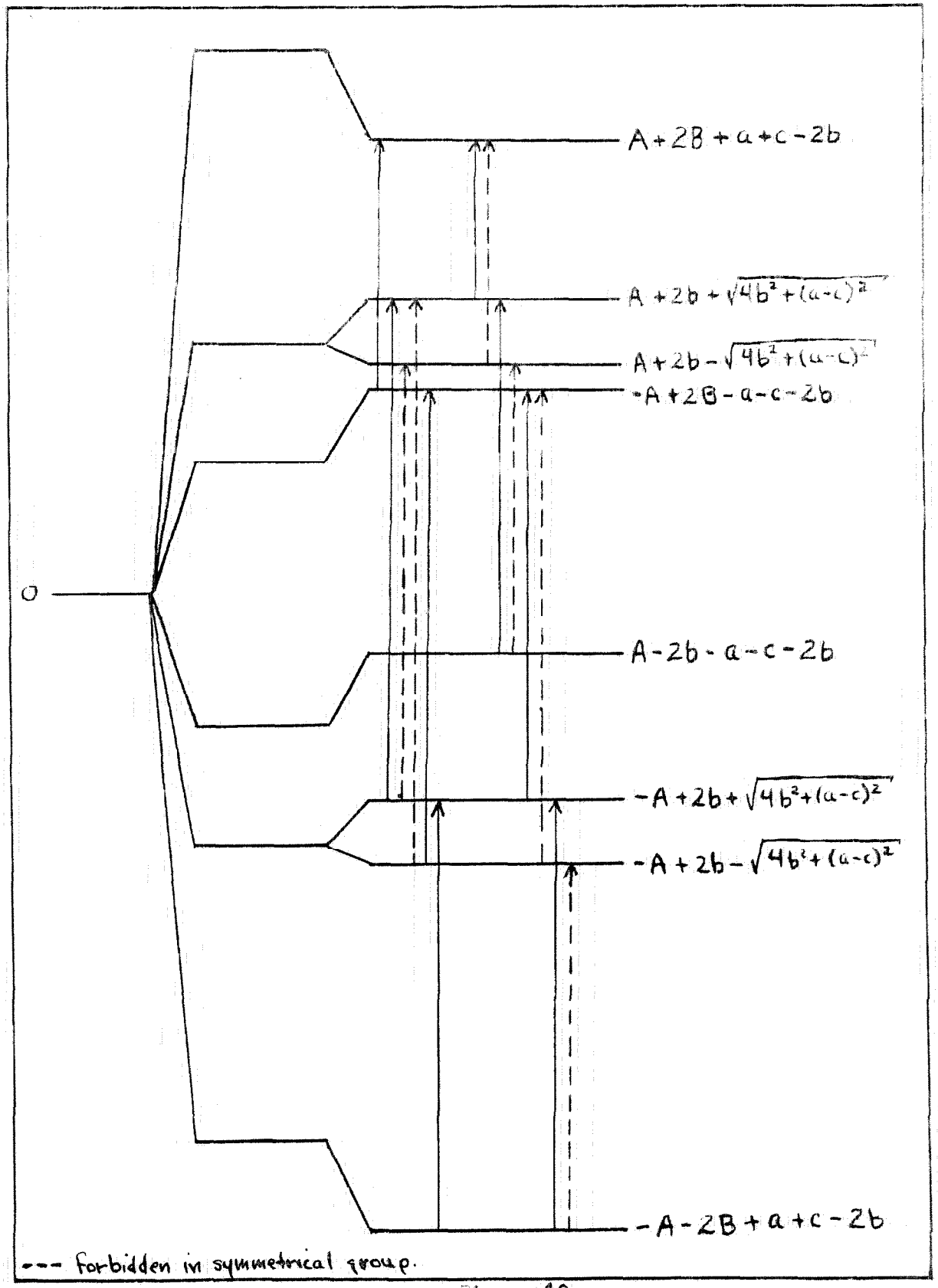
A+2B+a+c-2b
A+2b+√(4b²+(a-c)²)
A+2b-√(4b²+(a-c)²)
-A+2B-a-c-2b
0
A-2b-a-c-2b
-A+2b+√(4b²+(a-c)²)
-A+2b-√(4b²+(a-c)²)
-A-2B+a+c-2b
--- forbidden in symmetrical group.

Figure 10

where

$$R = \frac{\sqrt{4b^2 + (a - c)^2} - a + c}{2b} \qquad (2.2)$$

These, together with the states $|1\rangle$, $|4\rangle$, $|5\rangle$, and $|8\rangle$ of (1.3) make up the set of "correct zero'th order wave functions" for the system. Computation of the matrix elements of

$$M_+ = \mu_A \sigma_{+A} + \mu_B(\sigma_{+B_1} + \sigma_{+B_2}) \qquad (2.3)$$

yields the selection rules indicated in Figure 10, and the relative intensities of Table 3.

We thus have calculated the unbroadened fine structure as a function of the molecular parameters. Replacement of each component line by an appropriate bell - shaped curve gives the expected single crystal spectrum, and further transformation with the functions of Table 2 yields the absorption profile for a powder sample.

3. Limiting Behavior for Two Simple Cases:

In case one of the A - B distances is very large, the interaction constants b and c become vanishingly small. Application of L'Hôpital's Rule shows that $R \to 0$, and consequently all of the transitions shown in Figure 10 are equally allowed. The spectrum consists of doublets of separation $4a$ symmetrically

disposed about the unperturbed resonance fields for both A and B, and an undeviated line due to the resonance of the isolated nucleus of type B. The doublets are just the ones which would be calculated classically for a pair of unlike spins.

If both A - B distances are made much larger than the B - B separation, the coefficient R approaches unity, so that the mixed states of (2.1) become singlets and triplets for the B - B pair. The spectrum is made up of a single line at the unperturbed resonance position for A, and a symmetrical doublet of separation 6b in the vicinity of the Larmor field for nuclei of type B. This fine structure agrees with that calculated by Pake for a system of two identical spins, and applied in interpreting the spectrum due to the water molecules of hydration in the gypsum crystal.(35)

TABLE 3

Absorption Spectrum for an Isolated 3 - Spin System.

Transition	Energy	Relative Intensity
4 → 1	$2A + 2a + 2c$	1
6 → 2	$2A$	$2R/(1 + R^2)^2$
6 → 3	$2A - 2\sqrt{4b^2 + (a - c)^2}$	$1 - R^2/(1 + R^2)^2$
7 → 2	$2A + 2\sqrt{4b^2 + (a - c)^2}$	$1 - R^2/(1 + R^2)^2$
7 → 3	$2A$	$2R/(1 + R^2)^2$
8 → 5	$2A - 2a - 2c$	1
2 → 1	$2B - 4b - \sqrt{4b^2 + (a - c)^2} + a + c$	$(R + 1)^2/1 + R^2$
3 → 1	$2B - 4b + \sqrt{4b^2 + (a - c)^2} + a + c$	$(R - 1)^2/1 + R^2$
5 → 2	$2B + 4b + \sqrt{4b^2 + (a - c)^2} + a + c$	$(R + 1)^2/1 + R^2$
5 → 3	$2B + 4b - \sqrt{4b^2 + (a - c)^2} + a + c$	$(R - 1)^2/1 + R^2$
6 → 4	$2B - 4b - \sqrt{4b^2 + (a - c)^2} - a - c$	$(R + 1)^2/1 + R^2$
7 → 4	$2B - 4b + \sqrt{4b^2 + (a - c)^2} - a - c$	$(R - 1)^2/1 + R^2$
8 → 6	$2B + 4b + \sqrt{4b^2 + (a - c)^2} - a - c$	$(R + 1)^2/1 + R^2$
8 → 7	$2B + 4b - \sqrt{4b^2 + (a - c)^2} - a - c$	$(R - 1)^2/1 + R^2$

IV. DETERMINATION OF THE CONFIGURATION OF THE BIFLUORIDE ION.

1. Background:

The hydrogen atom has only a single 1s orbital which may be used in the formation of stable chemical compounds. However, a large number of substances exist whose properties cannot be satisfactorily explained unless it is assumed that certain hydrogen atoms are bound rather securely to two atoms simultaneously. Such couplings, in which two atoms (one of them always highly electronegative) are linked through a proton, are called hydrogen bonds.[36] They are definitely longer (2.4 to 3.0 A.U.) and weaker than normal covalent bonds, and normally are roughly equivalent to the combination of one covalent and one electrostatic bond.

In case the two hydrogen - linked atoms are identical, we may think of the proton as moving in a potential of two minima, each located approximately at the normal covalent distance from one of the atoms. The exchange of the relatively massive proton between the two equivalent positions does not contribute appreciably to the stabilization of the molecule.

The hydrogen bond in the bifluoride ion, HF_2^-, is anomalous in that its total length, 2.26 A.U.,[37] is considerable shorter than

any other known instance of this type of linkage. For the normal double - minumum potential to exist, both the covalent and the electrostatic parts of the bond must be significantly shorter than experience and qualitative theory would lead one to expect. One is tempted at least to entertain the idea that, in bringing together two isolated fluoride ions, the potential curves for hydrogen bonding merge to form a single minimum.

It is therefore of considerable interest to determine the true state of affairs in this ion, both for the sake of the information itself and for any light which it may throw on the theory of hydrogen bonding in general. Investigations of the problem have been made by a variety of techniques, and with considerable disagreement.

Ketelaar;[38] from an examination of the infrared absorption and reflection spectra of potassium bifluoride single crystals, concluded in 1941 that the usual two - minimum situation prevails. An estimate of 25 cm^{-1} for the splitting of the ground state of the asymmetric stretching vibration was interpreted to indicate a potential barrier of 7.35 kcal. $mole^{-1}$, separating the minima by 0.75 A.U.

Glockler and Evans[39] have interpreted the data of Buswell et. al.[40] on the 2.67 μ doublet to obtain a double minimum of separation 0.52 A.U. The height of the barrier was estimated at 33.4 kcal. $mole^{-1}$. In connection with the results of both of

these studies, it is well to note that barrier heights calculated from the splittings of vibrational states are quite sensitive to the form assumed for the potential.[41] In view of the fact that no good a priori conjectures can be made concerning its shape, it is likely that either of the above barrier height calculations could be considerably in error.

In 1949, Westrum and Pitzer published the results of a thermodynamic investigation of the system KHF_2, KF, HF.[42] Comparison of statistical entropies with those obtained from heat capacity measurements showed that no residual entropy exists at $0^{\circ}K$, thus indicating strongly that the structure is completely ordered and that the configuration is a symmetrical one. Maximum limits of 7 kcal. $mole^{-1}$ and 0.3 A.U. were set on the height and thickness, respectively, of the barrier.

Newman and Badger[43] then undertook an investigation of the polarized infrared spectrum of single crystals of KHF_2. This technique permits more clear - cut assignments of observed transition frequencies than does the more common unpolarized absorption method. The results of this study appear to support the thermodynamic results of Westrum and Pitzer, although it is difficult to explain the observed relative intensities for absorptions due to the bending vibration parallel with and perpendicular to the tetragonal crystal axis.

At this time it was felt desirable to reinvestigate the

problem by the completely independent method of nuclear magnetic resonance absorption. While this study was in progress, a reinterpretation of the infrared spectrum was made by Ketelaar and Vedder,[44] bringing it into accord with the single minimum hypothesis. Recently, Peterson and Levy have published the results of a neutron diffraction investigation of KHF_2, in which they conclude that the proton is centrally located within $\pm$ 0.1 A.U.[45] No research on the configuration of the bifluoride ion in any other than the potassium salt has been published. Rough x - ray diffraction data indicate the the F - F distance is longer in the sodium salt that in its potassium analogue. It would be interesting to verify this longer distance, and to ascertain whether or not a symmetrical situation prevails.

The only other bifluoride whose lattice parameters have been evaluated is the ammonium compound. The added complexity introduced by the presence of the perturbing protons of the NH_4^+ ion would make the interpretation of a nuclear magnetic resonance spectrum extremely uncertain.

2. The Effects of Motion:

It is clear from the x - ray diffraction data of Bozorth[46] that the bifluoride ion is a linear system of type B - A - B, with a total length of 2.26 A.U. in its equilibrium configuration. Before assuming that it can be treated by the methods appropriate to a rigid system, it is wise to consider the effects of the

various vibrational motions which are possible. In the case at hand these are:

a) a symmetric stretching vibration,

b) the corresponding asymmetric stretching,

c) a bending vibration,

d) a libration of the F - F axis,

e) the tunnelling of the proton between the two potential minima, which may have zero separation.

All of these motions are expected to be much more rapid than the Larmor precessions of the spins. b), c) and e), to a good approximation, involve only motion of the proton.

The complete Hamiltonian, including these effects, may be abbreviated

$$\mathcal{H} = \mathcal{H}^{(1)}(q) + \mathcal{H}^{(2)}(\sigma) + \mathcal{H}^{(3)}(q, \sigma) \qquad (2.1)$$

where $\mathcal{H}^{(1)}(q)$ includes the kinetic and potential energies for the molecular and lattice vibrations, $\mathcal{H}^{(2)}(\sigma)$ embodies the Zeeman effect for the isolated nuclei, and $\mathcal{H}^{(3)}(q, \sigma)$ is the dipolar interaction (7.5) of section I. q represents all of the "orbital" degrees of freedom, and σ stands for all the spin variables. We assume that wave functions of the form

$$\psi = \phi_k(q)\, X_m(\sigma) \qquad (2.2)$$

describe the system of uncoupled spins, and that the orbital motions are not appreciably altered by the perturbation $\mathcal{H}^{(3)}$. The validity of the latter assumption is indicated by the fact that the matrix elements of connecting different vibrational states are in magnitude roughly 10^{-9} times the separations of the most closely spaced vibrational levels.

The perturbing Hamiltonian occurs in the form

$$\mathcal{H}^{(3)}(q, \quad) = \sum_{i<j}\sum f_{ij}(q)\, g_{ij}(\sigma). \tag{2.3}$$

(viz. (7.5) of section I.) The matrix elements of the perturbation are then

$$\mathcal{H}_{mnkk} = \iint \sum_{i<j}\sum \phi_k^*(q)\, f_{ij}(q)\, \phi_k(q)\, X_m^*(\sigma)\, g_{ij}(\sigma)\, X_m(\sigma)\, d\tau_q d\tau_\sigma \tag{2.4}$$

since the ϕ's do not operate on the σ's nor the X's on the q's. This is just

$$\mathcal{H}_{mnkk} = \sum_{i<j} \langle f_{ij}(q) \rangle_{\text{av. } \phi_k} \int X^*(\sigma)\, g_{ij}(\sigma)\, X(\sigma)\, d\tau_\sigma . \tag{2.5}$$

That is, the perturbation treatment is carried out exactly as for a rigid lattice, except that the interaction parameters $f_{ij}(q)$ are replaced by their expectation values over the vibrational state of the system. It now remains to be seen to what extent

we may expect these averages to be different than the parameters calculated for a rigid system in the equilibrium configuration.

$f_{ij}(q)$ invariably has the form

$$f_{ij}(q) = \frac{K_{ij}}{r_{ij}^3} P_2(\cos \theta_{ij}) \tag{2.6}$$

All of the vibrations a) through d) are characterized by zero point energies on the order of 10^{-13} erg, and are separable as normal oscillatory modes. At room temperature ($kT \approx 4 \times 10^{-14}$erg) we may expect the ground states to be of predominant importance. Assuming harmonic potentials, the wave functions appropriate to these motions are Gaussians in the displacements X_n. Strictly speaking, therefore, one should take the necessary averages by evaluating integrals of the type

$$\left\langle f_{ij}(q) \right\rangle = \iiiint \prod_{n=1}^{4} e^{-k_n X_n^2} \; r_{ij}(X_1,\ldots,X_r)^{-3} \times P_2\left[\cos \theta_{ij}(X_1,\ldots,X_4)\right] dX_1 \cdots dX_4. \tag{2.7}$$

Needless, to say, such a process would be exceedingly difficult. In view of the facts that the potentials are certainly anharmonic to some degree, and that we have only meager knowledge of the force constants, it would also be somewhat absurd. A more satisfactory procedure is to estimate the orders of magnitude

of the corrections by calculating them for reasonable classical orbits.

The only important relative motions of the two F^{19} nuclei occur in the symmetric stretching vibration and the torsional oscillation of the ion axis. The first of these occurs at a frequency of about 300 cm^{-1}[43], corresponding to a classical oscillator amplitude of about 0.1 A.U. With a total F - F distance of 2.26 A.U., the correction to r^{-3} resulting from an average over a sinusoidal motion of this size is positive, and amounts to considerably less than 0.1%. (θ_{ff} is a constant over this motion.) According to Peterson and Levy[45] the libration (for which r_{FF} remains constant) has an amplitude of ca. 14°. The effect on an average of $P_2(\cos \theta_{FF})$ is indirect, and depends on the equilibrium value of θ_{FF}. For powder samples, the total width 3 α of the distribution function (8.4) of section I is not affected. The shape of $p(\Delta H_0)$ is altered slightly in this region, but for motions of the magnitude characteristic of the bifluoride ion, the corrections are of the order of 1%, and may consequently be neglected. Thus we conclude that the effect of motion on the interaction constant for the F - F pair is negligible, so that we can calculate this coupling assuming a rigid equilibrium separation.

Relative motion of the H - F pairs occurs in the asymmetric

stretching and bending vibrations, which have nearly the same force constants and an almost spherically symmetrical classical amplitude in the vicinity of 0.2 A.U.[43]. Integrating r_{HF}^{-3} over a sphere of this radius drawn about a proton position 1.1 A.U. from the F^{19} nucleus, we find that a positive correction of slightly less than 3% is necessary. We shall discover that the distinction between a single minimum and a bimodal potential involves much larger changes than this, and accordingly we may temporarily neglect it except to remember its presence. The oscillation of θ_{HF} occurring in the asymmetric stretching motion has an amplitude of roughly 10^{o}, and its effect may therefore be neglected to an even better approximation than the F - F libration. It is perfectly proper to consider the variations in r_{HF} and θ_{HF} separately in this case.

The only process which we have not yet considered, and the most important one by far, is the tunnelling of the proton which must occur if a double minimum situation prevails. Ketelaar[38], on the basis of his infrared measurements, concludes that this phenomenon occurs at an average rate of 25 cm^{-1}. While his frequency assignments are suspect, it is at least certain that the tunnelling occurs much more rapidly than the nuclear precession rates of ca. 10^{-3} cm^{-1} which are associated with the establishment of the spin energy levels. An immediate and vital consequence of this fact is that, for the purposes of a nuclear magnetic resonance

experiment, the proton cannot appear to be localized in one or the other potential trough, and the required average values of $r_{HF}^{(1)}$ and $r_{HF}^{(2)}$ are the same. The spectrum is therefore qualitatively that of a rigid symmetrical three - spin system, even though the instantaneous configuration may be far from a symmetrical one.*

The form of the potential in which the proton moves is unknown, so that we should be ill advised to attach too much importance to the choice between Morse functions, double parabola potentials, and the like. We can obtain a result of sufficient accuracy by assuming the proton to be localized with equal probability at either of two fixed, symmetrically placed points, corresponding to the minima of the actual potential. In the true situation, the probability distribution for the proton is actually skewed slightly farther from its nearest F^{19} neighbor than our potential allows. However, this fact is partially offset by the fact that the distances of closer approach are weighted more heavily in computing the average of r_{HF}^{-3}. In any case, it is reasonable to assume that we have already allowed for the fact that the proton is not completely localized when we considered the effect of the longitudinal vibrations of the ion.

---

* The proton wave function for the tunnelling motion is more properly represented by either the symmetric or the antisymmetric linear combination of the localized wave functions. Since these levels are established in times which are short in comparison with ω_L^{-1}, we wish the expectation value of r_{HF}^{-3} in one of these states. Since both squared wave functions are symmetrical with respect to interchange of the ends of the ion, the resulting average is the same for both H - F pairs.

Taking the effective interaction constants a_{eff} and c_{eff} of section III to be

$$a_{eff} = c_{eff} = k(\delta)\, a_{sym} = a_{sym}\left\{\frac{(1.13+\delta)^{-3} + (1.13-\delta)^{-3}}{2(1.13)^{-3}}\right\} \tag{2.8}$$

we find k as a function of the half separation δ of the potential minima to be as shown in Figure 11.

3. Predicted Line Shapes:

As we have just shown, the nuclear magnetic resonance absorption spectrum is expected to be that of the symmetrical B - A - B configuration calculated in section III. The energy levels, allowed transitions, and unbroadened fine structure for this case are shown in Figure 12 . The various constants , evaluated for the symmetrical situation, are

$$a_{sym} = -1.29 \times 10^{-22} \text{ erg} \qquad b = 7.6 \times 10^{-24} \text{ erg.}$$
$$A = 1.41 \times 10^{-23} H_0 \text{ erg} \qquad B = 1.33 \times 10^{-23} \text{ erg.} \tag{3.1}$$

For Zeeman fields on the order of 5000 gauss, it is clear that we are justified intreating $\mathcal{H}^{(3)}$ as a small perturbation on ψ .

Dividing the energy differences by the appropriate magnetic moments in each case, we find for a powder sample that

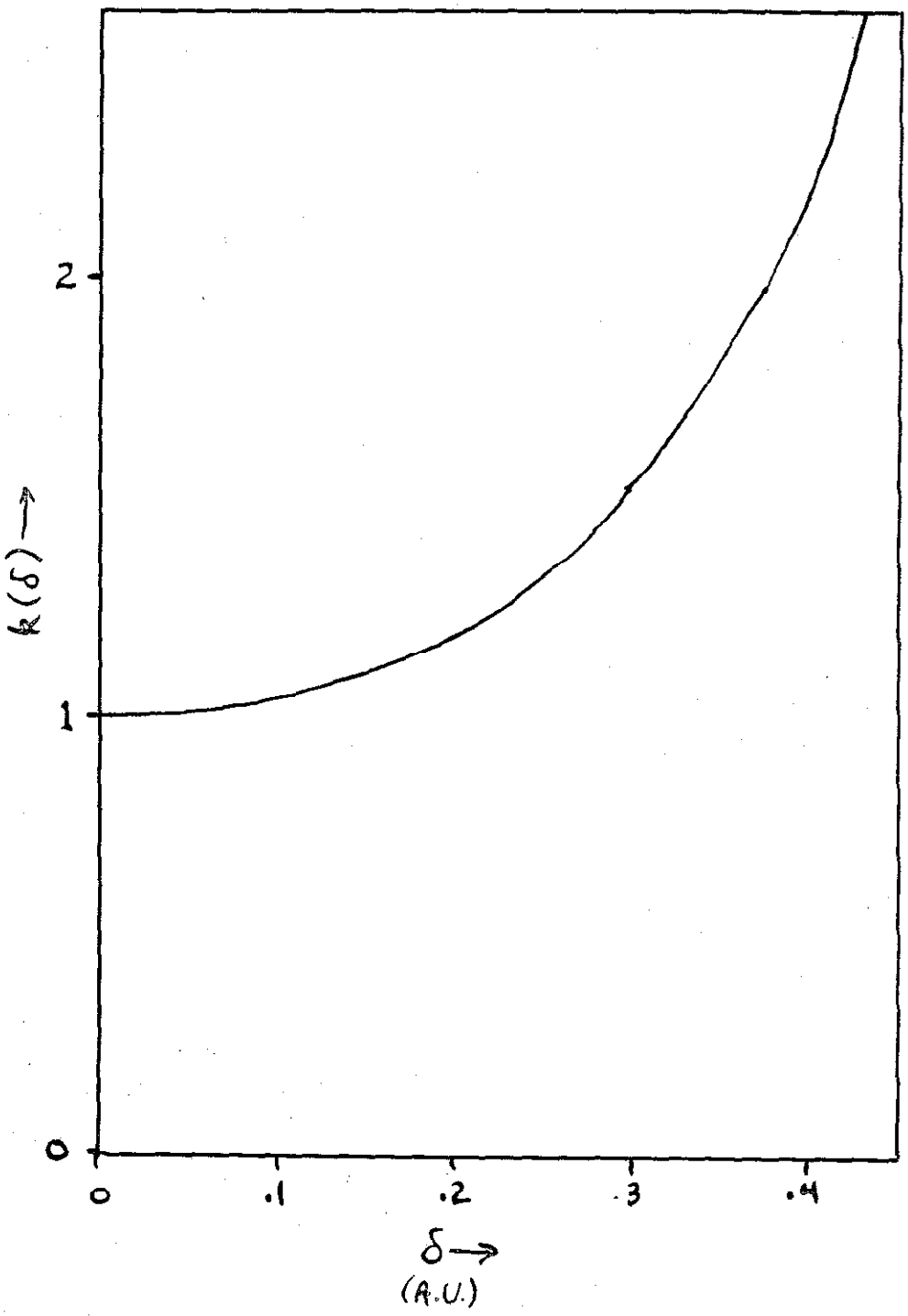

Figure 11

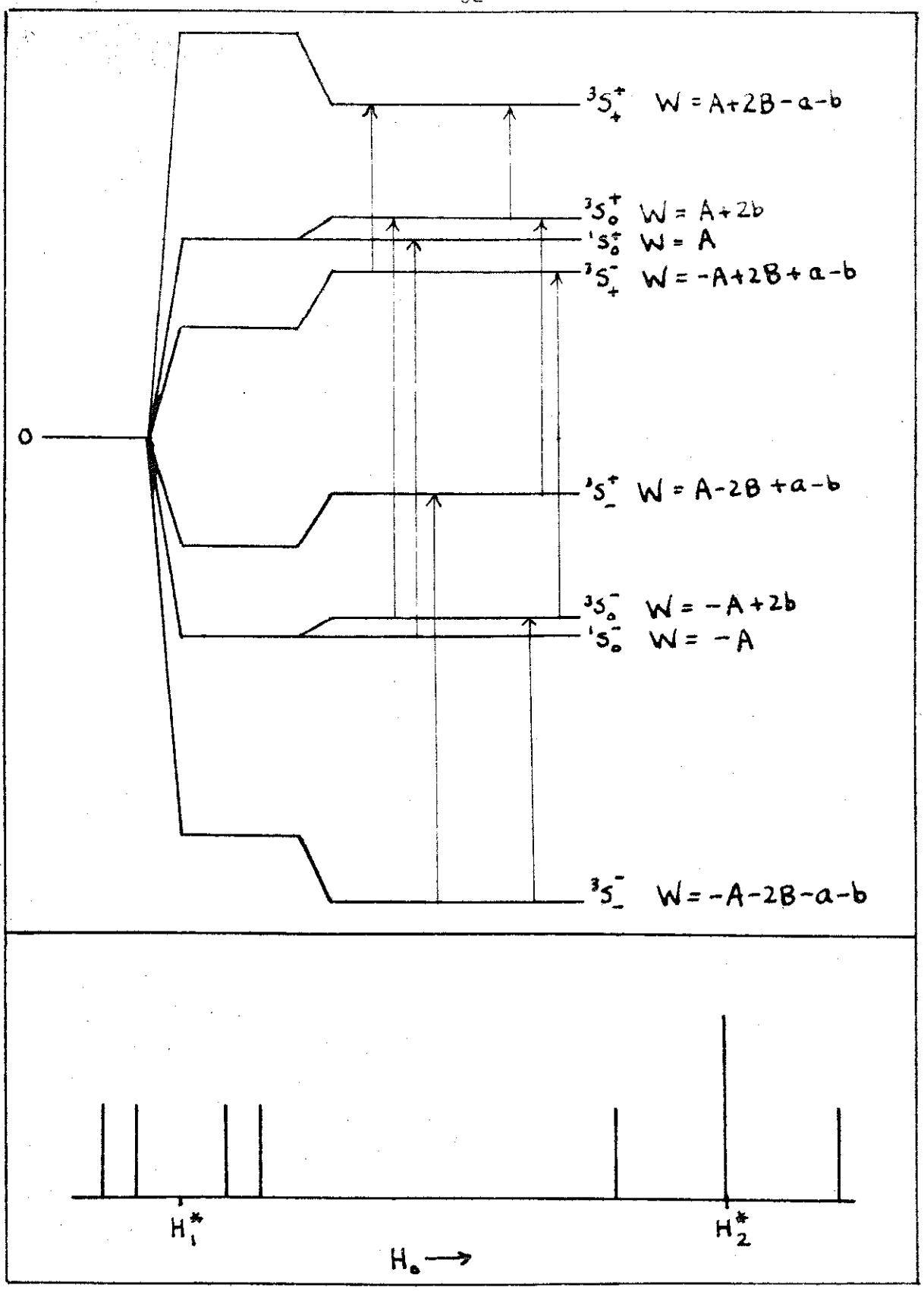
$^3S_+^+$ W = A+2B-a-b
$^3S_0^+$ W = A+2b
$^1S_0^+$ W = A
$^3S_+^-$ W = -A+2B+a-b
0
$^1S_-^+$ W = A-2B+a-b
$^3S_0^-$ W = -A+2b
$^1S_0^-$ W = -A
$^3S_-^-$ W = -A-2B-a-b
H_1^*
H_2^*
$H_0 \longrightarrow$

Figure 12

$$\frac{-4a_{sym}}{\mu_H \beta} = 18.4 \text{ gauss} ; \qquad \frac{-2a_{sym}}{\mu_F \beta} = 9.76 \text{ gauss} ;$$

$$\frac{3b}{\mu_F \beta} = 1.72 \text{ gauss} \qquad (3.2)$$

We therefore expect the following spectrum:

a) a triplet centered at the unperturbed proton resonance position, the central line having twice the intensity of either satellite, with a total splitting k(δ)(36.8) gauss, and

b) a pair of doublets at the fluorine resonance position. Each doublet is split by 3.44 gauss, and the doublet centers are separated by k(δ)(19.5) gauss.

This fine structure must be treated by the methods described in section I to make possible a comparison with experiment. Trial values for the extramolecular broadening may be obtained from a calculation of the appropriate second moment, using known crystal structure data.[46] KHF_2 crystallizes in a tetragonal lattice whose unit cell dimensions, in the conventional symbolism, are: a = b = 5.67 A.U., c = 6.81 A.U. The unit cell contains four molecules. The bifluoride ions lie in parallel planes $\frac{1}{2}$c apart, and each has its axis at right angles to those of its four nearest in - plane neighbors. The second moments external to a given HF_2^- ion for this overall structure are found by equation (6.5) of section I to be

$$\overline{\Delta H^2}\,(_1H^1) = 1.33 \text{ gauss}^2; \quad \overline{\Delta H^2}\,(_9F^{19}) = 2.48 \text{ gauss}$$

from which the appropriate Gaussian half - widths are approximately

$$\xi\,(H^1) = 1.16 \text{ gauss} ; \qquad \xi\,(F^{19}) = 1.58 \text{ gauss.}$$

4. Preparation of Samples:

KHF_2: Two commercial samples were available: Kalium bifluoratum Kahlbaum, No. 01958, and Potassium Acid Fluoride Merck, "pure". Both were recrystallized from aqueous solution in polyethylene and paraffin coated glass containers, and all crystals obtained were observed to have the habit characteristic of the salt. A weighed quantity of each sample was titrated with 0.1N. NaOH to a phenolphthalein end point, and the titers agreed in both cases with the calculated acid content within less than 1.5%. The Merck reagent was taken from the same lot as the samples used in the infrared investigation of Newman and Badger.

$NaHF_2$: A sample of Sodium Bifluoride "tech.", manufactured by the J. T. Baker Chemical Co., was recrystallized twice from aqueous solution in polythylene vessels. Neither the original samples nor the final product showed any traces of colored or insoluble impurities. A titration with 0.1N. NaOH gave the correct acid content within 2%.

The most likely impurities in the two substances are KF and NaF, respectively. From the known nuclear magnetic resonance spectrum of the former, it appears certain that the introduction

of either adulterant in quantities up to several percent would have no observable effect on the bifluoride resonances. It is therefore assumed that the samples are of sufficient purity.

After drying, samples of both substances were compressed in an arbor press into cylinders 0.32 inch in diameter and ca. one inch long, designed to fit snugly into the sample coil of the spectrometer probe unit. The pellets were mounted on the ends of 1/8" Lucite rods to facilitate their handling. Samples were initially stored in a desiccator over magnesium perchlorate, until it was found that storage in the open had no effect on either their weights or their nuclear magnetic resonance spectra.

Several attempts were made to prepare a single crystal of potassium bifluoride of sufficient size to permit a study of the dependence of nuclear magnetic resonance fine structure on the orientation of the crystal axes. The normal crystal habit is a square or rectangular plate, roughly one twentieth as thick as it is wide. Attempts to grow sufficiently thick crystals by slow evaporation of saturated aqueous solutions failed, owing to a tendency for branching of the well developed faces to occur at imperfections and dust grains. It is likely that the use of scrupulously cleaned solutions and a carefully temperature - controlled bath would enable one to grow adequate crystals by slow cooling of the solution. It is known that the habits of some crystals are changed by the addition of certain foreign

substances, e.g., : urea, gelatin, orgainic dyes, to the solutions from which crystallization takes place. It is possible that such a substance might be found which would improve the thickness - to - width ratio of the potassium bifluoride plates. However, the phenomenon is so poorly understood that any success in this direction would have to be achieved through a process of trial and error.

An attempt was also made to manufacture the equivalent of a single crystal by cementing together a number of the more easily obtained thin plates. Molten lambda sulfur was used as an adhesive, since it is one of the very few possible materials which contains neither of the interfering nuclei $_1H^1$ or $_9F^{19}$. Stacks of 10 - 20 plates were made, with the edges aligned with one another as carefully as possible. The edges were then trimmed with a hot wire to obtain a cylindrical sample which could be supported in a thin - walled glass tube which fitted into the sample coil of the spectrometer. Unfortunately, samples of large size and high density could not be obtained, so that the absorption signals were somewhat weaker than usual. Furthermore, the positions of the satellite absorption components depend strongly on the crystal orientation. Since they are extremely weak even in the case of a perfect crystal, the broadening introduced by small misalignments of the platelets causes them to become vanishingly weak. The recording of a derivative curve results in a further weakening. The result has been that no dependable

detection of the fine structure can be made. The few instances of structure observed at times when the spectrometer noise level was unusually low were reproducible on successive runs, but unfortunately could not be made to yield any quantitative information. Qualitatively, they appear to have the shape expected for a linear ion oriented in either of two directions in the lattice, as would be predicted from the known crystal structure of the salt. Owing to the undependability of the data, however, the single crystal project has for the present been reluctantly abandoned.

5. Comparison with Experiment: Proton Resonance:

A large number of line shape derivatives for the proton resonance in powdered KHF_2 have been obtained under widely varying conditions. The most satisfactory compromise between maximum signal strength and minimum distortion was found in a radiofrequency generator output in the neighborhood of .05 volt. and a field modulation amplitude of about 1.5 gauss. However, no single set of adjustments was entirely satisfactory for observation of all features of the absorption. The final experimental curves are the result of the synthesis of separate results on the central peak and the weak satellites. These latter are, in powder samples, near the threshold of sensitivity of the spectrometer, but have still been obtained reproducibly and measured with some accuracy. A sample absorption derivative is shown in Figure 13

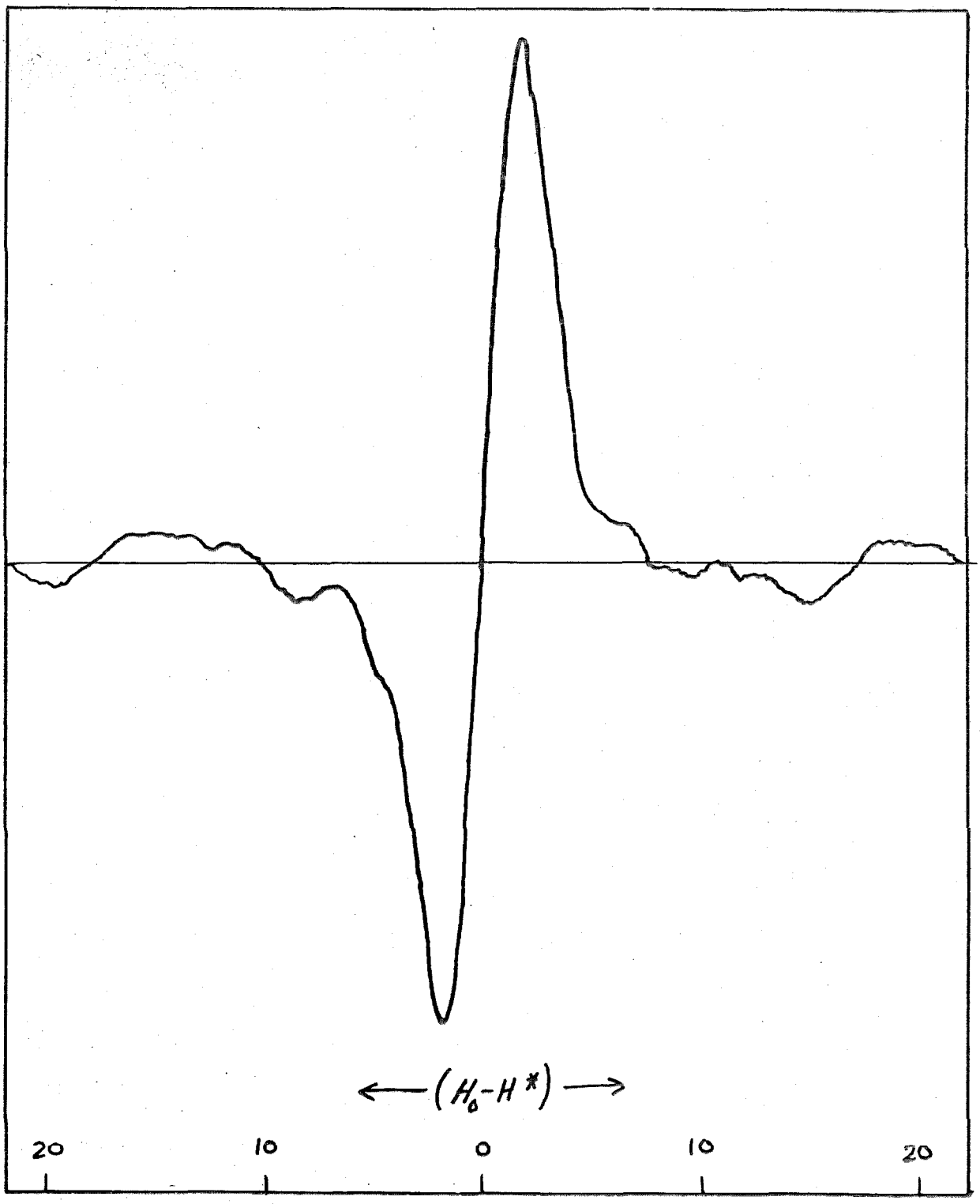

Figure 13

in the form in which it appears on the Brown Recorder chart. This tracing was taken with a narrow bandwidth in order to emphasize the wings of the absorption, and consequently the central component appears to be somewhat broader than it should be.

Since the undeviated peak is very well resolved from the satellite structure, a unique opportunity is afforded for determining the amount of extramolecular broadening by direct measurement of the width of this line. Except in its outermost regions it is very nearly Gaussian, so that its second moment is simply the square of the half - separation of the extrema of the derivative curve. A large number of measurements give an average value of $1.93 \pm .02$ gauss^2 for this quantity. The difference of 0.58 gauss^2 between this value and the theoretical one may probably be ascribed principally to field inhomogeneity and slight residual broadening by the slow response characteristics of the output detector.

The absorption derivative in the region of a wing of the curve has been calculated for several assumed ion configurations, using a broadening Gaussian of second moment 1.9 gauss^2. The result is compared in Figure 14 with the mean observed absorption in the same region, in the case of a symmetrical structure of total F - F distance 2.26 A.U. The results for double minimum models are qualitatively the same, except that the subsidiary peak is moved

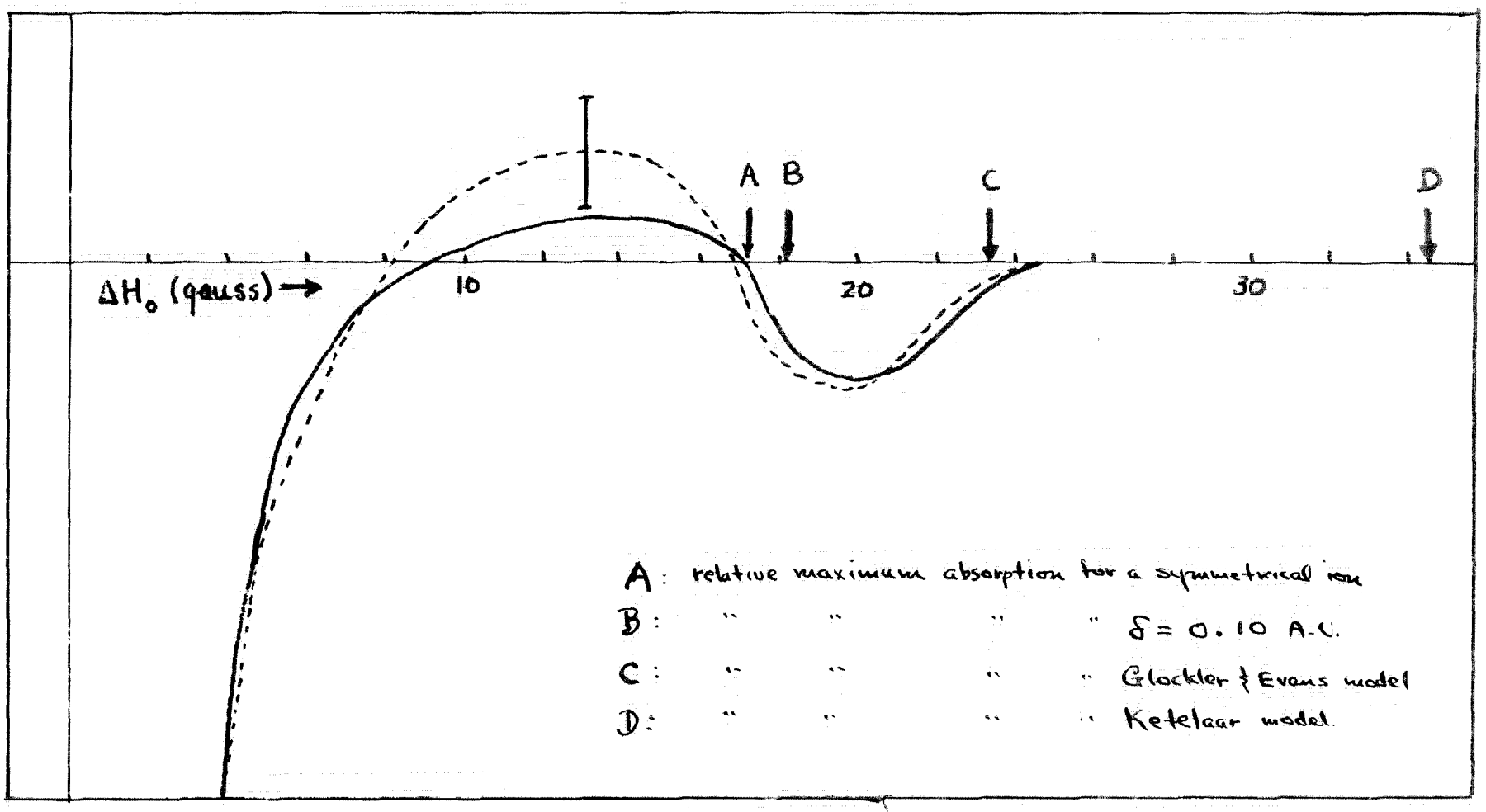
A B
C
D
ΔH_0 (gauss) →
10
20
30
A: relative maximum absorption for a symmetrical ion
B: " " " " $\delta = 0.10$ A.U.
C: " " " " Glockler & Evans model
D: " " " " Ketelaar model.

Figure 1b

out farther along the H_0 axis. The points of calculated relative maximum absorption are indicated for the asymmetrical models of Glockler and Evans and of Ketelaar. The precision of the experimental values is indicated in Table 4, in which are recorded the results of a set of measurements of the point of relative maximum absorption. From these data it is evident that both of the postulated dual potential configurations are inadmissible. Inclusion of corrections for vibrational effects would have the result of displacing the theoretical peaks outward from the line center, so that there is no danger of confusing the observed results with the absorption of a strongly - vibrating asymmetrical ion. Taking into account the effects of random errors and systematic discrepancies which might result from incorrect field calibration data, it is estimated that the equilibrium position for the proton lies within 0.07 A.U. of the center of the F - F axis.

6. Comparison with Experiment -- Fluorine Resonance:

F^{19} resonance data have been accumulated on several occasions for the resonance in powdered KHF_2. The absorption is extremely broad (about 55 gauss in toto) and correspondingly weak. Furthermore, saturation of the spin system occurs at radiofrequency power levels greater than about 50 mv. Even under the most favorable conditions, usable recording meter tracings could be

obtained only with the narrowest available system bandwidth, thus requiring very slow traversal of the resonance region in order to avoid distortion. Most of the final data were obtained at an R.F. level of 20 mv., and a field modulation amplitude in the neighborhood of 2 gauss.

Calculation from the crystal structure data of Bozorth yields an external broadening second moment of about 2.5 gauss^2 for a rigid lattice. Broadening of the calculated fine structures with a Gaussian of this width leads to a set of curves whose principal doublet separation, even for the minumum symmetrical case, is considerably greater than that observed experimentally. Traces of the (unresolved) subsidiary doublets appear in the theoretical results, but are completely absent in the experimental tracings, which have an obviously smeared simple doublet structure. It is true that the theory for the symmetrical case approaches agreement with experimental data more closely than does any asymmetrical model, but the agreement is far from flawless. We are then obliged, nolens volens, to introduce further artificial broadening to the theoretical profiles in an attempt to reconcile them with the actual results.

It is likely that the additional broadening stems from the following source: Observation of narrow, sharp resonances on the oscilloscope has shown that sharp, random fluctuations of the main magnetic field are constantly occurring, with amplitudes

in the vicinity of 1 or 2 gauss and at intervals averaging a few seconds. These appear to originate in fluctuations of the current supplied by the batteries, either in response to changing load conditions or to random changes in the batteries themselves. (Small fluctuations in the output of the sweeping power supply also occur, but apparently only in response to changes in flux through its magnet winding. This is shown by the fact that the variations do not occur with the main magnet current turned off.)

In the case of a stronger resonance than the one under discussion, the field may be swept through the absorption region rapidly enough so that the fluctuations appear only as small, random irregularities in the field scale of the recording chart. A composite of a number of observed resonances then approximates the true absorption profile by virtue of cancellation of the variations. When the field must be changed very slowly, however, it appears that the signal obtained at each point is a more - or - less complete average of the true absorption over the region of the fluctuations. If the averaging is complete and the variations are random in size, the effect is the same as a broadening of the true line with a normal error curve which represents the amplitude distribution of these changes.

Figure 15 shows a composite of a large number of experimental curves and the theoretical absorption for a symmetrical ion, broadened by a Gaussian of half width 3.1 gauss. A similar

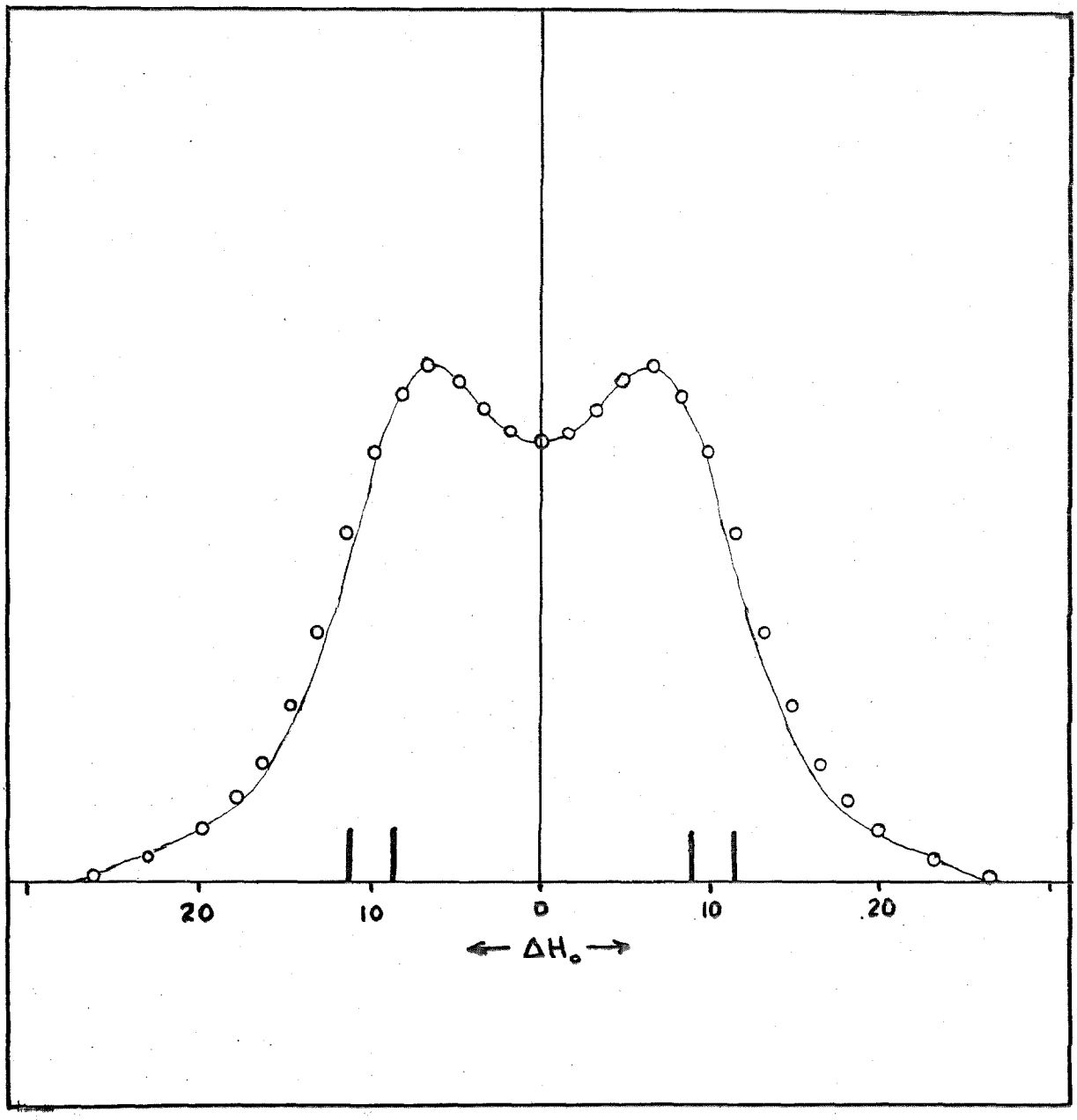

Figure 15

comparison, using the same broadening function, is made in Figure 16 with the double minimum model of Glockler and Evans. Ketelaar's model produces a discrepancy which is even considerably greater than this one. Attempts to reconcile the double minimum models with the experimental points by use of a still broader Gaussian function results in complete loss of resolution of the doublet, and even poorer agreement than that evidenced in Figure 16. A set of measurements of the observed doublet separation appears in Table 5. In view of the degree of arbitrariness involved in introducing a considerable amount of supplementary broadening, it is deemed the part of wisdom not to press the excellent agreement of Figure 16 too far in drawing conclusions regarding the configuration of the spin system. It is certainly true that a double minumum of as wide a separation as that of Glockler and Evans is to be excluded. However it seems discreet to regard these measurements chiefly as a verification of the proton resonance results.

7. Second Moments of the Absorption Lines:

Because of the extreme weakness of the outer reaches of the proton resonance, and the fact that it is just these regions which contribute most strongly to the second moment of the absorption, it is impossible to calculate a reliable value for this quantity from the experimental curves. In the case of the F^{19} absorption, the second moment was measured before a detailed line shape

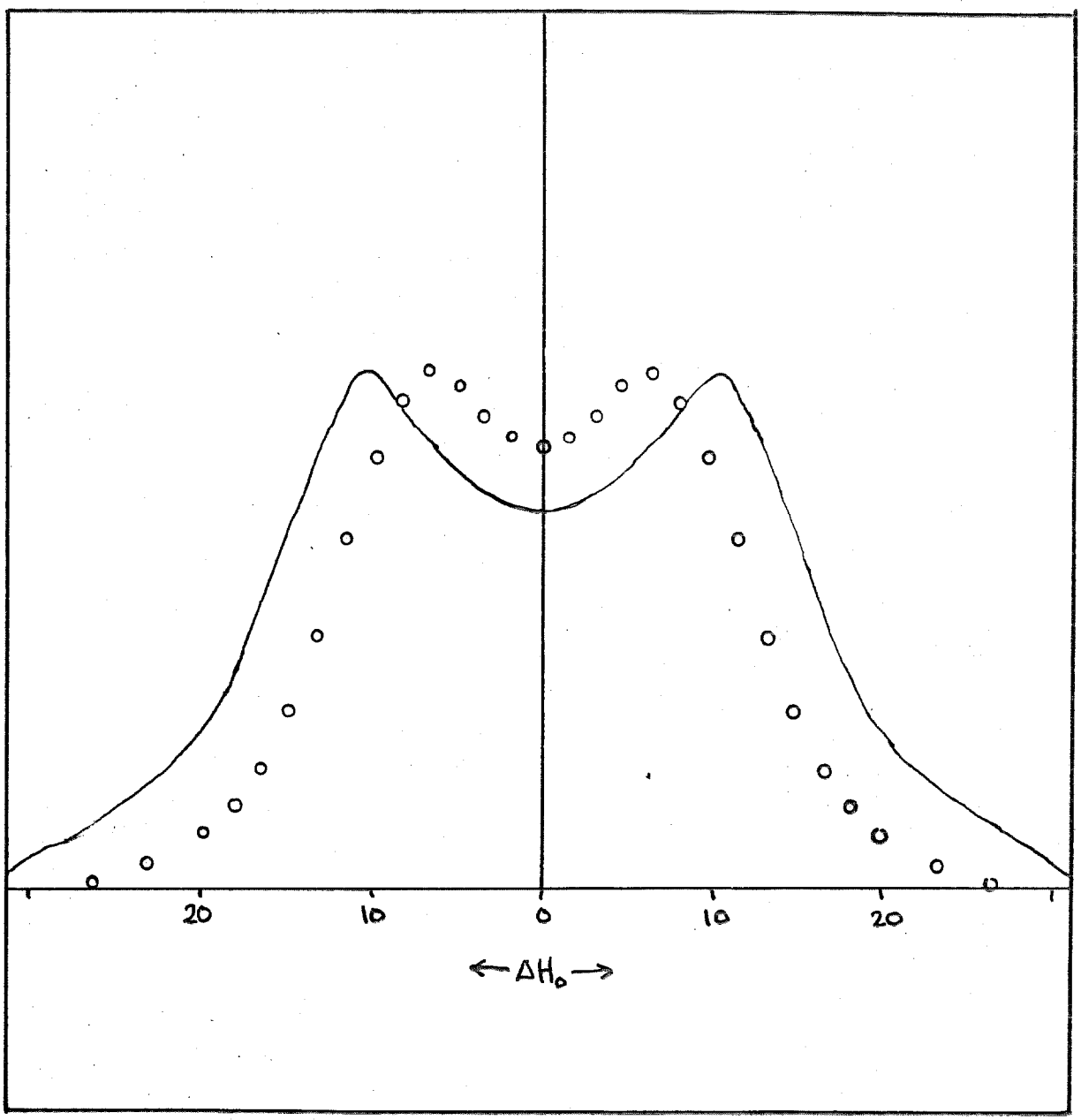

Figure 16

comparison was undertaken. The geometric mean of four such determinations, taken from the most symmetrical of the recorded derivative tracings, was found to be 93 ± 2 gauss^2. The rigid lattice second moment has been calculated by Van Vleck's formula as a function of the distance δ of the proton from the center of the ion axis, and the outcome is recorded in Figure 17. The value for a symmetrical ion, including the extramolecular contributions calculated from Bozorth's x - ray diffraction data, is 79.7 gauss^2. If to this we add 7.1 gauss^2 for the additional contribution of the arbitrary broadening Gaussian used in the line shape determinations, there remains a discrepancy of only 6.2 gauss^2. The corrections to the H - F interaction constants required by the vibrations of the proton, which were estimated to be in the vicinity of + 3%, would require about 6% correction to the calculated second moment, whose terms are proportional to r_{ij}^{-6}. If we add such a correction to the calculated value above, we obtain a final estimate of 91.6 gauss^2. The excellence of the agreement between this and the measured value is to be regarded as entirely fortuitous. The approximate nature of several of the assumptions made, particularly the one regarding the validity of the Gauss transform method for large broadenings, militate against the placing of a great deal of faith on a one percent agreement.

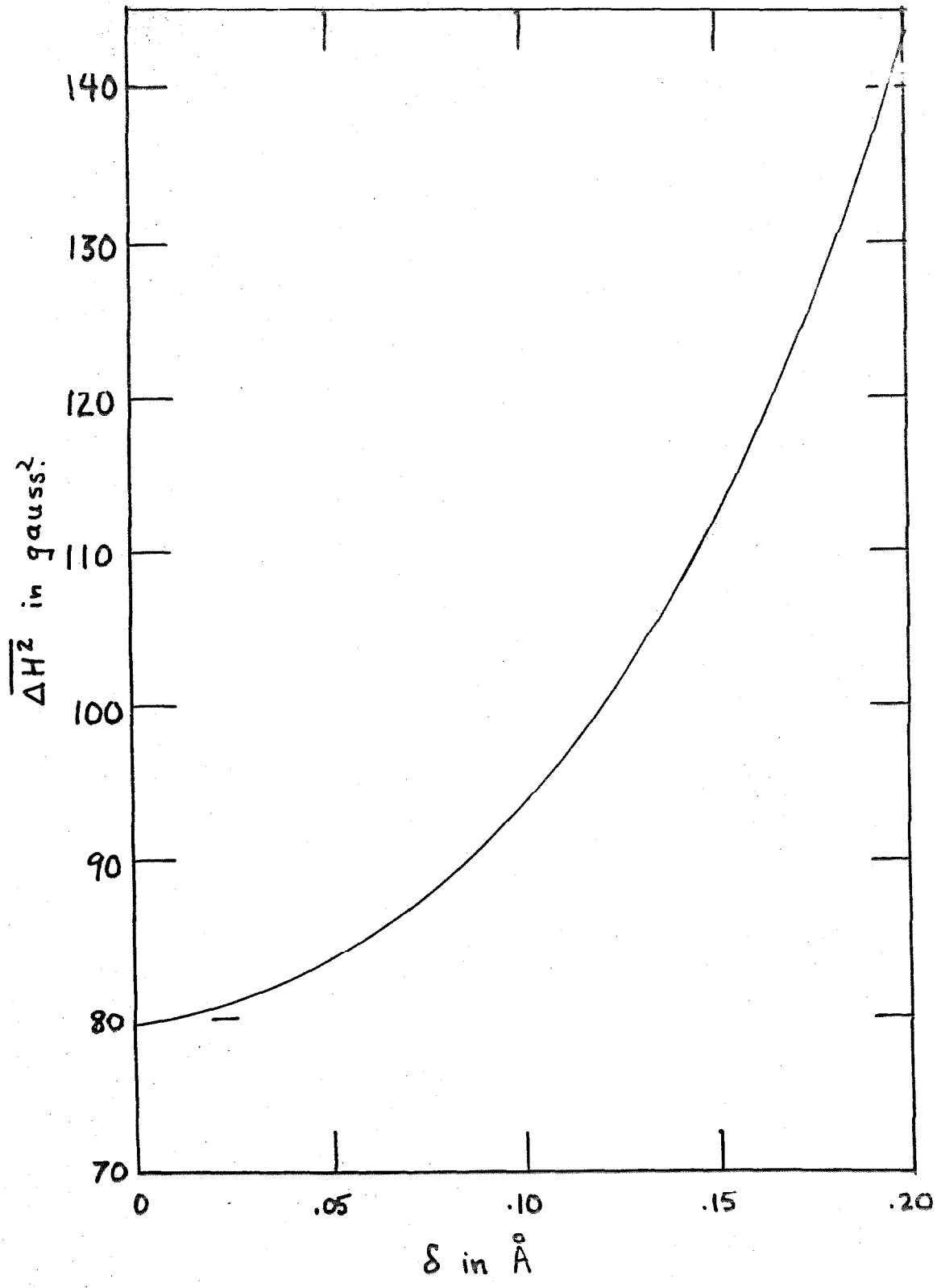
140
130
120
110
100
90
80
70
$\overline{\Delta H^2}$ in gauss^2.
0
.05
.10
.15
.20
δ in Å

Figure 17

The calculated second moment for the Glockler and Evans model amounts to some 200 gauss^2, and that for the more extreme Ketelaar structure is 460 gauss^2. It is perfectly clear from these figures alone that the double minimum interpretations based on infrared measurements are greatly in error. Reference to Figure 16 shows, however, that the variation of $\overline{\Delta H^2}$ with δ becomes much less rapid for smaller displacements. It seems reasonable to attach some validity to the assumption that the observed curves are broadened somewhat from their true shapes, and that we can subtract from the measured second moments an amount roughly equal to that of the broadening Gaussian. It thus seems reasonable on the basis of the second moment and line shape data for the fluorine resonance to assign a limit of.05 A.U. on δ.

In summary, we may then say with considerable certainty that the proton of the bifluoride ion, in crystalline potassium bifluoride, has its equilibrium position within 0.05 A.U. of the center of the ion axis. The possibility of a double minimum is not rigorously excluded, therefore, but appears extremely unlikely. The radial dependence of all atomic potential functions in common use is such that the barrier between two wells of separation 0.1 A.U. or less must inevitably be very low. According to the investigation of Newman and Badger[43], the zero point energy for the asymmetric stretching vibration is in the neighborhood

of 300 cm^{-1}. It is almost certain that this energy is larger than the height of the potential barrier, if one exists. Such a situation is ordinarily not described as a double - well configuration, since there is no important impediment to the motion of the proton even in the ground state, and tunnelling is a nonexistent process.

8. Resonances in Sodium Bifluoride:

A large number of observations have been made on the proton absorption in $NaHF_2$. The entire line, and especially the satellite structure, is notably weaker than is the case of the potassium salt. This circumstance is primarily the consequence of a longer spin - lattice relaxation time in the sodium compound, necessitating operation at a lower radiofrequency power level. While the fine structure is visible, its size is of the same order of magnitude as the zero drift of the spectrometer occurring during the time of a single measurement. Accordingly, no estimate of the half - splitting is possible beyond the statement that it lies in the range 16 - 21 gauss. The fact that the $F - F$ distance of 2.5 $\pm$ .2 A.U. reported for the salt is unreliable[36] largely vitiates any interpretation of the splitting in terms of the proton position.

The F^{19} resonance has been recorded with somewhat greater success, although it is weaker than that in KHF_2. The experimental derivative and intergrated absorption are shown in Figure 18. It is clear here that the fine structure is largely obscured by an amount of broadening even greater than that present in the KHF_2

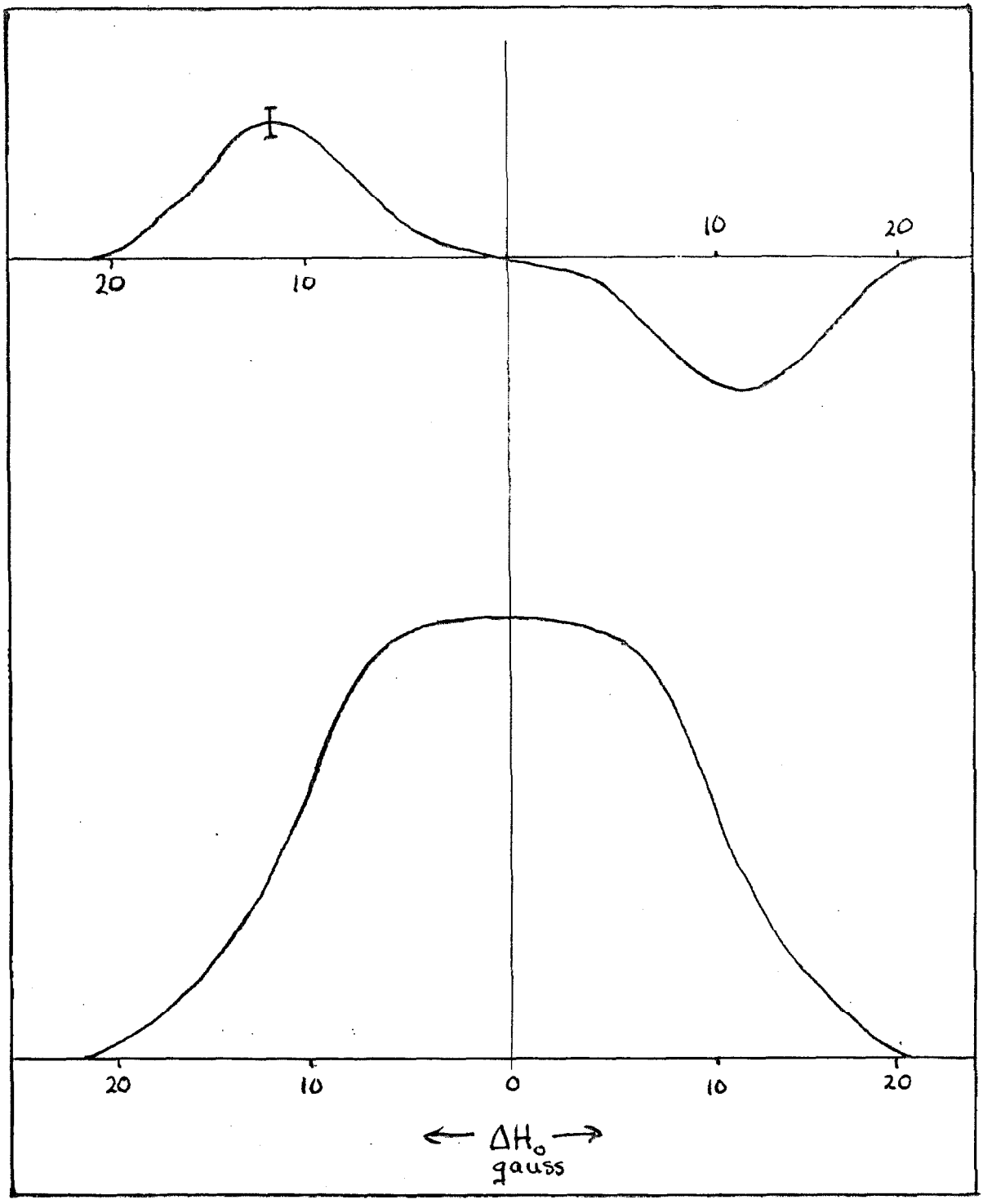

Figure 18

results. Since the data were taken under the same experimental conditions as the corresponding ones of § 6, we may assume that the spurious broadening due to magnetic field fluctuations is the same in each case. Apparently, then, the extramolecular broadening inherent in the sample is large in $NaHF_2$. This revelation is not unduly surprising in view of the lattice constitution of this salt. The structure is a rhombohedral one[8] with the very acute axial angle $39^{\circ}44'$. The bifluoride ions then are undoubtedly all parallel, and confined in rather close proximity to the sodium ions and to one another. We may thus speculate that large librations of the ion axis can introduce appreciable average interactions between F^{19} nuclei belonging to different ions.

The unusual amount of broadening present makes one reluctant to attempt a detailed comparison of observed and calculated line shapes. However some information can be obtained from a consideration of the second moment. The average of several experimental measurements of this quantity is 87 ± 4 gauss^2.

Comparison with the many trials made in fitting the experimental KHF_2 fluorine resonance data to the theory indicates that the second moment of the unbroadened fine structure should be obtained by subtraction of roughly 15 gauss^2 from the observed value, assuming the fine structure is qualitatively the same in both cases.

Taking the second moment to be 72 ± 10 gauss^2, we may establish the limits on the proton position shown in Figure 19, which is a plot of allowed combinations of the two proton - fluorine distances. The boundaries of the shaded region correspond to the limits of error taken for the second moment. The locus of all symmetrical configurations is shown, as is the region allowed under the conditions of the unreliable x - ray diffraction determination of the F - F distance. Were this distance known accurately, the separation of the proton from the ion center could be determined within rather narrow limits.* In the absence of this information, we can say only that neither H - F distance is less than 1.0 A.U. Since the corresponding separation in hydrogen fluoride is 0.92 A.U.[36] it is at least certain that appreciable modification of the hydrogen fluoride bond occurs upon approach of F^- to form a bifluoride ion.

---

* Note that the errors involved in this determination become considerably greater as a symmetrical configuration is approached.

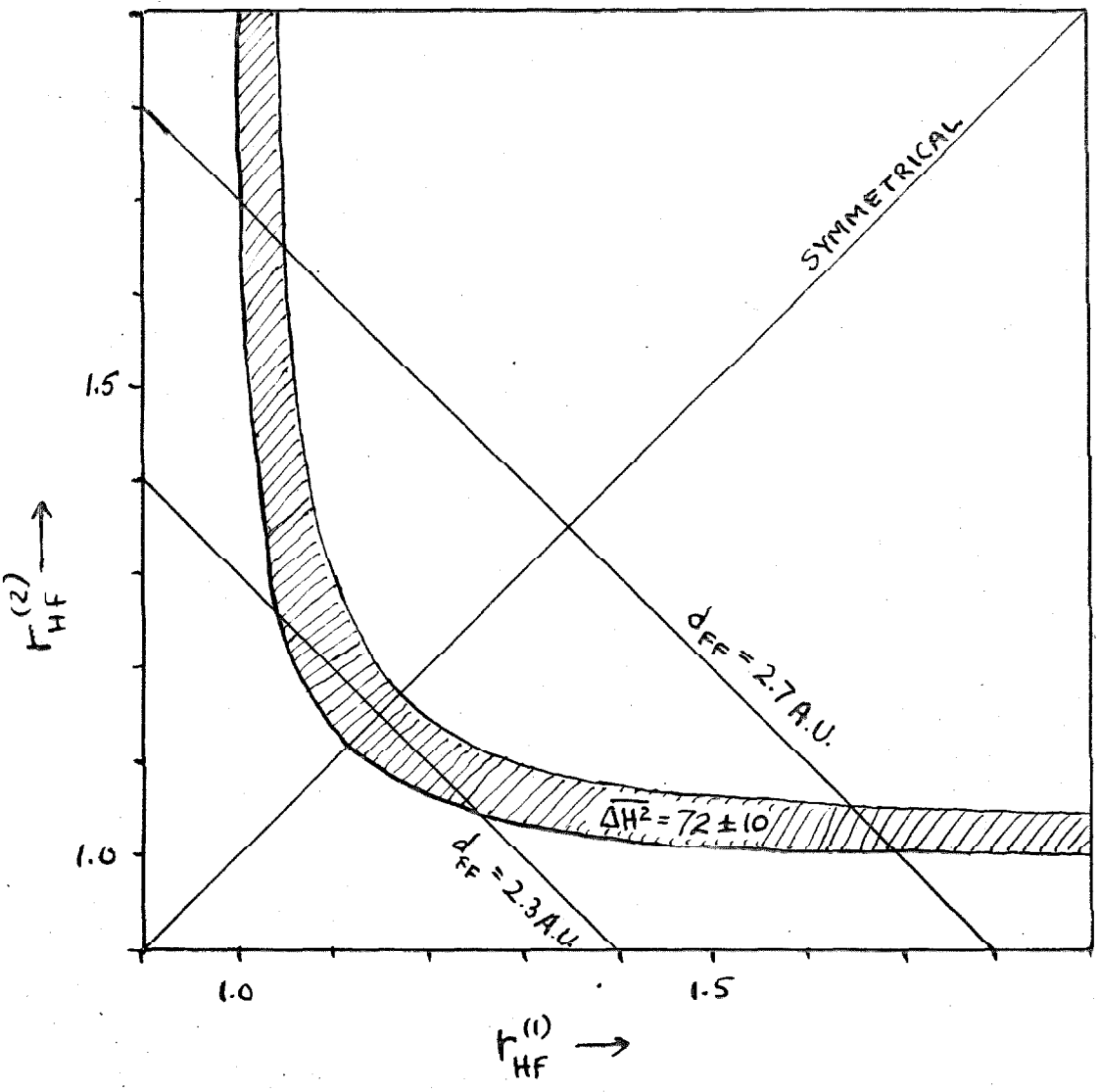
SYMMETRICAL
$d_{FF} = 2.7$ A.U.
$\overline{\Delta H^2} = 72 \pm 10$
$d_{FF} = 2.3$ A.U.
1.5
1.0
1.0
1.5
$r_{HF}^{(2)}$
$r_{HF}^{(1)}$

Figure 19

TABLE 4

Experimental Triplet Separations in the Proton Resonance of KHF_2.

$\frac{1}{2}$ - separation (cm)	$\frac{1}{2}$ - separation (gauss)
4.99	15.7
5.37	17.0
5.65	17.9
5.75	17.9
5.62	17.5
5.08	16.9
5.29	17.6
5.01	16.7
4.90	16.3
4.98	16.6
4.85	16.6
4.80	16.5
5.04	17.3

Average = 16.9 gauss $\pm$ 0.1

TABLE 5

Experimental Doublet Separations in the F^{19} Resonance of KHF_2.

separation (in)	separation (gauss)
1.80	14.0
1.80	14.0
1.65	12.8
1.53	13.0
1.53	13.0
1.42	11.8
1.58	13.2
1.57	13.2

Average $\frac{1}{2}$ - separation = 6.55 $\pm$ 0.10 gauss

V. MOLECULAR MOTIONS IN CERTAIN COMPLEX CRYSTALS.

1. Introduction:

Widespread study of the heat capacities of solids as functions of the temperature has resulted in the discovery of numerous cases of lambda point discontinuities, which are correlated with second order phase transitions. These transitions may for the most part be classified into two types: the cooperative onset of more or less free rotations, and the passage from a more ordered to a less ordered state. Preliminary work[13] has indicated that nuclear magnetic resonance absorption can function as a valuable tool for the study of these processes and for distinction between them.

It is perfectly possible for reorientations of the same sort to exist in the absence of phase transitions of any kind, so that they are not susceptible to detection by heat capacity measurements. An example will serve to make this clear: the ammonium halides crystallize in cubic lattices, in which each ammonium ion resides in a potential whose chief angular symmetry is octahedral. Since the NH_4^+ ion has tetrahedral symmetry, there are two different orientations possible for each ion, and these are equal in energy except for the relatively small effect of each ion on its neighbors. Each of the salts has a second order phase transition corresponding to the change from a state in which these small interactions dictate an ordered

arrangement of the NH_4^+ ions, to one in which they are distributed randomly between the two possible orientations. Were the NH_4^+ ion an octahedral one, or the lattice potential tetrahedral, no such phase transition could exist. Yet the tunnel effect responsible for the reorientations could still be possible. Thus no heat capacity anomaly would be detectable, even though the same characteristic motions were still present and capable of being studied by their effects on line widths and spin - lattice relaxation times in nuclear magnetic resonance absorption. An example of behavior of this type has been found, and is discussed in this section.

2. Preparation of Samples:

Cobalti - hexammine trichloride, $Co(NH_3)_6Cl_3$, was prepared (47) by air oxidation of an aqueous solution saturated with $CoCl_2$ and NH_4Cl, catalyzed by activated charcoal. The reaction mixture was then filtered to remove the carbon, and the salt precipitated by addition of 12 N. HCl which had been cooled to 0° C. The precipitate was washed with 65% and 95% ethyl alcohol and dried for several days at 110° C. Gravimetric analyses made by reduction with hydrogen to cobalt metal or conversion with oxygen to Co_2O_3 proved not to be reproducible. (The latter technique appears to give an unpredictable mixture of Co_2O_3 and CoO under all conditions that were tried.) Satisfactory results were obtained by dissolving the oxide in acid, followed by precipitation with $(NH_4)_2HPO_4$ and

weighing as $CoNH_4PO_4 \cdot H_2O$.[48] The average of several analyses, which had a precision of $\pm$ 0.5%, indicated 22.3% Co in the original complex, as compared with a theoretical value of 22.04%. The sample was stored *in vacuo* over anhydrous magnesium perchlorate.

Cobalti - tris - ethylenediamine trichloride, $Co((Ch_2NH_2)_2)_3Cl_3$, (henceforth abbreviated $Coen_3Cl_3$), was prepared by two similar methods. The more satisfactory of these[49] involved the air oxidation of $CoCl_2$, to which was added a mixture of 30% ethylenediamine and 6 N. HCl. The ethylendiamine (Eastman Kodak *tech.*) was redistilled before use. After the oxidation had proceeded to completion, the mixture was evaporated on a steam bath, acidified with 12 N. HCl, and the product precipitated by addition of ethyl alcohol. After cooling, the precipitate was washed with 65%, 95% and absolute ethyl alcohol and diethyl ether, and dried at 110° C. for several days. An analysis by precipitation as $Co(NH_4)PO_4 \cdot H_2O$ indicated a weight percentage of cobalt of 17.2, as compared with the predicted value of 17.05. The compound was stored *in vacuo* over $Mg(ClO_4)_2$.

A sample of azido - pentammine - cobalti - trichloride, $Co(NH_3)_5N_3Cl_3$, was obtained through the good offices of Dr. Alvin Cohen, of the U. S. Naval Ordnance Test Station, China Lake, California. The salt had been prepared by the method of Linhard and Flygare[50], and was found to contain 42.5% N, as compared with a calculated content of 43.6%. Dryness was assured by storage for several days in a vacuum desiccator.

A commercial sample of $AlCl_3 \cdot 6H_2O$, Baker and Adamson Reagent was used without further treatment.

Samples of all compounds were packed tightly into thin - walled glass tubes which fit snugly into the radiofrequency probe unit. Pellets prepared in the tablet press would not stick together unless painted with shellac, glyptal, or a similar adhesive. While the presence of these adulterants was never observed to have an effect on the nuclear magnetic resonance spectrum, it was felt desirable to use the purer, unpressed material. Although a smaller sample density is obtained in this way, the absorptions were all of sufficient intensity so that useful data could be obtained.

3. $Co(NH_3)_6Cl_3$:

The cobalt (III) hexammine ion possesses octahedral symmetry with respect to the distribution of nitrogen atoms about the central cobalt, and each ammonia molecule has threefold symmetry about its Co - N axis. There are therefore two distinct types of large scale motion to be considered: reorientation of the NH_3 groups about their C_3 axes, and tunnelling or free rotation of the entire ion in the lattice potential.

In order to evaluate the likelihood of rapid reorientations, we must have some information concerning the spatial disposition

of the atoms of the complex and of their neighbors. Inspection of the N - N distances (2.8 A.U.) within the ion makes it appear unlikely that appreciable freedom of rotation of the individual NH_3 molecules is possible.

Many of the $Co(NH_3)_6^{+++}$ salts (although not the chloride) have been investigated by x - ray diffraction, and are invariably cubic in structure with a unit cell edge in the vicinity of 10.4 - 10.9 A.U.* In the iodide[51] the complex ion resides at the center of a cube of iodide ions. The extension of each Co - N bond joins the centers of two opposite faces of this cube, whose side is 5.4 A.U. in length. It is assumed that the chloride has the same structure, probably with a somewhat smaller unit cell.

Since the $Co(NH_3)_6^{+++}$ ion has 18 hydrogen atoms at a common distance of 2.3 A.U. from the cobalt atom, and since each of them has an effective (Van der Waals) radius of something over 1 A.U. the complex presents from the exterior a nearly spherical aspect, and has a total Van der Waals radius in the vicinity of 3.3 A.U. Because of the nearly spherical symmetry it is to be expected that the barriers to rotation of the entire ion within the framework of chloride ions are not very high, particularly for

---

* The Laue diffraction patterns which have been obtained from these substances (presumably at room temperature) are invariably discrete, indicating that unhindered rotation of the complex ion does not occur. No such restriction can be made on possible motions of the NH_3 groups, since the hydrogen atoms are not detectable in the x - ray data.

rotations about the fourfold axes of the octahedron.

The distinction in nuclear magnetic resonance experiments among rigid lattice behavior, reorientation about the C_3 axis of ammonia, and tumbling of the entire ion in the lattice potential is most evident from second moment considerations. The chief contribution to $\overline{\Delta H^2}$ for a rigid lattice originates in the mutual interaction of the three protons within a single NH_3 molecule. Assuming the normal N - H distance for ammonia, and a tetrahedral system of bonds, this amounts to 35.4 gauss^2, as calculated by the methods of section I. In addition, we may expect an intermolecular contribution, whose magnitude is difficult to estimate with any accuracy. Rough measurements on a scale model of the complex indicate that this broadening is on the order of 10 gauss^2. This is sufficient to obscure any details of fine structure, and we therefore expect to observe a simple bell - shaped absorption line. The coupling between different $Co(NH_3)_6^{+++}$ ions, and that between each such ion and the chloride ions of the surrounding lattice, are small in comparison with these effects. We are therefore led to assign a total value of about 45 gauss^2 for the theoretical second moment.

For threefold rotation or tunnelling of the ammonia molecules, the intramolecular part of $\overline{\Delta H^2}$ is reduced[52] in powder samples to one fourth of its rigid lattice value, or 8.8 gauss^2. The interactions between different NH_3 molecules are expected to

retain their original orders of magnitude, leading us to predict a total second moment in the neighborhood of 15 gauss^2.

Reorientation of the entire complex ion, if it occurs at average intervals much shorter than ω_L^{-1}, is equivalent, because of the ion's octahedral symmetry,[52] to a complete averaging of all of the internuclear vectors over a sphere. The result is the vanishing of the second moment except for contributions from outside the rotating ion.

A number of proton resonance absorption derivatives have been recorded in $Co(NH_3)_6Cl_3$, and present a very narrow Gaussian appearance. Owing to the small line width and the high proton density in the sample, strong signals are obtained, and the signal - to - noise ratio is very high. The separation of points of extremal slope has been measured, and found to be $3.35 \pm .08$ gauss, corresponding to a Gaussian second moment of 2.8 ± 0.3 gauss^2. The conclusion to be drawn is, therefore, that tumbling of the $Co(NH_3)_6^{+++}$ ions occurs in the Cl^- lattice at a much higher rate than the Larmor precessions of the nuclei. The residual line width observed may be due in part to extra - ionic interactions, and partly to incomplete averaging of the internuclear vectors during one precessional period. Reorientation of the NH_3 molecules about their threefold axes may or may not occur in addition to this motion.

As mentioned above, the motion of the complex cannot be a

completely free rotation. The reorientation may occur by a pure tunnel effect, as we should expect in the case of very high, narrow barriers; or it may take place by an activation process, in which the barrier is surmounted as the ion is raised into an excited torsional oscillation state. The latter process is likely in the case of broad but low potential barriers. On qualitative grounds, one would predict rather shallow barriers in the present instance, so that the activation mechanism may play an important role. Certainly both effects are present to some extent, but in the absence of information concerning the form of the potential function, one cannot make any detailed statements concerning the mechanism of the tumbling.

Rushworth[53] has recently found a case in which the true, broad absorption of a rigid dipolar group had been overlooked in a previous investigation[54] in favor of a much stronger, narrow line due to small amounts of incompletely removed solvent. In the present work care has been taken to avoid misinterpretation of this sort. No evidence of any broad absorption can be found, even with the spectrometer gain increased to a point at which the extremes of the central peak are far off the scale of the chart recorder. No change in the observed absorption was detectable after rewashing of the sample in anhydrous ether and protracted drying at 110° C. and <u>in vacuo</u>. It is therefore felt that the narrow observed resonance is indeed characteristic of the complex compound itself.

4. $Coen_3Cl_3$:

The triply chelated complex compound cobalti - tris - ethylenediamine trichloride is chemically similar to the hexammine analogue just discussed, but has considerably lower symmetry, the configuration being of the type

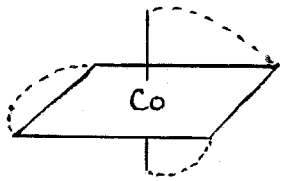

..... = en.

The outer boundary of this ion is much less nearly spherical than is that of the hexammine, and one might expect for this reason that rapid reorientation would be less probable. While the crystal structure of the anhydrous salt has not been determined, it seems a reasonable conjecture to assign it to the same system as the $Co(NH_3)_6^{+++}$ salts, except possibly for a larger unit of structure to allow for proper distribution of the enantiomers.

Nuclear magnetic resonance investigation of the ethylenediamine complex yields a broad line which has a roughly Gaussian shape, in accordance with the complexity and low symmetry of the spin system. The second moment is found, by numerical integration of the experimental derivative curves, to be 33 ± 2 gauss^2. The theoretical second moment contributed by the closest H - H pairs,

neglecting other interactions, is 15.4 gauss^2, where we have assumed tetrahedral angles and the bond lengths

$$d_{NH} = 1.01 \text{ A.U.} \; ; \quad d_{CH} = 1.09 \text{ A.U.}$$

Approximate measurements on a scale model of the ion indicate an additional broadening of about 15 gauss^2 for the other proton - proton, proton - nitrogen, and proton - cobalt interactions within the complex. Coupling between one complex ion and its neighbors is assumed to be small. We thus expect a total rigid lattice second moment of about 30 gauss^2, in good agreement with the measured value. It is therefore concluded that the $Coen_3^{+++}$ ion does not, at room temperature, have the freedom of reorientation possessed by the hexammine complex. A detailed comparison of the two cases would require a knowledge of the crystal structure of the ethylenediamine salt, and the results of line width studies at a variety of temperatures.

5. $\underline{Co(NH_3)_5N_3Cl_2}$:

X - ray photographs have been taken[55] to determine the crystal structure of azido - cobaltipentammine dichloride, but have not yet been analyzed. As a result, no complete comparison can yet be made with the closely related compound $Co(NH_3)_6Cl_3$. The rations are so nearly alike, however, that some interest attaches itself to a study of the proton resonance line width for the azido salt.

Qualitatively, one would expect the rigid lattice line widths in the two compounds to be very nearly identical, or about 45 gauss^2. The positive ions differ principally in the substitution in one of an ammonia molecule by a linear azide ion, which lowers the symmetry and is expected to inhibit any rotations except those about the axis of the N_3^- ion. If free reorientation about this axis (or the NH_3 threefold axes) occurs, the intramolecular second moment will be reduced to one fourth of its rigid lattice value, or about 11 gauss^2. If no appreciable tumbling occurs, one should observe the 45 gauss^2 mean square width mentioned above.

The experimental result is, in fact, that the second moment is 25.4 $\pm$ 2 gauss^2, or intermediate between the two limiting possibilities. It is conceivable that at room temperature the degree of freedom corresponding to the reorientation is just beginning to be excited, and that the available data are actually appropriate to a region of transition between rigid - lattice and freely tumbling states. The experimentum crucis would of course be a measurement of the line widths over a range of temperature. The spectrometer used in these experiments has not yet been adapted for operation at either high or low temperatures.

6. $Al(H_2O)_6Cl_3$:

The octahedrally hexahydrated aluminum ion possesses higher symmetry than $Co(NH_3)_5N_3^{+++}$ or $Coen_3^{+++}$, but is less nearly

spherical than the cobaltihexammine complex. The crystal lattice is rhombohedral[8] and locally similar to that of the hexammines.

Assuming that the principal proton - proton distances in the crystal are approximately the same as in free water, the second moment predicted for nuclear interactions within a single water molecule is 22.8 gauss^2 in powder samples. Some coupling between water molecules of the same complex ion is expected, but is difficult to estimate accurately. For a given metal - coordinated atom distance it is undoubtedly smaller than the 10 gauss figure taken for the hexammine cobalt (III) complex, by virtue of the smaller density of protons over the coordination sphere.

The second moment measured in $Al(H_2O)_6Cl_3$ is 25.7 $\pm$ 2 gauss^2, in satisfactory agreement with the theoretical rigid - lattice value. It is therefore concluded that no rapid, large - scale motions occur in this crystal. Apparently the symmetry required for such motion is very high, or the rotating group must be packed rather loosely in the lattice for such reorientations to occur.

VI. OTHER SUBSTANCES WHICH WERE STUDIED.

The structure of phosphorous acid is commonly believed to contain two hydroxyl groups and one hydrogen atom directly bonded to phosphorus. While this configuration appears to be a reasonable one, it appears that there is no direct evidence on the matter except for the fact that the acid has only two ionization constants of measurable magnitude in aqueous solution.

An attempt was therefore made to measure the nuclear magnetic resonance doublet separation expected for the H - P interaction, since even a rough determination of the H - P distance would suffice to distinguish between the accepted structure and one in which all three hydrogen atoms reside in hydroxyl groups. Anhydrous sodium phosphite, Na_2HPO_3 was selected as a sample material in order to avoid complication due to the extra hydrogen atoms of the free acid. The salt was prepared by titrating Baker and Adamson Reagent grade H_3PO_3 with sodium hydroxide to a thymolphthalein end point. The resulting solution was evaporated and the product dried in vacuo for several days. Samples of anhydrous Na_2HPO_4 and NaH_2PO_2 were also used for comparison purposes.

Unfortunately, the doublet splitting to be expected (approximately 1.5 gauss) was too small to be resolved. The low proton density in the samples necessitated the use of extremely

narrow bandwidth conditions, such that the spurious broadening from field fluctuations obscured any detail which might be present. Since it was felt undesirable to attempt any conclusions on the basis of second moment calculations, the project has for the present been reluctantly abandoned.

APPENDIX

Consider an arbitrary fine structure function f(x) and any even broadening function $\zeta\,(y - x)$. Both are assumed to be well - behaved and to vanish at $\pm\,\infty$ more rapidly than $1/x^2$. They are to be normalized so that

$$\int_{-\infty}^{\infty} f(x)\,dx = 1\ ; \qquad \int_{-\infty}^{\infty} \zeta\,(y - x)\,d(y - x) = 1.$$

The second moment of the broadened absorption is

$$\overline{\Delta\ y^2} = \int_{-\infty}^{\infty}\int_{-\infty}^{\infty} y^2\ \zeta\,(y - x)\ f(x)\,dy\,dx.$$

Making the change of variable $y \to y - x = u$,

$$\overline{\Delta\ y^2} = \int_{-\infty}^{\infty}\int_{-\infty}^{\infty} (u + x)^2\ \zeta\,(u)\ f(x)\,du\,dx.$$

This may be integrated immediately when written in the form

$$\overline{\Delta y^2} = \iint_{-\infty}^{\infty} x^2\,\zeta\,(u)\ f(x)\,du\,dx + \iint_{-\infty}^{\infty} u^2\,\zeta\,(u)\ f(x)\,du\,dx$$

$$+\ 2\iint_{-\infty}^{\infty} ux\ \zeta\,(u)\ f(x)\,du\,dx.$$

The first term is just the second moment of f(x), and the second

term is the second moment of the broadening function. The third term is the integral of an odd function of u over all u, and therefore, vanishes. Thus we have the important result that the second moment of the total absorption, obtained by the procedure of section I, is the correct second moment for all the interactions in the sample.

REFERENCES

(1) W. Pauli, Naturwiss. 12, 741 (1924).

(2) P. A. M. Dirac, Principles of Quantum Mechanics, 3d edition, Oxford, p. 144 (1947).

(3) B. T. Feld, Nuclear Electric Quadrupole Moments, (National Research Council, Washington, 1949) p.2.

(4) I. Newton, Principia, (Cajori ed.) (Univ. of Cal. Press, Berkeley, 1950), p.13.

(5) F. Bloch, Phys. Rev. 70, 460 (1946).

(6) E. Majorana, Nuovo Cimento. 9, 43 (1932).

(7) I. I. Rabi, Phys. Rev. 51, 652 (1937).

(8) Handbook of Chemistry and Physics, (Chem. Rubber Publ. Co., Cleveland, 1944).

(9) J. R. Zimmerman and D. Williams, Phys. Rev. 76, 350 (1949); 76, 638 (1949); 82, 651 (1951).

(10) H. W. Knoebel and E. L. Hahn, Rev. Sci. Inst. 22, 904 (1951).

(11) E. M. Purcell, Phys. Rev. 81, 2/15 (1951).

(12) N. Bloembergen, E. M. Purcell, and R. V. Pound, Phys. Rev. 73, 679 (1948).

(13) N. L. Alpert, Study of Phase Transitions by Means of Nuclear Magnetic Resonance Phenomena, Tech. Report No. 76, M.I.T. Electronics Laboratory (1948).

(14) L. I. Schiff, Quantum Mechanics, McGraw Hill, New York, p.144, (1949).

(15) I. Waller, Z. Phys. 79, 370 (1932).

REFERENCES (continued)

(16) L. J. F. Broer, Physica 10, 801 (1943).

(17) J. H. Van Vleck, Phys. Rev. 74, 1168 (1948).

(18) M. Ward, Lecture Notes in Mathematical Analysis, C.I.T. (1951).

(19) N. Bloembergen, Nuclear Magnetic Relaxation, (Martinus Nijhoff, The Hague, 1948) p.33.

(20) P. A. M. Dirac, op. cit. p. 161.

(21) W. Magnus and F. Oberhettinger, Formeln und Satze fur die Speziellen Funktionen der Mathematischen Physik, (Springer, Berlin, 1948).

(22) I. I. Rabi, Phys. Rev. 51, 652 (1937).

(23) F. Bloch, W. W. Hansen, and M. Packard, Phys. Rev. 70, 474 (1946).

(24) E. M. Purcell, H. C. Torrey, and R. V. Pound, Phys. Rev. 69, 37 (1946).

(25) D. Williams, Physica 17, 455 (1950).

(26) E. L. Hahn, Phys. Rev. 80, 580 (1950).

(27) G. M. Safonov, Ph.D. Thesis, (C.I.T. 1949).

(28) J. S. Waugh, J. N. Shoolery, and D. M. Yost, Rev. Sci. Inst., in press.

(29) H. L. Anderson, Phys. Rev. 76, 1460 (1949).

(30) C. A. Coulson, Valence (Oxford Univ. Press, Oxford, 1952).

(31) G. E. Pake, Am. J. Phys. 18, 473 (1950).

(32) G. E. Pake and E. M. Purcell, Phys. Rev. 74, 1184 (1948).

(33) S. Goldman, Frequency Analysis, Modulation and Noise (McGraw Hill, New York, 1948).

REFERENCES (continued)

(34) G. E. Valley and H. Wallman, Vacuum Tube Amplifiers (McGraw-Hill, New York, ;948).

(35) G. E. Pake, J. Chem. Phys. 16, 327 (1948).

(36) L. Pauling, The Nature of the Chemical Bond, (Cornell Univ. Press, Ithaca, 1939).

(37) L. Helmholz and M. T. Rogers, J. Am. Chem. Soc. 61, 2590 (1939).

(38) J. A. A. Ketelaar, Rec. Trav. Chim. 60, 523 (1941); J. Chem. Phys. 9, 775 (1941).

(39) G. Glockler and G. E. Evans, J. Chem. Phys. 10, 607 (1942).

(40) A. M. Buswell, R. L. Maycock, and W. H. Rodebush, J. Phys. Chem. 8, 362 (1940).

(41) E. Blade and G. E. Kimball, J. Chem. Phys. 18, 630 (1950).

(42) E. F. Westrum and K. S. Pitzer, J. Am. Chem. Soc. 71, 1940 (1949).

(43) R. Newman and R. M. Badger, J. Chem. Phys. 19, 1207 (1951).

(44) J. A. A. Ketelaar and W. Vedder, J. Chem. Phys. 19, 654 (1951).

(45) S. W. Peterson and H. Levy, J. Chem. Phys. 20, 704 (1952).

(46) R. M. Bozorth, J. Am. Chem. Soc. 45, 2128 (1923).

(47) W. C. Fernelius, Inorganic Syntheses, (McGraw-Hill, New York, 1935), p. 217.

(48) J. Dick, Z. Anal. Chem. 82, 401 (1930).

(49) W. C. Fernelius, op. cit., p. 221.

(50) M. Linhard and H. Flygare, Z. anorg. allgem. chem. 262, 328 (1950).

REFERENCES (continued)

(51) R. Wyckoff and T. P. McCutcheon, Am. J. Sci. 13, 223 (1927).

(52) H. S. Gutowsky and G. E. Pake, J. Chem. Phys. 18, 162 (1950).

(53) F. A. Rushworth, J. Chem. Phys. 20, 920 (1952).

(54) E. R. Andrew, J. Chem. Phys. 18, 607 (1950).

(55) A. Cohen, private communication.

(56) H. J. Emeleus and J. S. Anderson, Modern Aspects of Inorganic Chemistry, (Van Nostrand, New York, 1938).

IX. PROPOSITIONS.

1. Recent very strange results on the nuclear induction effect in glasses [1] make desirable a reliable determination of the nuclear spin of Si^{29}. It is suggested that an attempt be made to measure this quantity by observation of the quadrupole structure of rotational transitions of the symmetric rotor $SiHF_3$ at microwave frequencies. This experiment would also yield a value for the quadrupole coupling constant.

2. Simons et al. have attempted to measure electron affinities of some atoms and molecules by analysis of the scattering of slow electrons.[2] It is proposed for the following reasons, among others, that their conclusions are invalid:

a. Using the (classical) theory of these investigators, it is possible to change their reported electron affinity for Hg by 300%, and that for BF_3 by at least a factor of 10, without any loss of agreement with experiment.

b. The total cross sections observed are qualitatively what would be expected for classical electron interaction with any Fermi - Thomas atom, and so may have no connection with any specific electron affinity.

3. Electron exchange does not occur measurably at ordinary temperatures in solutions of $CoCl_2$ and $Co(NH_3)_6Cl_3$. Addition of very small quantities of $FeCl_3$ results in very rapid exchange. The kinetics of this reaction should be investigated in order to eluci-

date its mechanism.

4. Pake[3] attributes the narrowness of the observed proton resonance in $Na_2B_4O_7 \cdot 10\ H_2O$ at room temperature to tunnelling of the protons between equivalent positions in an ice - like structure.

a. It is proposed that such a process cannot account for the narrowing.

b. A study of line width and spin - lattice relaxation time as functions of temperature might produce information regarding other motions which might be responsible for the effect.

5. Bode and Klesper[4] report the preparation of the unusual compounds RbF_3 and CsF_3. It is likely that the constitution of these salts could be clarified by a study of their F^{19} magnetic resonance line profiles.

6. Three possibilities have been proposed for the microscopic constitution of silver bromide crystals containing small amounts of dissolved silver sulfide.[5] A distinction could be made by measuring the intensity of the paramagnetic resonance absorption of microwaves in such systems. It is possible that hyperfine structure would be observable to sharpen the distinction.

7. It appears likely that the optical isomers of the o.-phenanthroline complexes $Fe(ophen)_3^{++}$ and $Fe(ophen)_3^{+++}$ racemize very slowly in solution. It would be interesting to measure the rates of electron exchange for the various pairs of resolved enantiomers of this simple system, using radioactive Fe^{59} as a tracer.

8. The initial logarithmic oxidation law obeyed by certain metals (e. g., iron, stainless steel)[6] follows from the assumption that the rate determining step is an essentially free migration of metal atoms or ions through contiguous, randomly distributed lattice imperfections in the oxide layer. This assumption could be tested by a careful study of the temperature dependence of the oxidation rate.

9. Extremely low - lying rotational levels of certain molecules should be detectable by minima in the spin - lattice relaxation times of nuclei which they contain.

10. In certain experimental investigations, e. g.: the study of phase transitions by nuclear magnetic resonance effects, it is desirable to have a rapid and direct means of temperature measurement. For applications in which accuracy of the order of $\pm$ 3°C is sufficient, a circuit of the type shown on the following page may be expected to afford convenient, direct, and stable readings in the range -200° to +1200°C.

REFERENCES.

1. S. S. Dharmatti, private communication.
2. J. H. Simons and R. P. Seward, J. Chem. Phys. 6, 790, (1938) and subsequent papers.
3. G. E. Pake, J. Chem. Phys. 16, 327, (1948).
4. W. Rode and E. Klesper, Z. Anorg. Allgem. Chem. 267, 97, (1951).
5. O. Stasiw and J. Teltow, Z. Anorg. Chem. 257, 109, (1948). J. W. Mitchell, Phil. Mag. 40, 249, (1949).
6. E. A. Gulbransen, Trans. Electrochem. Soc. 91, 573, (1947).

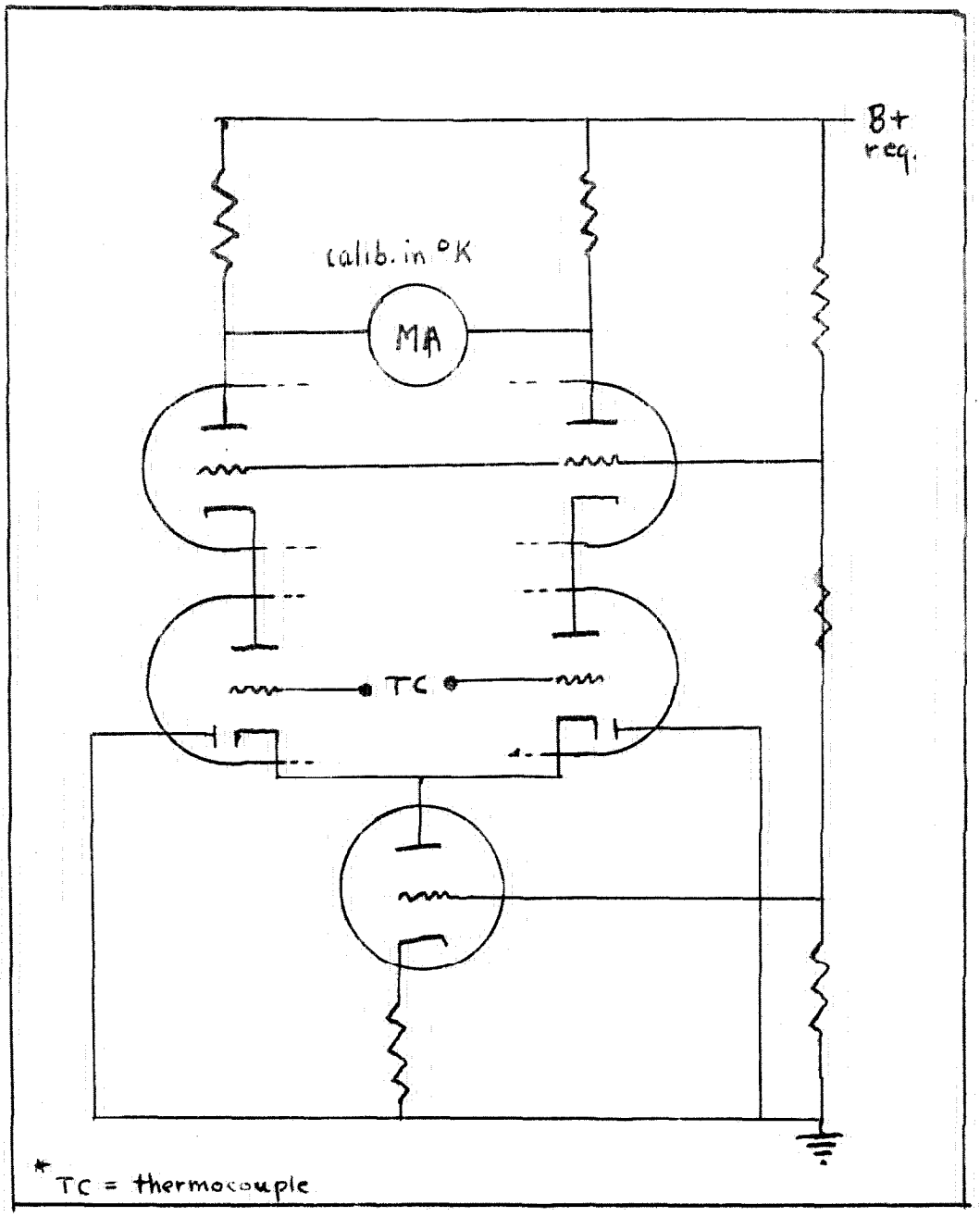
B+
req.
calib. in °K
MA
TC
* TC = thermocouple